

DESIGN OF PEPTIDE-BASED PRODRUG CHEMISTRY AND ITS APPLICATION
TO
GLUCAGON-LIKE PEPTIDE I

Arnab De

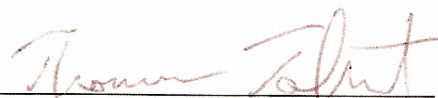
Submitted to the faculty of the University Graduate School
in partial fulfillment of the requirements
for the degree
Master of Sciences
in the Department of Chemistry ,
Indiana University
August' 2007

Accepted by the Graduate Faculty, Indiana University, in partial fulfillment of the requirements for the degree of Master of Science in Chemistry.

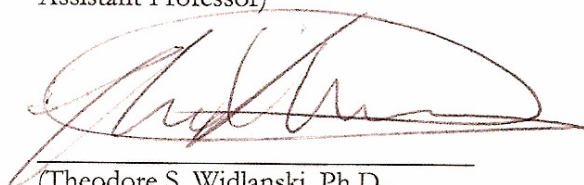
Master of Science Committee



(Richard Dimarchi, Ph.D.,
Linda and Jack Gill Chair in
Biomolecular Sciences and Professor
in Chemistry)



Thomas J. Tolbert, Ph.D.,
Assistant Professor)



(Theodore S. Widlanski, Ph.D.,
Professor of Chemistry and Dean for
Research and Infrastructure)

Inasmuch as this candidate has completed all other requirements, I recommend on behalf of the Department of Chemistry that, upon completion of the course program, s/he be granted the degree of Master of Science in Chemistry.

Graduate Adviser in Chemistry



Daniel J. Mindiola, Ph.D.,
Associate Professor)

© 2007
(Arnab De)
ALL RIGHTS RESERVED

DEDICATION

This thesis is dedicated to my parents, my family and my mentor, Professor Richard DiMarchi.

I would like to take this chance to sincerely thank my parents for my education, for helping me to imbibe the values that helped to get past difficult times. I also want to thank them for their wisdom especially in the times I thought I did not need it.

I want to convey my deepest regards to my mentor for his unwavering support at bitter and disappointing times. His unbridled excitement, enthusiasm and encouragement in my progress helped to introduce me to the world of research. I shall be forever grateful to him for all my scientific achievements and otherwise for he was my first teacher. It is in this light that I shall remember him all my life.

Thank you so much, Ma, Baba and Professor!

ACKNOWLEDGMENTS

I express my gratitude to everybody in the Department of Chemistry, Indiana University, Bloomington who helped my growth as a scientist. I am indebted to my mentor, Professor DiMarchi for all his valuable contributions towards my education on all fronts. He has always guided me both as a researcher and a teacher. I thank my committee members, Professor Tolbert, Professor Widlanski and Professor Clemmer for their viewpoints and vital feedback. I thank everyone in the DiMarchi laboratory for all their help without which I could not complete this thesis. I profusely thank Mr. Jay Levy and Mr. David Smiley for their help in the chemical aspect of my work. I was fortunate to be assisted by Dr. Vasily Gelfanov in the bio-assays and Dr. Todd Parody with his suggestions during my work.

Lastly, I want to thank my dearest 'Ri' for pitching in with her patient and invaluable feedback. It was enjoyable discussing some of the science with her. I am going to remember my MS thesis with fond memories and anticipation.

DESIGN OF PEPTIDE-BASED PRODRUG CHEMISTRY AND ITS APPLICATION
TO GLUCAGON-LIKE PEPTIDE I

ABSTRACT – Peptide-based drugs are highly effective medicines with relatively short duration of action and of variable therapeutic index. Glucagon-like peptide 1 is a hormone that offers promise in the treatment of Type II diabetes. However, the biggest problem in the therapeutic use of GLP-1 is its extremely short half-life in plasma (~2 min). A prodrug of GLP-1 should extend and improve the pharmacodynamics of this peptide hormone. We have designed prodrugs that slowly convert to the parent drug at physiological conditions of 37C and pH 7.2 driven by their inherent chemical instability without the need of any enzymatic cleavage. We observed that amide prodrugs could not convert to the active peptides under physiological conditions. Consequently, we decided to synthesize peptide drugs which had a hydroxy-terminal extension instead of a N-terminal amine. Ester prodrugs were prepared using these hydroxy-peptides as the scaffold. We explored the diketopiperazine and diketomorpholine (DKP and DMP) strategy for the chemical flexibility that it offers to develop prodrugs with variable time actions. The esters proved to be more labile than the corresponding amides and the dynamic range in rate of cleavage ranged from an hour to almost half a week. We found that the rate of cleavage depends on the structure and stereochemistry of the dipeptide pro-moiety and also on the strength of the nucleophile. The careful selection of appropriate functionality that balances chemical, biological and immunological features under physiological conditions has also been reported.

Contents

A) Introduction - Peptide Hormones in the Treatment of Diabetes

- I. Diabetes
- II. Insulin
- III. Glucagon Incretin Peptide 1 (GLP-1)
- IV. Prodrug

B) Hypothesis & Prodrug Design (Application of diketopiperazines to prolongation of GLP-1 pharmacodynamics)

C) Experimental procedure

- I. Peptide synthesis (Boc method)
- II. Peptide synthesis (Fmoc method)
- III. Depsi-peptide synthesis (Amino ester formation)
- IV. Depsi-peptide synthesis (Hydroxyl ester formation)
- V. HF cleavage of the peptidyl-resin
- VI. Analysis by mass spectrometry
- VII. Analysis by High Pressure Liquid Chromatography (HPLC)
- VIII. Preparative purification using HPLC
- XI. Bioassay: Luciferase-based assay for cAMP detection

D) Experimental Results and Discussion

- I. GLP-Oxyntomodulin
- II. Adding dipeptides to the N terminus of GLP-1
- III. Adding dipeptides to the N terminus of F⁷,GLP(8-36)-CEX
- IV. Depsi-peptides and Esters
- V. Adding dipeptides to the OH terminus of HO-F⁷,GLP(8-36)-CEX
- VI. Bioassay of selected longer-acting prodrug candidates
- VII. Ester prodrugs at internal peptide sites
 - a) Hypothesis & Design
 - b) Synthesis and analysis

E) Conclusion

Figure Legends

- I. Figure 1: Primary structure of Insulin
- II. Figure 2: Pharmacodynamics of common insulin analogues
- III. Figure 3A: Primary structure of GLP-1(7-36) amide and action of DPP IV
- IV. Figure 3B: Primary structure of GLP-1(7-37) acid and action of DPP IV
- V. Figure 3C: 2D-NMR structure of GLP-1
- VI. Figure 4: Pictorial explanation of GLP-1 therapy
- VII. Figure 5A: General prodrug chemistry hypothesis
- VIII. Figure 5B: Hypothesis (N-terminal amide and ester prodrugs)
- IX. Figure 6: Cleavage of amide and ester prodrugs
- X. Figure 7: Pictorial explanation of luciferase reporter gene assay
- XI. Figure 8A: Peptide synthesis (Boc method)
- XII. Figure 8B: Peptide synthesis (Fmoc method)
- XIII. Figure 9: Depsi-peptide synthesis (Amino ester formation)
- XIV. Figure 10: α -Hydroxyl- N terminal peptide extension
- XV. Figure 11A: Mass spectra of purified GLP-oxytomodulin chimeric peptide
- XVI. Figure 11B: Bioassay results of GLP-oxytomodulin chimeric peptide
- XVII. Figure 12A: Schematic synthesis of Class I prodrugs
- XVIII. Figure 12B: Cleavage of an amide bond to form DKP and H⁷,GLP(8-37)
- XIX. Figure 12C: Cleavage of an amide bond to form DKP and F⁷,GLP(8-37)
- XX. Figure 13: Mass spectra of G⁵P⁶H⁷,GLP(8-37)
- XXI. Figure 14A: Dipeptide extended F⁷,GLP(8-36)-CEX
- XXII. Figure 14B: Schematic synthesis of Class II prodrugs

- XXIII. Figure 15: HPLC analysis of $G^5G^6F^7, GLP(8-36)-CEX$
- XXIV. Figure 16A: Schematic synthesis of $HO-F^7, GLP(8-36)-CEX$
- XXV. Figure 16B: Bioassay results of $HO-F^7, GLP(8-36)-CEX$
- XXVI. Figure 17A: Schematic synthesis of Class III prodrugs
- XXVII. Figure 17B: Schematic synthesis of Class IV prodrugs
- XXVIII. Figure 17C: Cleavage of Class III and Class IV prodrugs
- XXIX. Figure 18A: $HO-F^5X^6-O-F^7, GLP(8-36)-CEX$
- XXX. Figure 18B: $F^5V^6-O-F^7, GLP(8-36)-CEX$
- XXXI. Figure 19: Formation of $HO-F^7, GLP(8-36)-CEX$ (MALDI data)
- XXXII. Figure 20: $HO-G^5X^6-O-F^7, GLP(8-36)CEX$
- XXXIII. Figure 21: Dipeptide extended $HO-F^7, GLP(8-36)-CEX$
- XXXIV. Figure 22: Transition State diagram
- XXXV. Figure 23: Structures of the peptides represented in Figure 24 and Table 8
- XXXVI. Figure 24A: Bioassay results of select longer-acting GLP-1 prodrugs
- XXXVII. Figure 24B: Histogram showing the potency of various prodrugs
- XXXVIII. Figure 25: Bioassay results that show the reversal of prodrugs to drugs
- XXXIX. Figure 26A: $(H7F), (E9Q), GLP(8-36)-CEX$
- XL. Figure 26B: $(H7F), (E9Q), (T11S), GLP(8-36)-CEX$
- XLI. Figure 27: Bioassay of internal serine/ threonine ester drug candidates
- XLII. Figure 28: Formation of $(H7F), (E9Q), (T11S), GLP(8-36)-CEX$
- XLIII. Figure 29: Representative kinetic profile for appearance of a drug
- XLIV. Figure 30: Ester prodrugs resistant to cleavage
- XLV. Figure 31A: Relative potency of $G^5V^6-O-F^7, GLP(8-36)CEX$

XLVI. Figure 31B: Relative potency of HO-F⁵F⁶-O-F⁷,GLP(8-36)-CEX

XLVII. Figure 32: Prodrugs of varying half lives

Index of Tables

- I. Table I: Pharmacodynamics of common insulin analogues
- II. Table II: Attempted Cleavage of H⁷,GLP(8-37) prodrugs to form native GLP-1
- III. Table III: Attempted Cleavage of Di-peptide extended F⁷,GLP(8-37)
- IV. Table IV: Attempted Cleavage of dipeptides attached to the N terminus of F⁷,GLP(8-36)CEX
- V. Table V: Attempted Cleavage of dipeptides at the N terminus of G⁷,GLP(8-36)CEX
- VI. Table VI: Cleavage of dipeptide esters attached to the OH terminus of HO-F⁷,GLP(8-36)-CEX
- VII. Table VII: Cleavage of esters to yield HO-G⁵X⁶-O-F⁷,GLP(8-36)CEX
- VIII. Table VIII: Bioassay of select longer-acting ester prodrugs
- IX. Table IX: Bioassay results validating the conversion of prodrugs to drugs
- X. Table X: Bioassay results of internal serine/ threonine drug candidates

Appendix

- I. Appendix I: Schematic synthesis of longer-acting prodrugs
- II. Appendix II: Structure of peptides in Table 2
- III. Appendix III: Structure of peptides in Table 3
- IV. Appendix IV: Structure of peptides in Table 4
- V. Appendix V: Structure of peptides in Table 5
- VI. Appendix VI: Structure of peptides in Table 6
- VII. Appendix VII: Structure of peptides in Table 7
- VIII. Appendix VIII: Acylation of HO-His⁷,GLP(8-37)
- IX. Appendix IX: Synthesis of (H7F),(E9Q),(T11S),GLP(8-36)-CEX
- X. Appendix X: Synthesis of F⁷Q⁹-S¹¹-(Gly-Gly)-GLP(8-36)-CEX
- XI. Appendix XI: A note on nomenclature

Design of Peptide-based Prodrug Chemistry and its Application to Glucagon-Like Peptide I

A) Introduction

I) Diabetes:

Diabetes is an ancient disease that continues to affect a diverse population in modern times. The first recorded cases of diabetes date to ancient times in Egypt and India (where it was called Madhumeha in ancient Ayurvedic medicine).¹ The term "diabetes" was first coined by a Greek physician named Aretaeus of Capasdocia.¹

The prevalence of diabetes has grown steadily over the last thirty years, largely as a result of poor diet and a rapid rise in the prevalence of obesity. Diabetes is a disease associated with sizable morbidity and excessive mortality. It imposes an immense financial burden on those afflicted with the disease and general societal health care costs. It is broadly accepted that there currently is a worldwide epidemic of Type 2 diabetes (often referred to as adult-onset diabetes). Moreover, numerous clinical studies have shown that most cases could be prevented or managed by lifestyle modifications and proper medication.² In certain demographic populations, like the Pima Indians of North America, as much as 30% of the adult population has been diagnosed with Type 2 diabetes. In the United States alone, 18 million people (6.3%) currently suffer from diabetes which in turn is a leading cause of blindness and heart attacks, as well as kidney and vascular disease^{3,4}.

The primary physiological cause of diabetes is the defective utilization of glucose by insulin-responsive cells in the body. Consequently, blood glucose levels increase despite elevations in insulin concentrations and hyperglycemia eventually emerges. The

glucose accumulates in the blood instead of being absorbed and metabolized. Therefore, the cells do not generate enough energy to perform their normal activities while the persistently high blood glucose concentration is damaging to numerous tissues, especially the eyes, kidney and nerves.

There are three different forms of diabetes that are distinguished by their etiological onset and progression. The physiological effects vary in severity and cause, but all induce similar types of damage to physical health.

1) Type 1 diabetes: Type 1 diabetes is often referred to as juvenile diabetes because the majority of cases strike before adulthood. This is a chronic disease of childhood and approximately 150,000 people under the age of 18 and more than a million people in total are afflicted by this disease in the United States alone. Its prevalence is rising at a rate of 3% a year.⁵ Over time, Type 1 diabetes can lead to serious medical complications such as cardiovascular diseases, diabetic retinopathy and diabetic neuropathy.⁶ Type 1 diabetes is most often the result of a humoral based auto-immune response against β cells of the islets of Langerhans which are located within the pancreas. These cells are responsible for producing the insulin required for normal metabolic homeostasis. Such patients typically lose about 80-90% of their β cells⁷ and the remaining population is insufficient to meet the body's normal insulin requirements. This leads to hyperglycemia or what is also known as "insulin-dependent diabetes". People diagnosed with Type 1 diabetes need to be treated with daily insulin injections.

Type 1 diabetes also presents us with a challenging paradox. If the subjects could be identified before hyperglycemia occurs, the initiation of the autoimmune process

might be prevented, thus halting the development of diabetes. Unfortunately, a definitive diagnostic method to determine who will eventually develop Type 1 diabetes does not exist and attempts to develop such methods would require large numbers of test subjects. Without such a diagnostic, the development of an efficacious therapy is difficult since finding the subjects is very hard and the risk-benefit ratio of an experimental medicine in a subject prior to disease onset is unknown.⁶

2) Type 2 diabetes (non insulin-dependent): This is the more common form of diabetes. A healthy person's body secretes enough insulin to maintain a steady blood glucose level. In Type 2 diabetes, the body does not produce enough insulin in a relative and often an absolute sense. Resistance to insulin action is a physiological hallmark feature of this disease. This resistance to insulin is often caused by obesity⁸. Although this is not a universal phenomenon, underweight patients are often found to have had impaired insulin secretion while the obese exhibit "insulin resistance".⁹

Approximately 90-95% patients that suffer from diabetes reportedly have Type 2 diabetes¹⁰ which normally occurs after 40 years of age. Hence it is known as "adult-onset diabetes". Due to changes in dietary habits and lack of exercise, it is no longer uncommon for Type 2 diabetes to occur in younger people, even adolescents. This shows a strong correlation with the alarming rise in the prevalence of obesity and a sedentary lifestyle.

3) Gestational diabetes: This occurs in pregnant women, hence the name. If the blood glucose level is high in a woman during pregnancy but not at other times, then she is said to have gestational diabetes. The cause is currently unknown but seems similar to

Type II diabetes where pregnancy imposes a level of insulin resistance. Approximately 4% of pregnant women are purported to have this disease, and around 135,000 new cases are reported every year.¹¹ Further observations show that approximately 50% of gestational diabetes reappears as Type II diabetes within two years of child bearing.¹¹

II) Insulin:

In two landmark papers^{12, 13} in 1922, Fredrick Banting, Charles Best, James Collip and John Macleod reported the extraction of insulin from the pancreas of a dog. This extract was subsequently shown to lower the blood glucose level in surgically induced diabetic animal models. The clear demonstration that diabetes is caused by the deficiency of insulin and could be reversed pharmacologically makes these two of the more important scientific papers of the 20th century.

Insulin is a rather small protein, with a molecular weight of slightly less than 6,000 Daltons. The primary amino acid sequencing was accomplished by Sanger in 1959.¹⁴ It is composed of two peptide chains, designated as the A chain and B chain. The A chain has 21 amino acids while the B chain has 30.

The chains are linked by two disulfide bonds (residues A7 to B7, and A20 to B19). In addition, there is a third intramolecular disulfide bond in the A chain (residues A6 to A11) (Fig 1). The complete conservation of these three disulfide bonds throughout the mammalian phylum underscores the critical importance of this bonding pattern. This also increases the structural complexity of the molecule and makes it more difficult to synthesize as compared to a single peptide chain.

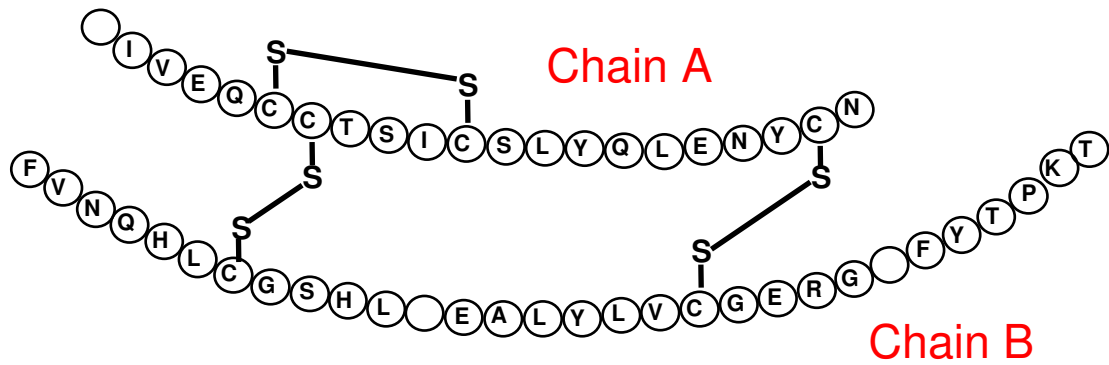


Figure 1: Primary structure of Insulin

There are three important pharmacodynamic characteristics of a drug: its onset (duration to biological action), its peak time (time at which the biological effect is strongest), and finally its duration (sustained time of biological activity). There are several unique forms of insulin designed to meet an individual patient's daily glucose demands (meal and fasting level). They are commonly classified into four broad categories by their duration of action: very fast, fast, slow, and very slow (Table I).

	Onset	Peak Action*	Duration*
Humalog®	0.25 hr	0.5 – 1.5 hrs	3-5 hrs (very fast)
Regular	0.5 hr	2-4 hrs	6-8 hrs (fast)
NPH, Lente	1-3 hrs	6-12 hrs	18-24 hrs (slow)
Ultralente	4-8 hrs	12-18 hrs	24-28hrs (very slow)

*Since patients respond to insulin differently, the peak action and duration are given as ranges.

Table 1: Pharmacodynamics of common insulin analogs

The time action curves of some common insulin analogs are shown in Figure 2. Ultralente is a very slow acting insulin, hence it is usually used with Humalog® (very fast acting) or native regular insulin (fast acting)¹⁵ to more accurately mimic the normal daily physiological variation in insulin activity.

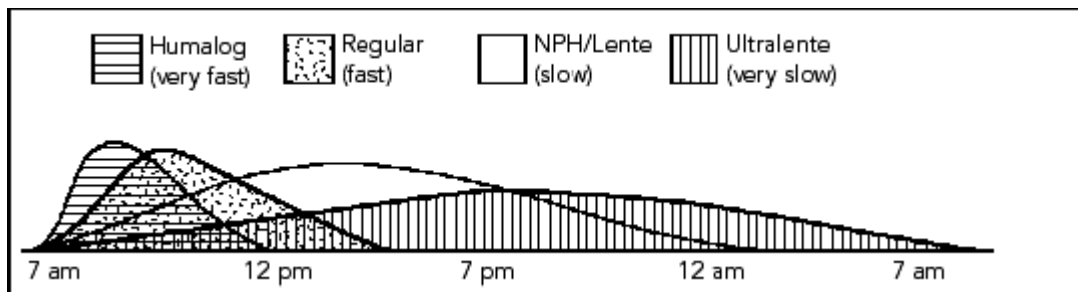


Figure 2: Pharmacodynamics of common insulin analogs.

Numerous combinations of these insulin analogs facilitate regulation of blood glucose in virtually all forms of diabetes. However, they all have several severe limitations. The most relevant is the finding that insulin overdose is the single most

potent cause of life-threatening hypoglycaemia¹⁶. This has been confirmed by many clinical trials, most notably by the Diabetes Control and Complications Trial Research Group¹⁷. Studies performed in representative populations clearly demonstrate that weight gain is another problem associated with insulin therapy¹⁸. Such weight gain can paradoxically increase insulin resistance and thus the amount of insulin needed. Obesity also increases cardiovascular risks¹⁹.

While insulin is a miraculous substance it is a challenging medicine. Its complex structure, especially its intra and intermolecular disulfide bonds makes it difficult to synthesize in an inexpensive manner and the molecule hard to formulate. Furthermore, the natural tendency of insulin to form insoluble multimeric complexes at high concentrations seriously complicates its commercial production. Additionally, the narrow therapeutic index and thermal instability of insulin over extended periods of time makes refrigeration a necessity. Lack of adequate refrigeration is a major issue in many parts of the world.

What is most needed is a medicine that is capable of normalizing blood glucose without the risk of hypoglycemia. In this context, it is helpful to note that Glucagon-like peptide 1 (GLP-1) therapy has been shown to increase native insulin synthesis and secretion without inducing hypoglycemia²⁰.

III) Glucagon like peptide 1 (GLP 1):

Glucagon-like peptide 1 is a hormone that offers the promise of revolutionizing the treatment of Type II diabetes. In a landmark paper published in 1985,²¹ two endogenous peptides were reported which had a high sequence homology to glucagon

and, like insulin, displayed high conservation across a range of different species. These two peptides were Glucagon-like peptide-1 (GLP-1) and Glucagon-like peptide-2 (GLP-2) which were first identified in the course of cloning the gene for proglucagon. Upon testing, it was found that GLP-1 stimulated insulin release while GLP-2 did not²¹. Early clinical experiences suggested that GLP-1 has an attractive pharmacologic profile²². Throughout this thesis, GLP-1(7-37)-acid has been denoted simply as GLP with changes added to this nomenclature to signify related peptides.

GLP is secreted from the gut in response to a meal²³. It is an incretin hormone that has the potential to offer an ideal treatment for Type 2 diabetes²⁴. GLP enhances the secretion of insulin²⁵ only when the blood glucose level is high, eliminating the risk of hypoglycemia. It inhibits glucagon secretion therein maintaining an optimal ratio of insulin and glucagon²⁶. GLP has further been shown to reduce food intake via its effects on gut motility (it inhibits the motility of the upper gut), leading to weight loss and decreased obesity²⁶. Thus, GLP by virtue of its multiple biological actions has emerged as a valuable tool in the treatment of Type 2 diabetes, and related metabolic syndromes.

There is another more physiological factor to rationalize GLP therapy. Type 2 Diabetes is characterized by insufficient insulin secretion and declining β -cell function. This β -cell defect partly results from the progressive loss in β -cells function, as noted previously. GLP also has an apparent mitogenic effect on the β -cells of the pancreas²⁷, and thus stimulates the *in vivo* biosynthesis of insulin (thus addressing the main defect of progressive decay in β -cell capacity)²⁶. Additionally, recent research demonstrates that almost two thirds of the insulin secreted in response to a meal is because of the action of insulinotropic actions of the incretin hormones, like GLP²⁸. Indeed patients with Type 2

Diabetes have been long known to exhibit a variable loss in the incretin action of GLP²⁹. In this way, GLP therapy addresses the physiological replacement for the loss in incretin action associated with Type 2 Diabetes.

GLP stimulates the secretion of insulin by interacting with the GLP G-Protein Coupled Receptor (GPCR) expressed on the surface of β -cells of the pancreas. This receptor is coupled positively to the adenylyl cyclase system³⁰. After ligand activation, the adenylyl cyclase is stimulated leading to an increase in cAMP concentration within the β -cells³¹. This in turn activates protein kinase A that leads to an avalanche of additional biochemical events³². GLP mediated receptor action via adenylyl cyclase is the basis of our *in-vitro* bio-assay, and has proven useful in design of GLP analogs with therapeutic promise (see Experimental Design of Bioassays). It is to be noted that this insulinotropic effect of GLP is strictly glucose dependent³³.

Glucagon-like peptide 1 physiologically exists in two forms of comparable biopotency³⁴. The first is the more abundant³⁴ GLP(7-36) amide where the C terminus is an arginine amide (Figure 3A). The second form is the GLP(7-37) acid where the C terminus is a glycine (Figure 3B). The secondary structure of GLP-1 is shown in Figure 3C.

Human Glucagon Like Incretin Peptide (7-37)-OH

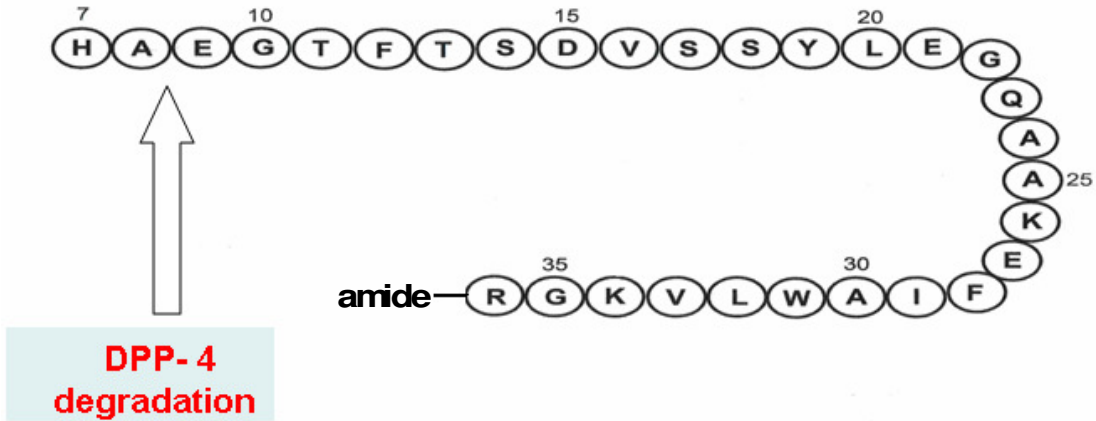


Figure 3A: Primary structure of GLP-1(7-36) amide and action of DPP IV

Human Glucagon Like Incretin Peptide (7-37)-OH

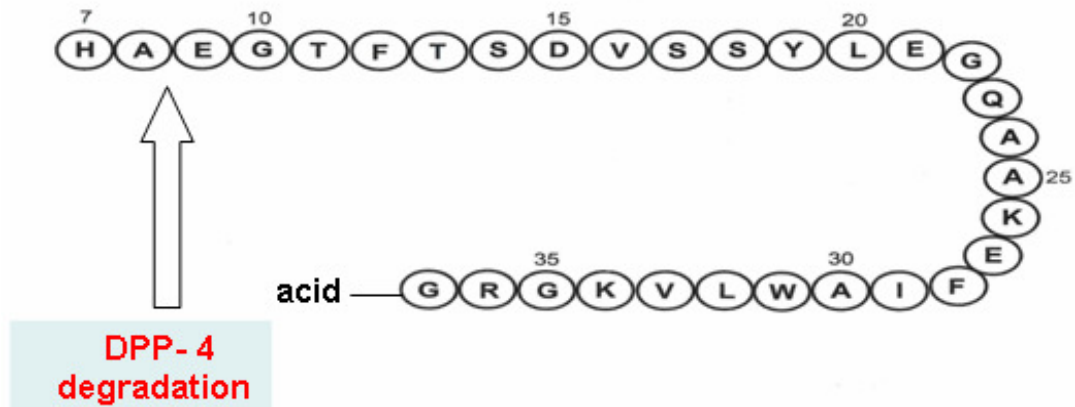
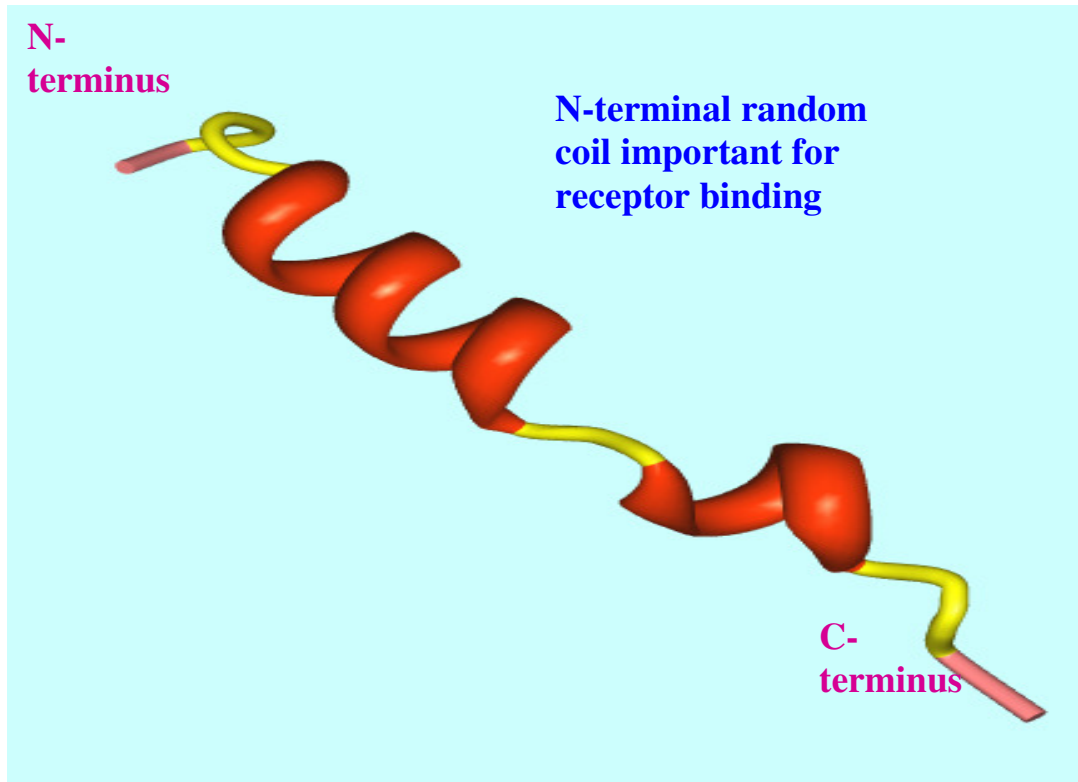


Figure 3B: Primary structure of GLP-1(7-37) acid and action of DPP IV.



The 2D-NMR structure of GLP-1 has revealed that the first 7 residues show a random coil (pink) followed by a turn (yellow). This is followed by a helical region (red; residues 7-14), a linker region (yellow; residues 15-17) and another helical region (red; residues 18-25). The C-terminal region of GLP-1 is again a random coil. It is speculated that the N-terminal random coil region interacts with the receptor. The structure has been drawn using PDB Protein Workshop software. (Hui, H., et al. (2005) *Diabetes/Metabolism Research and Reviews* 21: 313-331)

Figure 3C: 2D-NMR structure of GLP-1

As illustrated in Figure 3C, it is thought that the N-terminal random coil region is important for receptor binding. Structure-activity relationship studies have shown that the N terminal histidine is especially important for the potency of GLP and the N-terminally extended forms severely diminish biological potency³⁵. We intend to take advantage of this finding to further advance our research hypothesis (see Hypothesis).

The biggest problem in the therapeutic use of GLP is its extremely short half-life in plasma (~2 min)³⁶. The short half life results from the rapid degradation by Dipeptidyl Peptidase IV (DPP-IV) and the circulating levels further decrease due to high renal

clearance³⁷. As shown in Figure 3A and 3B, DPP-IV cleaves GLP between the alanine residue at position 8 and the glutamic acid residue at position 9³⁸. This cleavage not only inactivates the peptide but it also yields the residual GLP(9-36) amide; an antagonist at the GLP receptor³⁹. Hence, to obtain reasonable glycemic control, the GLP should be administered continuously for a prolonged period³⁶.

Two other strategies have been formulated to use GLP signaling to treat Type 2 diabetes: use of a DPP-IV inhibitor⁴⁰ or design of a longer-acting variant of GLP (pictorially represented in Figure 4).

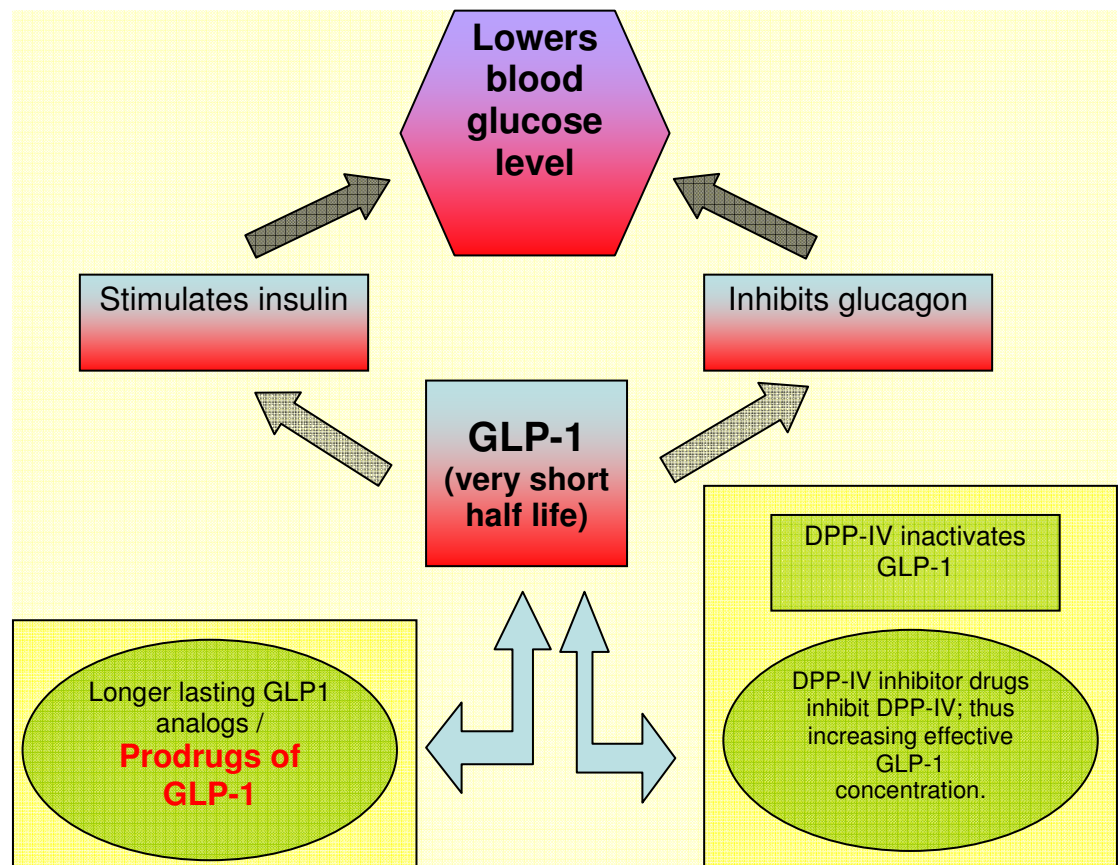


Figure 4: Pictorial explanation of GLP-1 therapy

The most obvious difference between these two therapies seems to be their effect on body weight. While native GLP and its analogs promote loss of weight, the DPP-IV inhibitors act by preventing gain of weight⁴¹. Additionally, several other issues regarding the feasibility of using DPP-IV inhibitors need to be addressed before effective therapeutic use⁴². Even after treatment with DPP-IV inhibitors it is not clear if there would be enough GLP to attain peak efficacy in the body. This is because the amount of endogenous GLP secreted is severely reduced in diabetes. The fact that DPP-IV non-specifically acts on peptides other than GLP adds to its efficacy but is also a matter of concern. The larger issue pertains to the other useful functions of DPP-IV in different tissues, such that adverse effects of DPP-IV inhibitors are theoretically possible⁴².

Our work concentrated on designing a prodrug for GLP i.e., a longer-acting variant of GLP. A few longer-acting analogs of GLP have been identified, two of which will be discussed below. The first peptide is Exendin-4 which is an agonist for GLP receptor⁴³ and is found in the saliva of the Gila monster⁴⁴ (*Heloderma* species native to several American States). Exendin-4 was discovered by John Eng, an endocrinologist at the Bronx Veteran's Affairs Medical Center in New York. It is being marketed by Amylin Pharmaceuticals. Exendin-4 functions in a manner similar to that of native GLP with which it shares 53% amino acid homology. Several important functional residues like the N-terminal histidine are conserved. It is much more resistant to cleavage by DPP-IV than GLP as a result of the glycine at the second residue instead of alanine. Thus, it is found that Exendin-4 has all the biological functions of GLP, but with a longer half life (60-90 minutes)⁴⁵. While the $t_{1/2}$ is much greater as compared to native GLP ($t_{1/2}$ ~2min), an even longer-acting drug is highly desirable. Finally, since Exendin-4 is of non-human

origin, it has been reported to induce an immune response that compromises long-term clinical efficacy⁴⁶.

Another longer-acting GLP analog is called Liraglutide. In this peptide analog, there is an arginine in the 34th position instead of a lysine. Additionally, a glutamic acid residue is added to the lysine residue at position 26⁴⁷ and the α -amine of this glutamate is acylated with a C16 fatty acid. Upon entering the bloodstream, the fatty acid non-covalently binds to serum albumin (a protein facilitating plasma transport)⁴⁸. The serum albumin distributes the drug throughout the body and also protects against cleavage⁴⁷. As a result Liraglutide's $t_{1/2}$ is increased to about 10-14 hrs and the drug can be injected once a day. This drug is being developed by Novo Nordisk and has now entered Phase 3 trials.

The N-terminal histidine of GLP (7th position as shown in Figure 3B) is important for pancreatic receptor activation of GLP and exendin-4. Previous amino acid substitutions for this histidine with lysine and alanine have resulted in a large loss of bioactivity³⁵. Hence it has been concluded that the imidazole ring of the histidine is necessary for the full potency of the molecule. GLP lowers blood glucose in diabetic patients, and might restore β cell sensitivity to exogenous insulin secretagogues. Studies so far have yielded evidence that GLP therapy is safe and effective for Type 2 diabetics⁴⁹. We want to develop a longer-acting GLP prodrug, possibly with weekly or even monthly duration of in vivo biological action.

IV) Prodrug:

A prodrug is the precursor of a drug. According to The International Union of Pure and Applied Chemistry (IUPAC), the term prodrug is defined as “any compound that undergoes biotransformation before exhibiting its pharmacological effects. Prodrugs can thus be viewed as drugs containing specialized non-toxic protective groups used in a transient manner to alter or to eliminate certain limiting properties in the parent molecule”⁵⁰. The term “prodrug” was first introduced by Albert in 1950 to signify pharmacologically inactive chemical derivatives that undergo conversion endogenously to become an active pharmacological agent to increase their usefulness or decrease their toxicity⁵¹. In this regard, prodrugs can be used for various purposes. Most prodrugs are designed to facilitate high cellular absorption following administration⁵² (i.e. valaciclovir). Prodrugs must be soluble in an aqueous media to be absorbed properly. Insolubility of a drug can also cause significant pain at the site of injection. An example is clindamicyn where injections are painful, but its phosphate ester prodrug improves solubility and alleviates the pain⁵³. The prodrug should be non-toxic, stable in storage and must be resistant to degradation in different body fluids until that point when it reaches its site of action. Finally after reaching the specific site of action, there should be a quantitative release of the drug⁵³.

The prodrug approach is commonly utilized with small molecules (less than 500 Daltons)⁵⁴ to enhance oral delivery. The main obstacle to using peptides as potential drugs is their short half life in the systemic circulation because of proteolytic hydrolysis and the rapid clearance by blood, liver and kidney⁵⁵. A second limitation is their limited

oral absorption⁵⁵. Due to these problems of short half life and poor oral bioavailability, alternative routes of delivery are being explored⁵⁶.

The prodrug that we envision has certain unique characteristics. Through structural refinement, we intend to appropriately extend the biological half life and broaden the therapeutic index of GLP. Our prodrug concept is not focused on oral bioavailability as with conventional small drug approaches, but upon extended biological half life. Consequently, many of the stringent necessities of conventional prodrugs are not relevant. Most prodrugs as described above are designed to facilitate transport across biological membranes. Our prodrug is used to delay the time of action by inhibiting recognition by the corresponding receptor. Receptor recognition is the primary means of degradation and thus termination of biological activity of our drug. We seek to convert our prodrugs to active peptides by controlling the chemical conversion to structures that can be recognized by the receptor. The speed of this chemical conversion will determine the time of onset and duration of in vivo biological action (Figure 5).

The final element of this work is the application of selective pegylation⁵⁷ to delay non-productive, premature, in-vivo clearance. Peptides are easily cleared because of their relatively small molecular size when compared to plasma proteins. Increasing the molecular weight of a peptide above 40kDa exceeds the renal threshold and significantly extends duration in the plasma. The judicious choice in the site of attachment of a polyethylene glycol polymer that is ten fold larger than insulin or GLP is a sizable challenge.

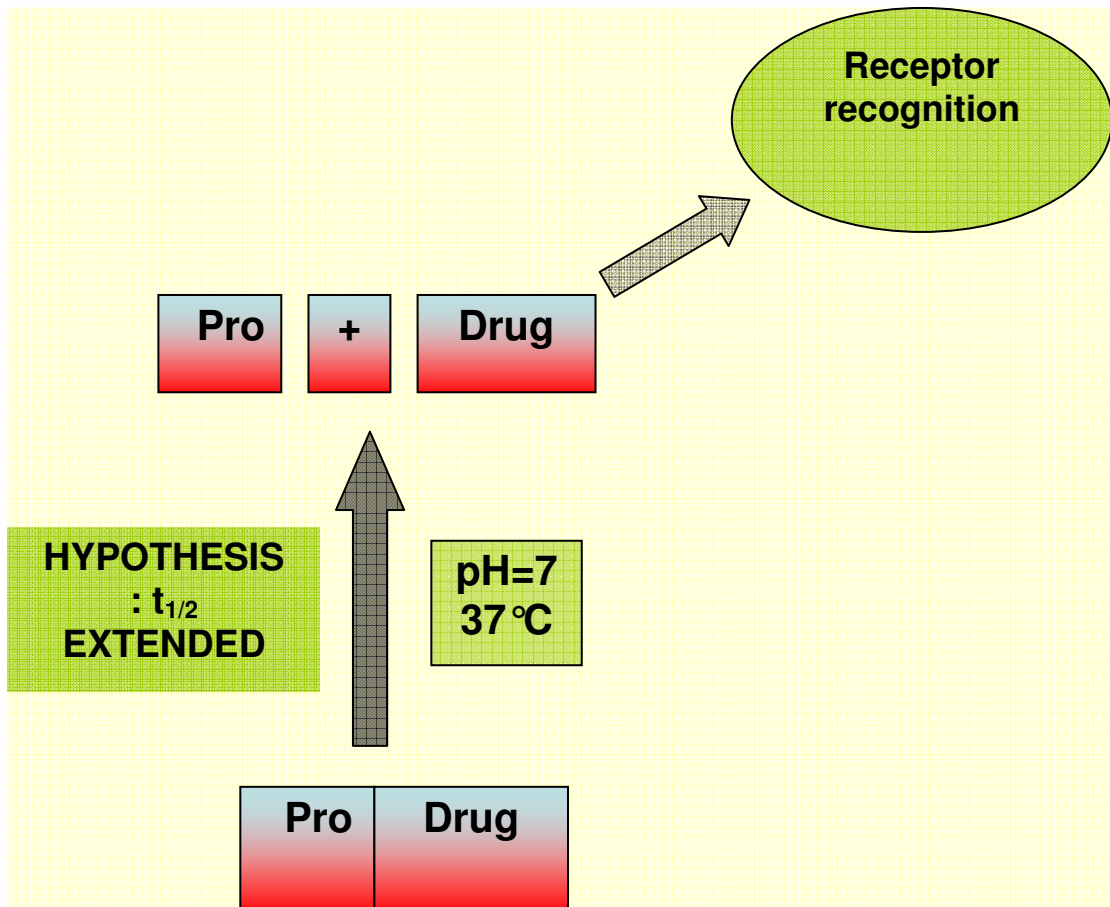


Figure 5A: General prodrug hypothesis

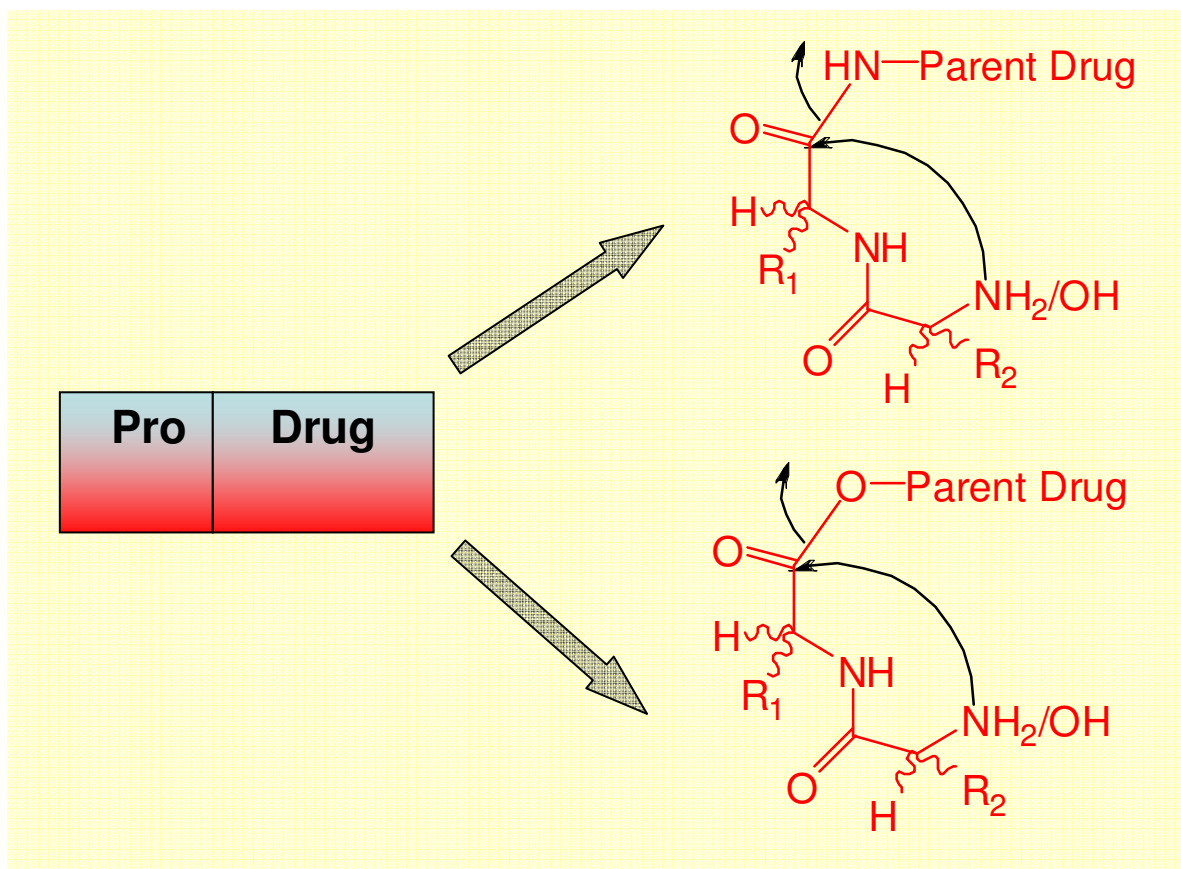


Figure 5B: Hypothesis (N-terminal amide and ester prodrug)

B) Hypothesis:

We believe that by making a prodrug at the N-terminal end of GLP, it should be possible to extend and improve the pharmacodynamics of this peptide hormone (Figure 5A and 5B).

The ideal prodrug should be soluble in water at a pH of 7.2 and 37°C, and it should be stable in the powder form for long term storage. It should be immunologically silent and biologically inactive when injected in the body; and be quantitatively converted to the active drug within a defined period of time. Our greatest interest lies in prodrugs with a $t_{1/2}$ of between 10-100 hrs (weekly, or even monthly duration) under physiological conditions (pH of 7.2 and 37°C).

During the course of this research, we identified four GLP analogs that are physically and chemically stable, and whose conversion from prodrug to the active drug form under normal physiological conditions ranges within the optimal range. One of these peptides converts to GLP with a half life of 64 hrs. The *in vivo* extension in duration of action of this magnitude would constitute the longest acting peptide prodrug ever designed. These analogs possess a minimal alteration to the native amino acid sequence, and this should minimize potential adverse immunogenic affects. The bioactivities of these synthetic peptides have been determined using *in vitro* cellular assays.

At the beginning of this research, many strategies were considered for constructing our prodrugs. It was contemplated that the protecting groups of the prodrug could be cleaved by enzymes as reported for nucleotide prodrugs⁵⁸. However, we decided to design a prodrug that would slowly convert to the parent drug at physiological

conditions of 37°C and pH 7.2 driven by inherent chemical instability. The pH and temperature were relied upon for this conversion, as they are virtually invariant physiologically. We are seeking a prodrug that converts quantitatively to the drug under physiological conditions without the aid of any enzyme. The establishment of prodrug chemistry at the N-terminal end of GLP should be translatable for use with other peptides where this specific site is vital to bioactivity.

We decided to synthesize a chemical derivative of GLP that would convert to GLP spontaneously as stated above. A few possible choices were contemplated before deciding that our primary target in prodrug chemistry would be diketopiperazine formation. The N-terminal histidine is important for the potency of our drug, and a reversibly modified histidine side chain was considered, as has been reported for Thyrotropin-Releasing Hormone (TRH)⁵⁹. However, we dispensed with this approach since this prodrug chemistry is specific to the imidazole ring. This means that the prodrug chemistry requires the presence of a histidine, and possibly also at an N-terminal site.

Thiol esters could also be synthesized by thioesterification⁶⁰. However, a thiol ester is relatively unstable in physiology and thus would likely cleave too fast, thereby resulting in rapid clearance of the prodrug in its active form. Additionally, the use of thiol-based chemistry is fraught with other difficulties, such as instability of disulfide bonds. We decided to forgo this course of action.

Our work therefore focused on making amide and ester prodrugs at the N-terminus that upon cleavage of the suitable amide or ester bond generates the desired drug. Esters are normally more labile than amides; however they are easily hydrolyzed by the ubiquitous serum esterases⁵³. Hence, amide bond based prodrugs were a much more

attractive design, although the risk of peptidase degradation may potentially complicate *in vivo* application.

In considering amide prodrugs, it is reported that histidyl-proline amide cyclizes to a cyclo (His-Pro)⁶¹ at a pH of 7 and 37°C with a $t_{1/2}$ of 140 minutes, with the release of NH_3 . The imidazole ring is purported to be playing a catalytic role at this pH. Hence, other dipeptides that did not have a histidine cleaved more slowly, and tripeptides did not cleave at all⁶¹. Thus, it seemed from this work that there might be a basic difference in the rate of diketopiperazine formation from the cleavage of a secondary amide (as in a tripeptide) as compared to a primary one (as in a dipeptide amide).

In another paper⁶², the intramolecular aminolysis of Phe-Pro-p-nitroanilide (Phe-Pro-pNA) to Phe-Pro-diketopiperazine (Phe-Pro-DKP) was studied as a function of pH. The pH-rate plot showed that the rate of the formation of the DKP was dependent on the degree of ionization of the N-terminal amino group, with the unprotonated free amine being more reactive than the protonated form. In their experiment, the authors used an activated, strongly electron withdrawing p-nitroanilide dipeptide instead of a natural tripeptide. This was because these p-nitroanilide dipeptides dissociate by DKP formation more rapidly than amino acid amides (i.e., natural dipeptides), thereby greatly facilitating their use in kinetic studies. The calculated $t_{1/2}$ of conversion of a Gly-Pro-p-nitroanilide (Gly-Pro-pNA) dipeptide to Gly-Pro-diketopiperazine (Gly-Pro-DKP) under physiological conditions was about 120 hours. This is consistent with the previous assertion that there is a significant difference in the dissociation rate between a primary (around 140 minutes as in previous example⁶¹) and an activated secondary amide. It is

also important to note that in a natural tripeptide, the half life of the DKP formation would be further extended since there is no electronic assistance from the pNA.

In both these papers^{61,62}, it seems that the presence of proline in the C terminus of the dipeptide extension accentuates the formation rate of the DKP. This is likely due to contribution of the cis-proline conformer in the facilitation of the dipeptide's adoption of an optimal steric conformation for formation of DKP. The observations with modifications of an N-terminal residue upon the rate of DKP formation at pH 7.0 have been more varied. Reports suggest that it might depend on the pKa of the residue⁶¹, on its bulk⁶³, or on the conformational stability of the resulting DKPs⁶².

We also envisioned modification of a hydroxyl group at what otherwise would be the N terminus to prepare a depsi-peptide and thus make an ester prodrug. An ester can cleave hydrolytically^{64,65} or via the formation of five^{66,67} or six membered rings (like DKP). The ester prodrugs of Floxuridine (FUdR)⁶⁵ convert by general ester hydrolysis i.e., a nucleophilic attack by water on the ester carbonyl. For the most part, the bulk of the pro-moiety influenced the hydrolysis of the FUdR prodrug (the Val ester prodrugs dissociated the slowest). In another paper, the authors studied the cyclization of the dipeptide esters in paracetamol to form a diketopiperazine⁶⁸. They observed that they could obtain differential time action depending on the dipeptide structure. They also considered the possibility that in paracetamol, the drug release might have been via the general mechanism of ester hydrolysis and not the formation of a DKP ring. However, they eliminated it as in that case the nature of the dipeptide would have a lesser effect on reactivity. The proof of labile esters cleaving very fast under physiological conditions is

exemplified by the fast cleavage of the dipeptide esters in paracetamol where all the prodrugs had a $t_{1/2}$ of less than 20 minutes⁶⁸.

In another investigational report, this time with cyclosporine-A prodrugs^{69,70} it has also been seen that through modulating the chemical nature of dipeptide esters it was possible to get conversion rates at physiological conditions ranging from minutes to several hours, but not longer. In these papers^{68,69}, it seems that the presence of a minimally bulky glycine residue in the C terminus of the dipeptide extension accentuates the rate of formation of the DKP. This might be because of less bulk and the preferred conformational effect of glycine. However in the cyclosporine prodrug⁶⁹, it seems unexpected that the presence of a proline in the C terminus of the DKP actually attenuates the rate of the conversion.

In another investigation⁷¹, the C terminal amides of glycine were rapidly hydrolyzed at 25°C and a pH of 7 when the N-terminus was N-hydroxyethylated. The $t_{1/2}$ of bis-N-2-hydroxyethylglycinamide is three hours. In this case, the C terminal amide bond is activated by H bonding with the N-hydroxyethyl group. However, there was no practical way that one could modify the structure of the N-hydroxyethyl group as the precise Vander Waal radii were required to activate the amide group.

Consequently, we explored the intramolecular cyclization reaction of dipeptide esters and amides to form diketopiperazine as an example of a chemoreversible prodrug (Figure 6). This chemistry is reasonably straightforward and allows at least four points (stereochemistry of R1 and R2, nature of the nucleophile and leaving group as shown in Figure 6A and 6B) where structure can be stereochemically controlled to refine the rate

of formation with release of the active peptide. Lastly, they can also be prepared from readily available alpha-amino acids using established chemistry⁷².

As shown below (Figure 6A and 6B), prodrugs of varying half lives were designed by modifying R1 and R2. In the reaction below, there is an N-terminal histidine residue (native peptide), and an amide bond is being broken (Figure 6A). In the second equation, the ester bond of phenyllactic acid (hydroxyl phenylalanine) is being broken (Figure 6B). Though it might be beneficial to use the histidine in the 7th position of GLP, alternatives to the native N-terminal histidine were utilized for synthetic and analytical ease. Once the chemistry of a longer-acting prodrug is established, it is plausible to return to the histidine or for that matter any other suitably potent amino acid at the N-terminus.

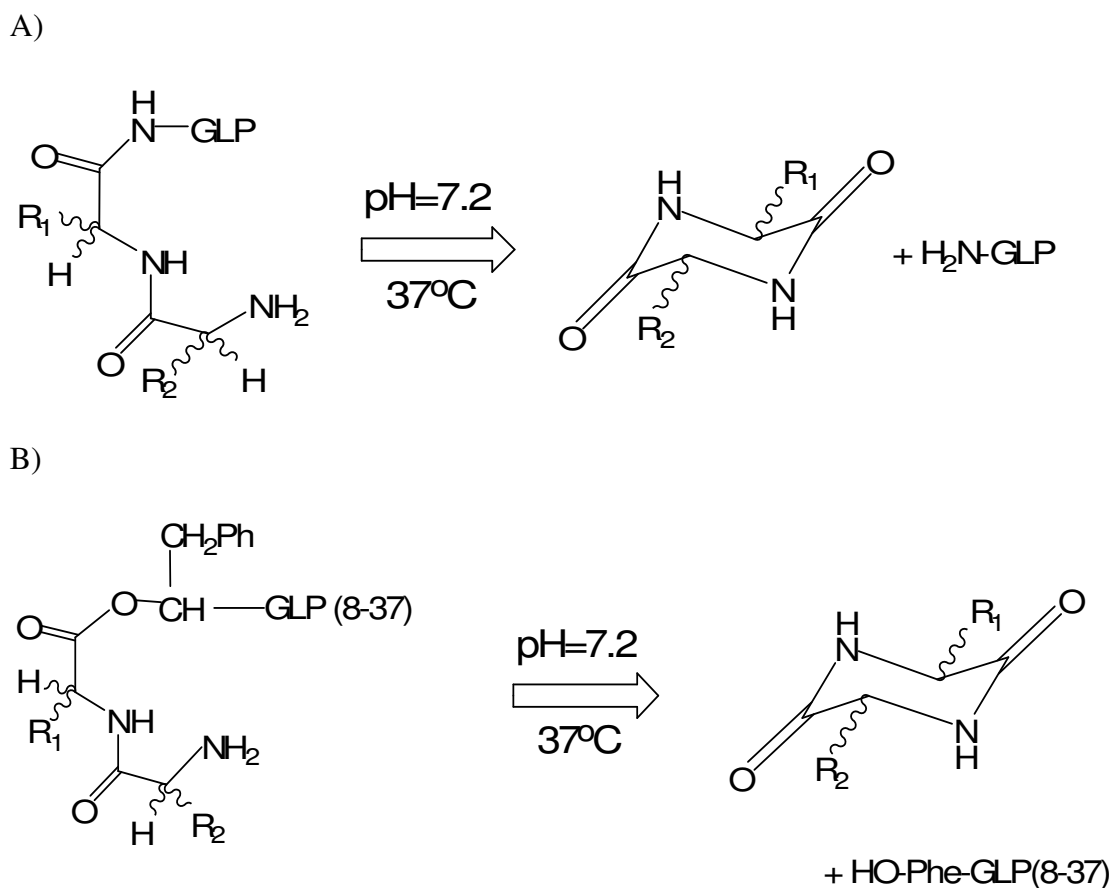


Figure 6: Cleavage of amide (A) and ester prodrugs (B)

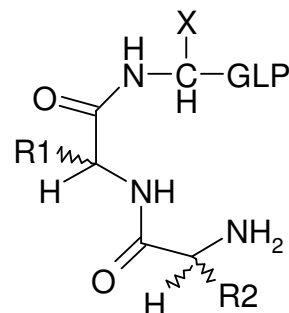
Thus, we propose to make a prodrug that will slowly convert ($t_{1/2}$ between 10-100 hrs) to the parent drug at physiological conditions of 37°C and pH 7.2 so that they could be administered at a weekly or monthly frequency. As far as possible, a native sequence shall be used in the prodrug so as to minimize the chances of an immunological response. We rely on the pH and the temperature for this intramolecular conversion, as they are virtually invariant. It is of essence to note that this reaction should be concentration independent.

Four such peptides were identified with protracted half lives, with minimal potency as compared to the drug in the luciferase-based bioassay. These prodrugs

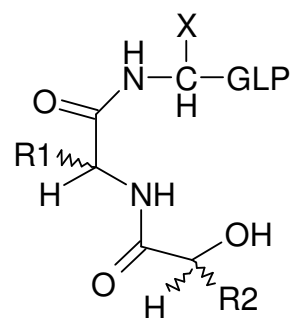
regained their potencies after incubation in PBS buffer at a pH of 7.2 and temperature of 37°C.

Prodrugs of this thesis can be broadly classified into 4 different types of prodrugs:

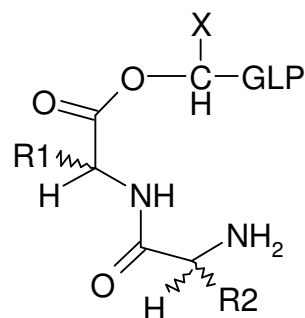
1. An amine nucleophile cleaving an amide bond (Class 1): This will dissociate with the formation of the corresponding 2,5-diketopiperazine.



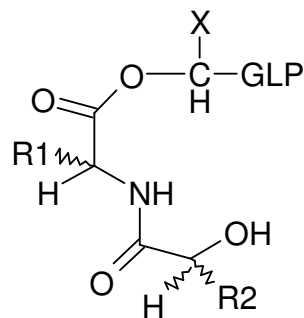
2. A hydroxyl nucleophile cleaving an amide bond (Class 2): This will dissociate with the formation of the corresponding 2,5-diketomorpholine.



3. An amine nucleophile cleaving an ester bond (Class 3): This will dissociate with the formation of the corresponding 2,5-diketopiperazine.



4. A hydroxyl nucleophile cleaving an ester bond (Class 4): This will dissociate with the formation of the corresponding 2,5-diketomorpholine.



The initial analysis was performed with the crude peptides. The rate of this reaction was not different from the pure peptides as this is an intramolecular cyclization. Additionally, it is also possible to observe our molecules of interest (both the prodrug and the drug) with a HPLC and MALDI analysis even in the midst of contaminating material. In most cases, an excellent mass balance for the disappearance of the prodrug and the appearance of the drug was observed. After we were satisfied that the crude prodrug had the required $t_{1/2}$, the prodrug was purified and a standard luciferase-based bioassay was conducted to obtain relative potencies.

The experimental design of our bioassay was based on the general principles of “reporter gene technology”⁷³ (Figure 7). In our case, the luciferase-based reporter gene assay for cAMP detection was used. The changes in the intracellular cAMP concentrations⁷⁴ caused by the GLP receptor-mediated interactions are detected by the changes in the expression level of the luciferase gene. The transcription of this gene is regulated by the cAMP response-element binding protein (CREB) binding to cAMP response element (CRE).

This is an artificially created test system where the luciferase gene is downstream to the CRE which resembles nature’s response system all the way up to the point of gene expression where the luciferase gene is expressed. This modification is necessary as the concentration of activated luciferase is easier to measure than that of cAMP.

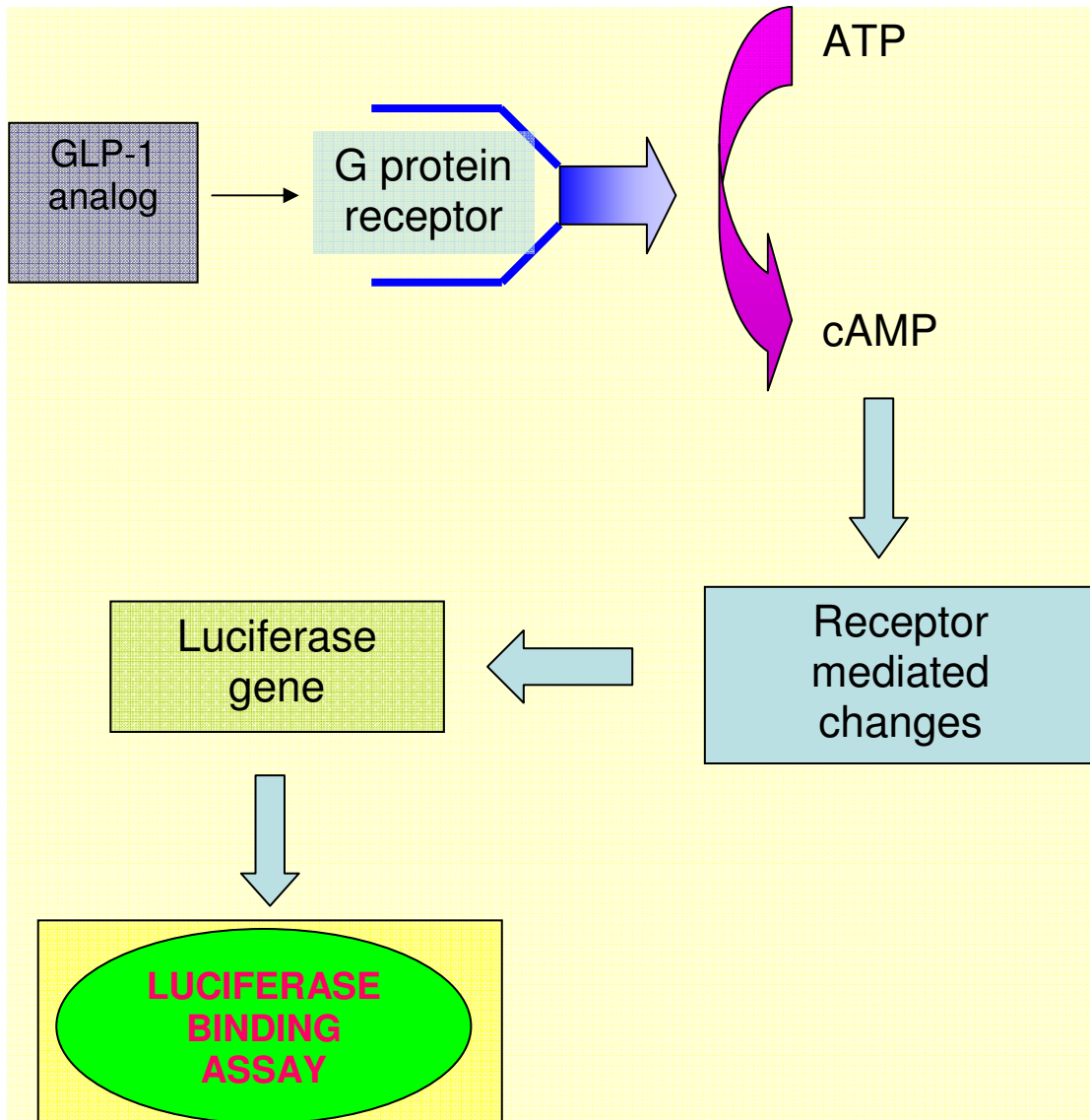


Figure 7: Pictorial Explanation of luciferase-based reporter gene assay

C) Experimental Procedure: *Synthesis of GLP analogs*

In this project, numerous GLP analogs were synthesized. The standard procedure is described briefly here, and the details are discussed later.

PAM resin (PAM resin is OCH₂phenylacetamidomethyl–copolystyrene-1% divinylbenzene), (100-180 mesh, 1% DVB cross-linked polystyrene; loading of 0.7-1.0mmol/g), Boc-protected and Fmoc protected amino acids were purchased from Midwest Biotech. Other reagents such as the α -hydroxy-acids (phenyllactic acid and glycolic acid) were purchased from Aldrich. The solid phase peptide syntheses using Boc-protected amino acids were performed on an Applied Biosystem 430A Peptide Synthesizer⁷⁵. Fmoc protected amino acid synthesis was performed using the Applied Biosystems Model 433 Peptide Synthesizer. The manual synthesis of depsi-peptides was performed in sintered reaction vessels using analogous procedures^{75,76}.

I) Peptide synthesis (Boc amino acids/ HF cleavage):

The bulk of the synthesis was accomplished by using this method (Figure 8A).

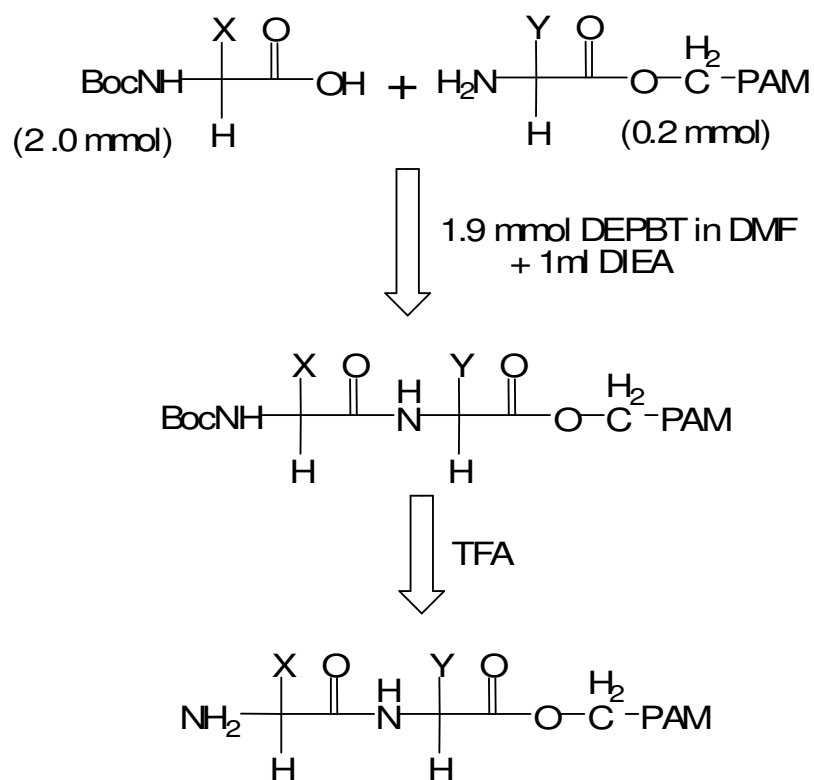


Figure 8A: Peptide synthesis (Boc method)

Synthesis of these analogs was performed on the Applied Biosystem Model 430A Peptide Synthesizer. Synthetic peptides were constructed by sequential addition of amino acids, and activated esters of each amino acid were generated by the addition of 1.9mmol (3.8 ml of a 0.5M solution) of 3-(Diethoxy-phosphoryloxy)-3H-benzo[d][1,2,3] triazin-4-one (DEPBT) in DMF to a cartridge containing 2mmol of Boc protected amino acid. The amino acids were dissolved by bubbling Nitrogen gas through the cartridge. 1 ml of N,N-Diisopropylethylamine was added to the cartridge to effect ester formation. This solution was transferred to the reaction vessel containing the 0.2 mmol of the C-terminal residue attached to the PAM resin, vortexed several times, and allowed to couple to the resin for

10 minutes. After washing to remove the unreacted reagents, the N-terminal Boc protecting group was removed by treatment with trifluoroacetic acid (TFA) for 5 minutes. The resin was washed with DMF and the cycle was repeated for the desired number of steps until the chain was assembled. The reaction vessel at the end of the synthesis (typically 30 amino acids) contained approximately 1.2-1.5g of protected peptidyl-PAM resin. The resin was washed numerous times with dimethylformamide (DMF), treated with trifluoroacetic acid to remove the last tBoc protecting group and finally washed several additional times with DMF, dichloromethane (DCM) and dried.

The peptidyl-resin was treated with anhydrous HF (procedure explained later in this section), and this typically yielded approximately 350 mg (~50% yield) of a crude deprotected-peptide.

II) Peptide synthesis (Fmoc amino acids/ HF cleavage):

This synthesis scheme was performed manually with a few amino acids at selective sites. In this work, the Fmoc amino acids were used only to synthesize the internal serine prodrugs, as a part of a wider synthetic strategy. Here, it is to be noted that although Fmoc chemistry has been used in the synthesis, the peptides have always been built on PAM resin that required treatment with HF to cleave the peptide from the solid support. The yield of these peptides is approximately as stated earlier for Boc/PAM synthesis.

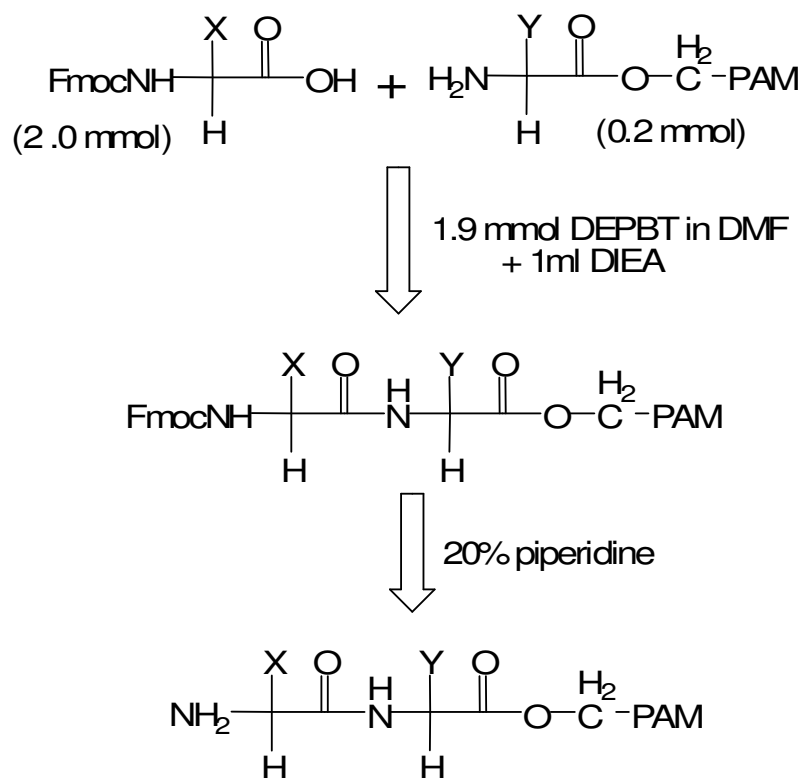


Figure 8B: Peptide synthesis (Fmoc method)

The synthesis was carried out as described in the previous section. At the end of the coupling step, the peptidyl-resin was treated with 20% piperidine to remove the N-terminal Fmoc protecting group. It was washed repeatedly with DMF and this repetitive cycle was repeated for the desired number of coupling steps. The peptidyl-resin at the end of the entire synthesis was dried by using DCM, and the peptide was cleaved from the resin with anhydrous HF.

III) Depsi-peptide synthesis (Amino ester formation):

These syntheses⁷⁶ were performed manually (Figure 9). In this case, the peptidyl-resin had an α -hydroxyl-N terminal extension instead of a N-terminal amine and the acylation was done at the α hydroxyl group. This reaction takes a longer time than that of the amide bond formation, as the hydroxyl group is a weaker nucleophile as compared to the amine. The reaction time was typically 12 hours.

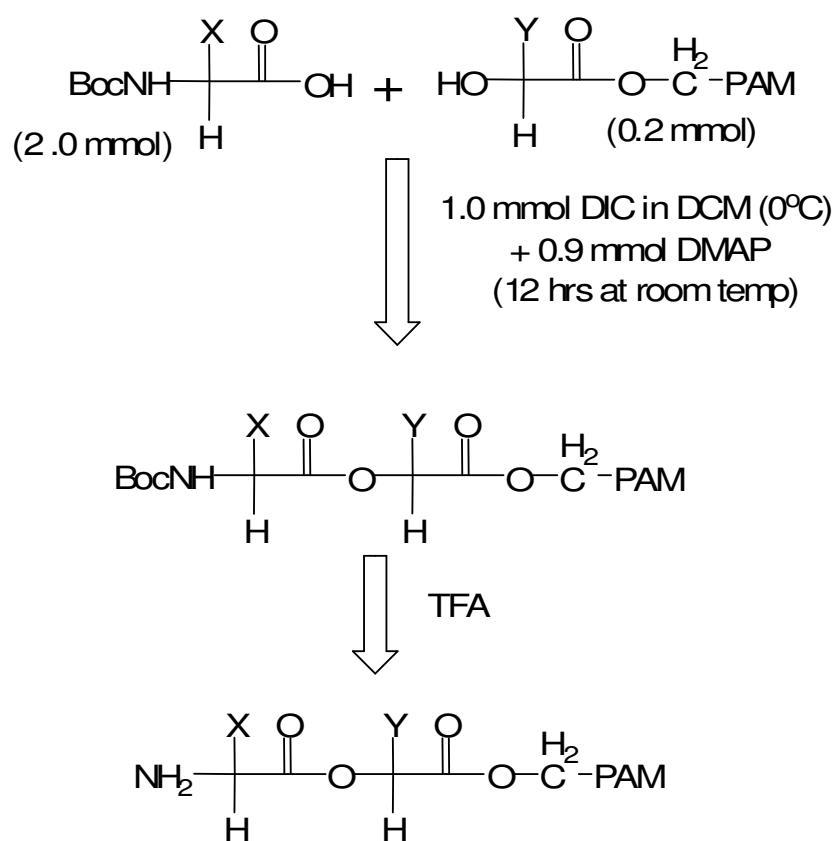


Figure 9: Depsi-peptide synthesis (Amino ester formation)

Initially, the activated esters of each amino acid were generated by the addition of 1mmol (0.155 ml of Diisopropylcarbodiimide (DIC) to a cartridge containing a solution

of 2mmol of Boc protected amino acid residue in 2 ml DCM. This was cooled to 10°C for 10 minutes. 0.9 mmol (244 mg) of dimethylaminopyridine (DMAP) was added to the cartridge to accelerate ester formation. This mixture was transferred to the reaction vessel containing the peptidyl-resin upon which the peptide was synthesized. The reaction vessel was stirred for 12 hours.

The peptidyl-resin was dried using DCM and the synthesis of the desired peptide was continued. The peptidyl-resin at the end of the entire synthesis was dried by using DCM, and finally treated with anhydrous HF to generate the desired peptide.

IV) N-terminal hydroxyl peptide synthesis (α hydroxyl- N terminal extension)⁷⁴:

In this reaction, the free amine of the peptidyl-resin reacts with an α hydroxyl acid to form an α hydroxyl- N terminal extension (Figure 10).

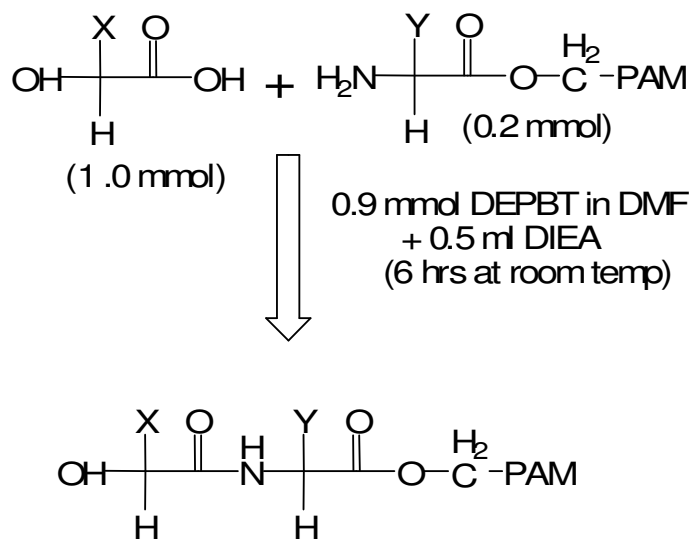


Figure 10: α hydroxyl- N terminal extension

In this regard, only two such α hydroxyl acids were used namely, glycolic acid (OH-glycine) and phenyllactic acid (OH-phenylalanine). These syntheses were also performed manually. The peptides were constructed by addition of the α hydroxyl acid, and activated esters of the α hydroxyl acid were generated by the addition of 0.9mmol of DEPBT (270 mg) to a cartridge containing a solution of 1mmol of Boc protected residue in 2 ml DMF. 0.5 ml of DIEA (N, N-Diisopropylethylamine) was added to the cartridge to accelerate ester formation. This mixture was transferred to the reaction vessel containing the peptidyl-resin upon which the peptide was synthesized. The reaction time was 6 hours.

The peptidyl-resin was dried using DCM and the synthesis of the desired peptide was continued. The peptidyl-resin at the end of the entire synthesis was dried by using DCM, and cleaved by anhydrous HF to generate the free peptide.

V) HF treatment of the peptidyl-resin:

The peptidyl-resin (30mg to 200mg) was placed in the hydrogen fluoride (HF) reaction vessel for cleavage. 500 μ L of p-cresol was added to the vessel as a carbonium ion scavenger. The vessel was attached to the HF system and submerged in the methanol/dry ice mixture. The vessel was evacuated with a vacuum pump and 10ml of HF was distilled to the reaction vessel. This reaction mixture of the peptidyl-resin and the HF was stirred for one hour at 0°C, after which a vacuum was established and the HF was quickly evacuated (10-15 min). The vessel was removed carefully and filled with approximately 35 ml of ether to precipitate the peptide and to extract the p-cresol and small molecule organic protecting groups resulting from HF treatment. This mixture was

filtered utilizing a teflon filter and repeated twice to remove all excess cresol. This filtrate was discarded. The precipitated peptide dissolves in approximately 20ml of 10% acetic acid (aq). This filtrate, which contained the desired peptide, was collected and lyophilized.

VI) Analysis using mass spectrometry:

The mass spectra were obtained using a Sciex API-III electrospray quadrupole mass spectrometer with a standard ESI ion source. Ionization conditions that were used are as follows: ESI in the positive-ion mode; ion spray voltage, 3.9 kV; orifice potential, 60 V. The nebulizing and curtain gas used was nitrogen flow rate of .9L/min. Mass spectra was recorded from 600-1800 Thompsons at 0.5 Th per step and 2msec dwell time. The sample (about 1mg/mL) was dissolved in 50% aqueous acetonitrile with 1% acetic acid and introduced by an external syringe pump at the rate of 5 μ L/min.

When the peptides were analyzed in PBS solution by ESI MS, they were first desalted using a ZipTip solid phase extraction tip containing 0.6 μ L C4 resin, according to instructions provided by the manufacturer. (<http://www.millipore.com/catalogue.nsf/docs/C5737>)

VII) High Pressure Liquid Chromatography (HPLC) analysis:

Preliminary analyses were performed with these crude peptides to get an approximation of their relative conversion rates in Phosphate Buffered Saline (PBS) buffer (pH, 7.2) using high performance liquid chromatography (HPLC) and MALDI analysis. The crude peptide samples were dissolved in the PBS buffer at a concentration

of 1mg/ml. 1ml of the resulting solution was stored in a 1.5ml HPLC vial which was then sealed and incubated at 37°C. Aliquots of 100µl were drawn out at various time intervals, cooled to room temperature and analyzed by HPLC.

The HPLC analyses were performed using a Beckman System Gold Chromatography system using a UV detector at 214 nm. HPLC analyses were performed on a 150mm x 4.6mm C18 Vydac column. The flow rate was 1ml/min. Solvent A contained 0.1% TFA in distilled water, and solvent B contained 0.1% TFA in 90% CH₃CN. A linear gradient was employed (40% to 70%B in 15 minutes). The data was collected and analyzed using Peak Simple Chromatography software.

The initial rates of hydrolysis were used to measure the rate constant for the dissociation of the respective prodrugs. The concentrations of the prodrug and the drug were estimated from their peak areas respectively. The first order dissociation rate constants of the prodrugs were determined by plotting the logarithm of the concentration of the prodrug at various time intervals. The slope of this plot gives the rate constant 'k'. The half lives of the degradation of the various prodrugs were then calculated by using the formula $t_{1/2} = .693/k$.

VIII) Preparative purification using HPLC:

After we were satisfied that the prodrug had an appropriate $t_{1/2}$, the prodrug was purified. The purification was performed using HPLC analysis on a silica based 1 x 25cm Vydac C18 (5µ particle size, 300Å° pore size) column. The instruments used were: Waters Associates model 600 pump, Injector model 717, and UV detector model 486. A wavelength of 214 nm was used for all samples. Solvent A contained 10% CH₃CN /0.1%

TFA in distilled water, and solvent B contained 0.1% TFA in CH₃CN. A linear gradient was employed (0 to 100%B in 2 hours). The flow rate is 1.2ml/min and the fraction size was 6ml. From ~350 mgs of crude peptide, 80 mgs of the pure peptide (~23% yield) was typically obtained.

IX) Bioassay Experimental Design: Luciferase-based reporter gene assay for cAMP detection

The ability of each GLP analog or prodrug to induce cAMP was measured⁷⁷ in a firefly luciferase-based reporter assay (Figure 7). The cAMP production that is induced is directly proportional to the GLP binding to its receptor. HEK293 cells co-transfected with the GLP receptor and luciferase gene linked to cAMP responsive element were employed for bioassay.

The cells were serum-deprived by culturing 16 hours in Dulbecco Minimum Essential Medium (Invitrogen, Carlsbad, CA) supplemented with 0.25% Bovine Growth Serum (HyClone, Logan, UT) and then incubated with serial dilutions of either GLP analogs or prodrugs for 5 hours at 37°C, 5% CO₂ in 96 well poly-D-Lysine-coated “Biocoat” plates (BD Biosciences, San Jose, CA). At the end of the incubation, 100 µL of LucLite luminescence substrate reagent (Perkin Elmer, Wellesley, MA) were added to each well. The plate was shaken briefly, incubated 10 min in the dark and light output was measured on MicroBeta-1450 liquid scintillation counter (Perkin-Elmer, Wellesley, MA). The effective 50% concentrations (EC₅₀) were calculated by using Origin software (OriginLab, Northampton, MA).

D) Experimental Results and Discussion

I) *GLP-Oxyntomodulin*

The GLP-oxyntomodulin chimeric peptide shown below was synthesized. The last eight amino acids were derived from oxyntomodulin and are shown in red.

HAEGTFTSDVSSYLEGQAAKEFIAWLVKGRGKRNRNNIA

The rationale behind synthesizing this chimeric peptide is two fold. First, to demonstrate that a peptide of a mass of around 4300 Da could be synthesized. Second, if this peptide is biologically potent, then a GLP analog with an extended C-terminus could be used for any future modification that might be required. This peptide has a mass of 4322.5 Daltons (Figure 11A). In this way, the synthesis of GLP-oxyntomodulin was confirmed. The receptor binding activity of GLP-oxyntomodulin was determined in the GLP-receptor Luciferase assay (Figure 11B).

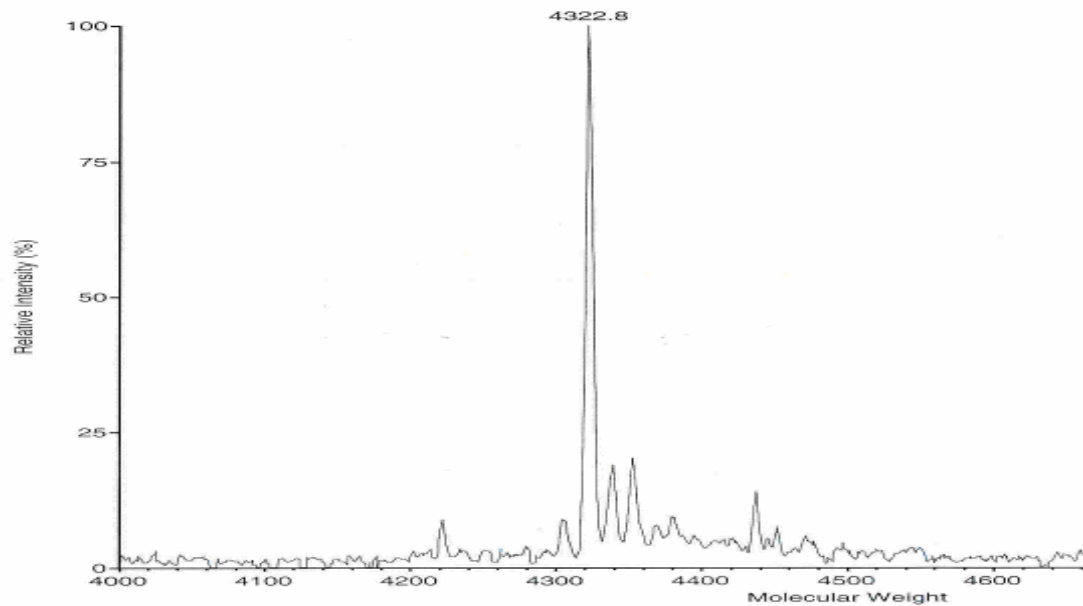


Figure 11A: Mass spectra of purified GLP-oxyntomodulin chimeric peptide.

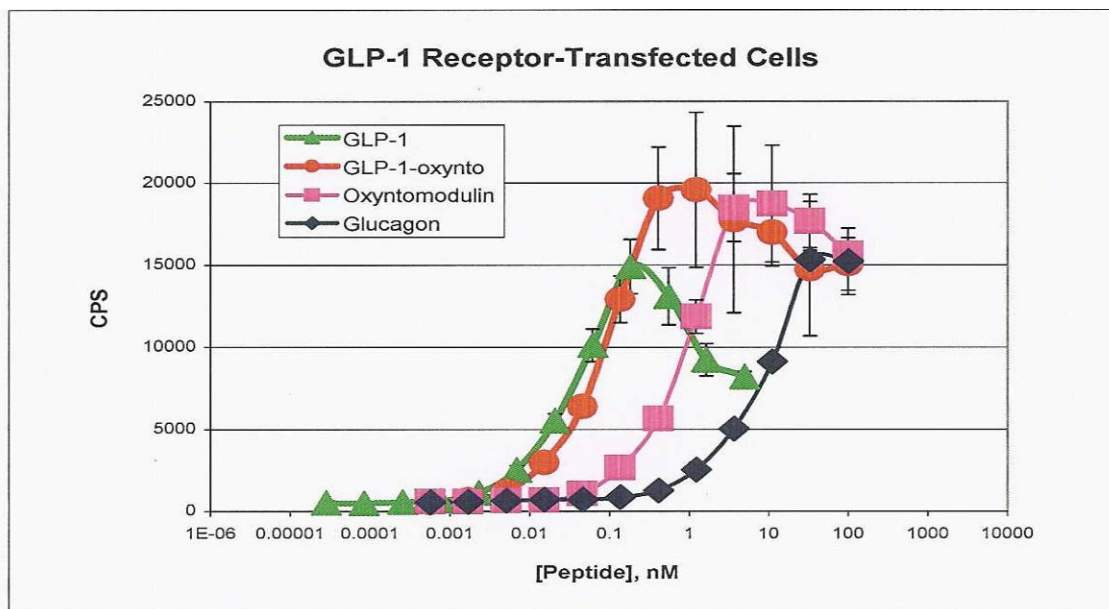


Figure 11B: Bioassay results of GLP-oxytomodulin chimeric peptide

The GLP-oxytomodulin was found to be at least as potent as the native GLP peptide in the luciferase assay. The GLP-oxytomodulin also has a higher apparent maximal efficacy as compared to GLP (Figure 11B). This observation warrants additional study as the less potent oxyntomodulin also demonstrated super-efficacy. This signifies that the first portion of the project is successful and we focused on the central element of this study, specifically the N-terminal prodrug design.

II) Adding dipeptides to the N terminus

Dipeptides were covalently attached to the N-terminus of GLP (sequence in Figure 3B) to study differential tendencies for intramolecular cyclization and cleavage through diketopiperazine formation. This is represented schematically in Figure 12A. All class I prodrugs were synthesized by analogous procedures.

The biologically inactive dipeptide-extended GLP was converted to the active GLP upon cleavage of the amide bond along with the DKP (Figure 12B and Table 2). In Figure 12C (Table 3 and 4), the same conversion is shown with the phenylalanine in the 1st position of GLP. Prodrugs of varying half lives were envisioned by chemically modifying the R1 and R2 positions. This validates our reason for probing the DKP formation strategy.

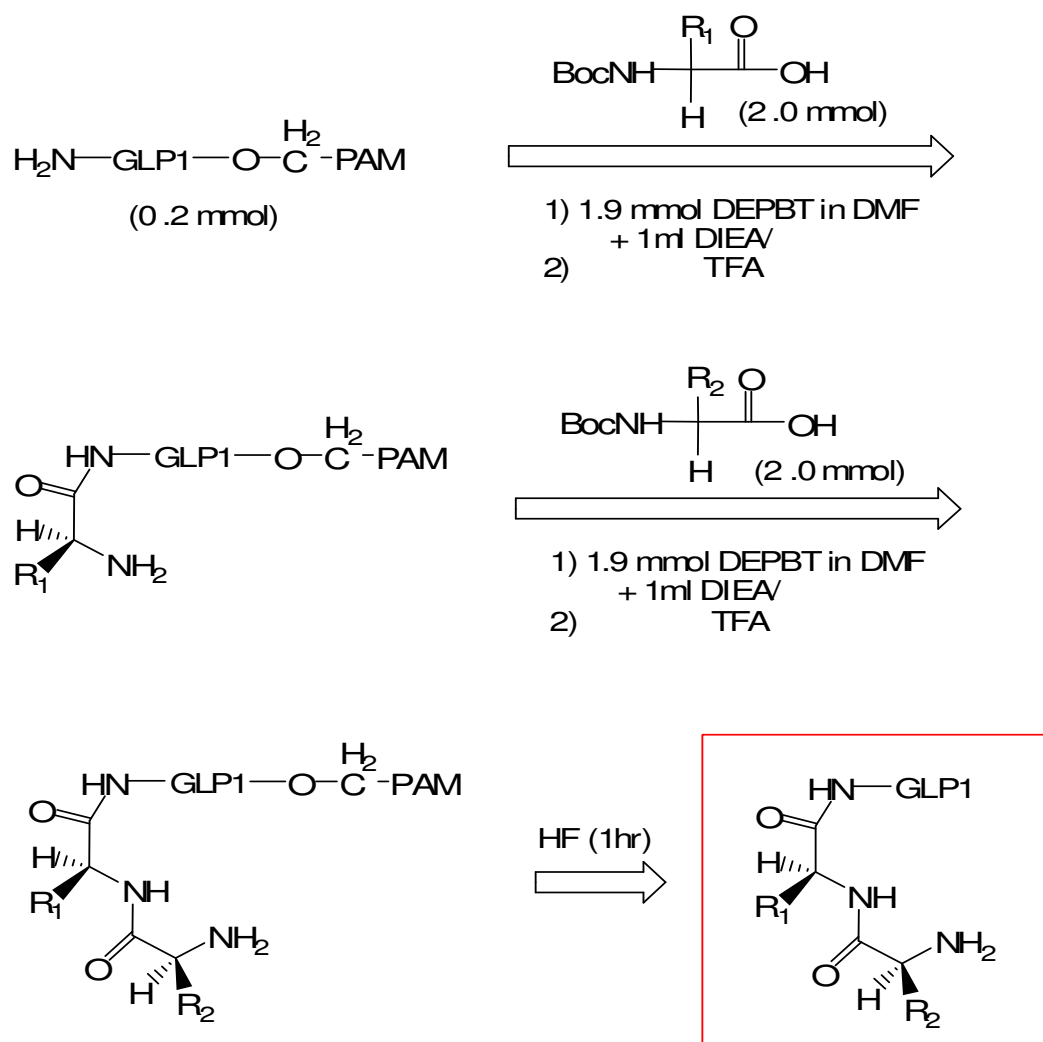


Figure 12A: Schematic synthesis of Class I prodrugs

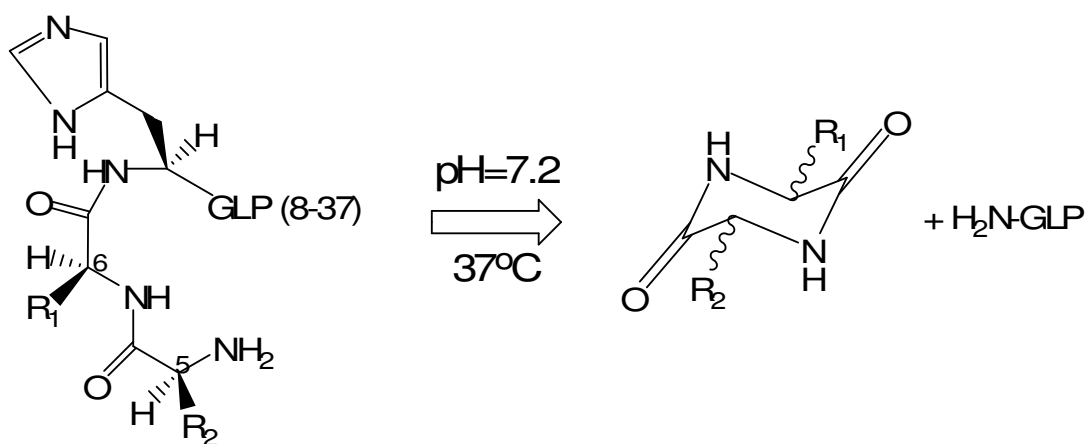


Figure 12B: Cleavage of amide bond to form DKP + H⁷,GLP(8-37)

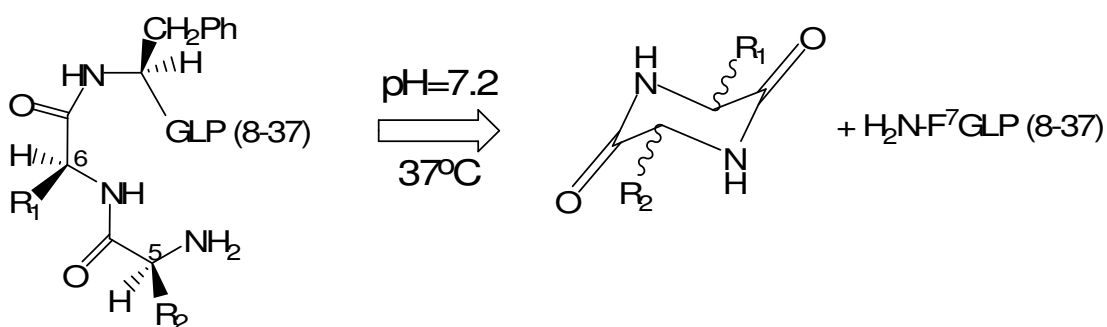


Figure 12C: Cleavage of amide bond to form DKP + F⁷,GLP(8-37)

The results of the cleavage in the prodrugs are shown in Table 2. The first peptide synthesized was named G⁵P⁶H⁷,GLP(8-37) where the R1 is the side chain for proline and R2 refers to the side chain for glycine (peptide 1 in Table 2). All peptides mentioned hereafter will have the same systematic nomenclature and the stereochemistry was assumed to be the l-isomer unless otherwise stated. The peptide was prepared synthetically by solid phase synthesis as described earlier. The synthesis was confirmed by MALDI-MS analysis (3509.5 Da) as shown in Figure 13.

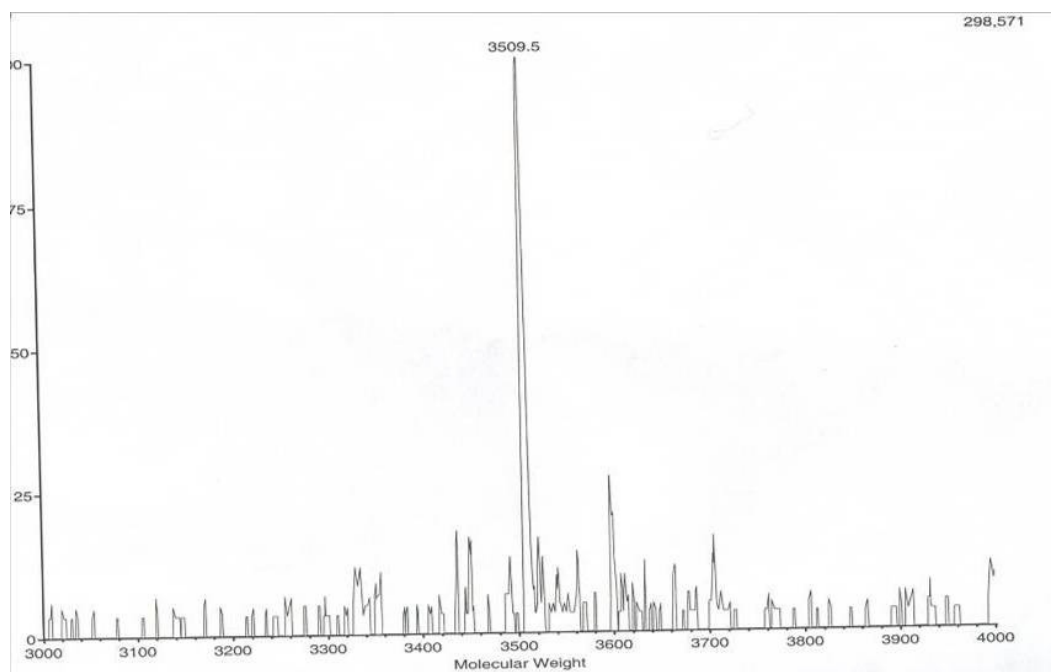


Figure 13: Mass spectra of $G^5P^6H^7$,GLP(8-37)

To explore the possible formation of DKP, and simultaneous regeneration of the H^7 ,GLP(8-37), the $G^5P^6H^7$,GLP(8-37) was incubated in PBS buffer at 37°C for approximately a week. Additionally, the peptide was heated at 100°C to accelerate the amide bond cleavage. Analysis by reverse phase HPLC showed no apparent cleavage of the amide bond in this first set (Table 2). The structures of the peptides in Table 2 are illustrated in Appendix II.

To investigate the propensity of various prodrugs to undergo DPK formation, all subsequent peptides were similarly synthesized and analyzed by MS and HPLC following treatment at 100°C and 37°C as described above.

Serial No	Peptide (Xaa ¹ Yaa ² -GLP1)	Rate of cleavage at 100°C	Rate of cleavage at 37°C
1	GP	No cleavage	No cleavage
2	PP	No cleavage	No cleavage
3	γ Glu	No cleavage	No cleavage
4	E	No cleavage	No cleavage
5	P	No cleavage	No cleavage
6	H	No cleavage	No cleavage
7	PH	No cleavage	No cleavage

In 4, 5 and 6, there is just a single amino acid added to the N terminus of GLP-1. In 7, the dipeptide modification was made to sandwich the carbonyl bond of interest between two histidines. In all these cases there is histidine in the 1st position (histidyl leaving group) of GLP-1.

Table 2: Attempted cleavage of H⁷,GLP(8-37) prodrugs to form native GLP-1

The dipeptide extension of peptides 1 and 2 in Table 2 were synthesized to facilitate DPK formation by sterically assisting in the cleavage of the amide bond. It was thought that the cis-orientation of proline would contribute in the facilitation of the dipeptide's adoption of an optimal steric conformation for the formation of DKP. However, the amide bond is quite robust and did not cleave. In peptides 3, 4, 5 and 6, an acid-base catalyzed general hydrolysis of the amide bond was attempted. Since, the leaving group will be the histidine at the N-terminus, it was purported that the imidazole ring might in some way assist in the cleavage by general acid-base catalysis. In 7, the carbonyl bond of interest is sandwiched between two histidines (amino acid Y and the

histidyl leaving group). This design was directed at a proton assisted cleavage of the amide bond via diketopiperazine formation. But even this prodrug did not cleave.

At this point, it was speculated that perhaps the imidazole nucleus was playing an attenuating role in the cleavage of the amide bond. To test this possibility, a different leaving group was studied. F⁷,GLP(8-37) was synthesized and purified using the standard procedure described above. It was determined to be a full agonist with 10% the potency of native GLP. Dipeptides were added to this GLP analog to study the same type of reaction as described above (Table 3; reaction shown in Figure 12C). The structures of the peptides in Table 3 are drawn out in Appendix III.

Serial No	Peptide (Xaa ¹ Yaa ² - F ^{7a} -GLP8-37)	Rate of cleavage at 100°C	Rate of cleavage at 37°C
1	GP	No cleavage	No cleavage
2	GSar ^b	No cleavage	No cleavage

^a: In all these cases there is phenylalanine in the 1st position (phenylalanyl leaving group) of GLP.

^b: Sar represents sarcosine

Table 3: Attempted cleavage of dipeptide extended F⁷,GLP(8-37)

The dipeptide extension of peptides 1 and 2 (Table 3) were designed to sterically assist in the cleavage of the amide bond. In peptide 2, sarcosine was used⁶⁹, as it has been previously reported to enhance the rate of cleavage. However, the amide bond remained resistant to cleavage.

A minor difficulty was encountered at this point. It seemed that the F⁷,GLP(8-37) analogs were not very soluble in PBS at 37°C. Hence, we focused on a modified GLP

analog; GLP(7-36)-CEX amide where the C terminus is a serine amide. The CEX sequence is the C-terminal nine amino acids of exendin-4. The last nine amino acids were derived from exendin-4 and are shown in red.

H⁷AEGTFTSDVSSYLEGQAAKEFIAWLVKGRPSSGAPPPS-
amide

This peptide been observed in our laboratory to be ten times more potent *in vitro* than the native GLP sequence, and its analogs are appreciably soluble in PBS. Throughout this thesis, GLP(7-36)-CEX amide has been denoted simply as GLP(7-36)-CEX with changes added to this nomenclature to signify related peptides.

III) Adding dipeptides to the N terminus of F⁷,GLP(8-36)-CEX

G⁵G⁶F⁷,GLP(8-36)-CEX (class 1) and OH-G⁵G⁶F⁷,GLP(8-36)-CEX (class 2) were synthesized to determine if either of the nucleophiles (amine or hydroxyl) could cleave the amide bond by 2,5-diketopiperazine or 2,5-diketomorpholine formation respectively and thus regenerate the F⁷,GLP(8-36)-CEX. The two compounds are shown below (Figure 14A). The schematic synthesis of the class 2 prodrug is represented in Figure 14B. All subsequent Class II prodrugs were synthesized by analogous procedures.

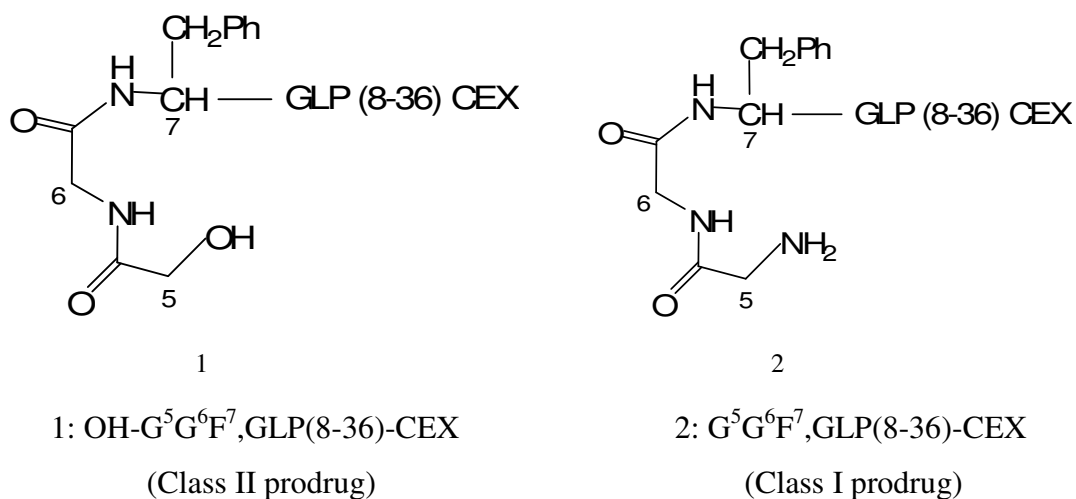


Figure 14A: Dipeptide extended F⁷,GLP(8-36)-CEX

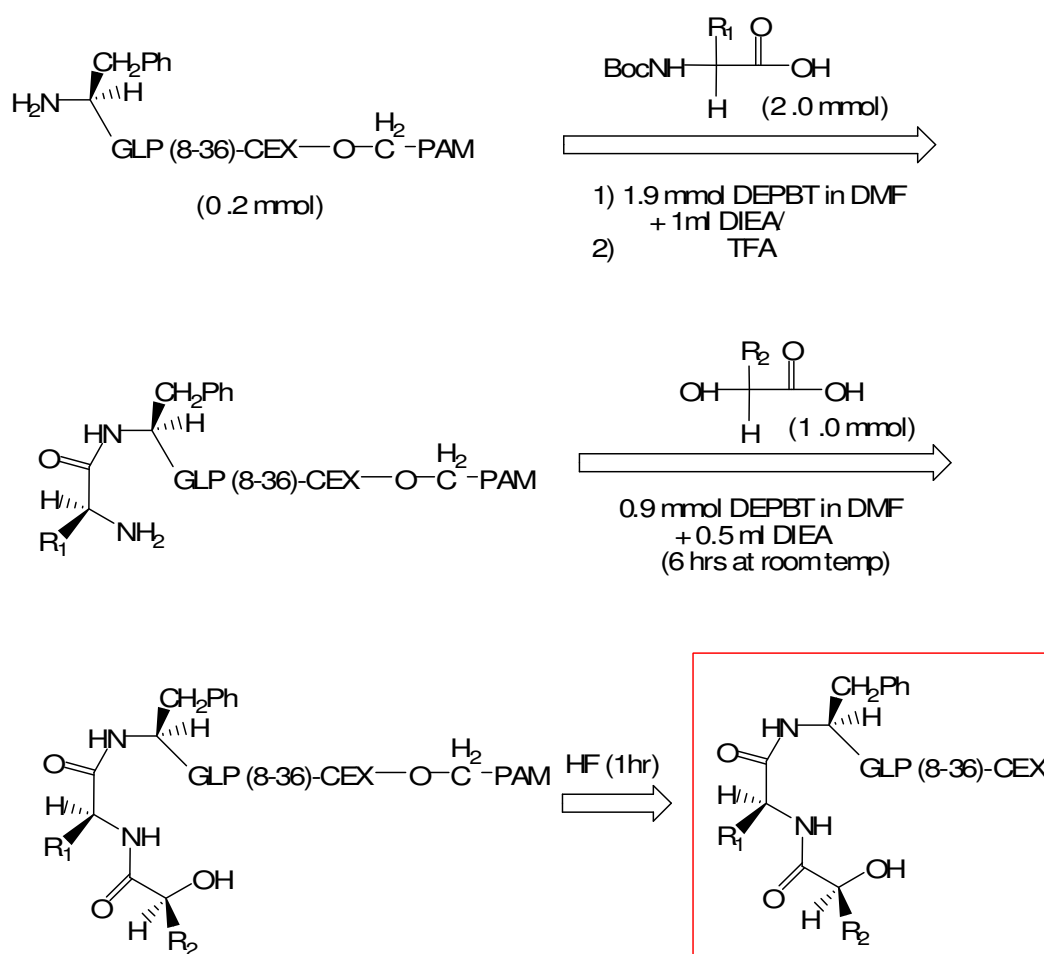


Figure 14B: Schematic synthesis of Class II prodrugs

The analyses of the two peptides after incubation in PBS (Figure 14A and Table 4) showed that neither the amine, nor the hydroxyl nucleophile could cleave the amide bond. The structures of the peptides in Table 4 are also illustrated in Appendix IV (along with the relevant stereochemistry).

Serial No	Peptide (Xaa1Yaa2-F ^{7a} -GLP-CEX)	Rate of cleavage at 100°C	Rate of cleavage at 37°C
1	GG (class 1)	No cleavage	No cleavage
2	HO-GG (class 2)	No cleavage	No cleavage

^a: In all these cases there is phenylalanine in the 1st position (phenylalanyl leaving group) of GLP.

Table 4: Attempted cleavage of dipeptides attached to the N terminus of F⁷,GLP(8-36)-CEX

Representative HPLC analyses of G⁵G⁶F⁷,GLP(8-36)-CEX dissolved in PBS before and after treatment at 100°C for two hours is shown in Figure 15. This analysis was done with the crude peptide. The amide bond did not cleave and the DKP was not generated. This was reflected by the absence of a shift of the HPLC peak in the elution profile of the prodrug to that of the dipeptide-shortened peptide drug F⁷,GLP(8-36)-CEX (not shown here) even when heated at 100°C.

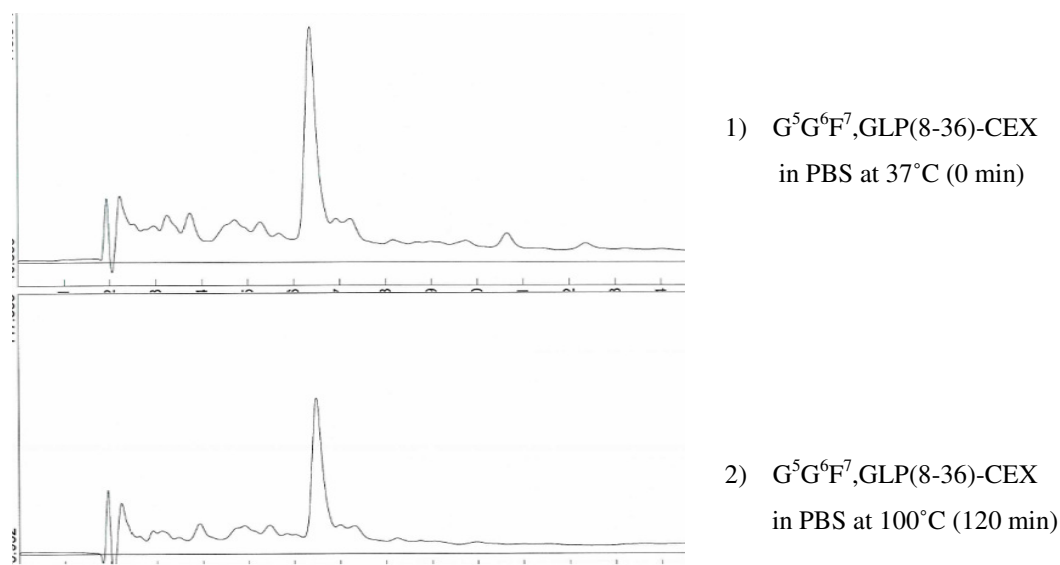


Figure 15: HPLC analysis of $G^5G^6F^7, GLP(8-36)-CEX$

In Table 5, the analyses of two peptides with a glycine at the N-terminal position are shown. These peptides were tested to check the effect of the less bulky glycyll leaving group, as opposed to the previously studied phenylalanine in Table 4. The structures of the peptides in Table 4 are displayed in Appendix V.

Serial No	Peptide (Xaa1Yaa2- G^{7a} - GLP-CEX)	Rate of cleavage at 100°C	Rate of cleavage at 37°C
3	GG (class 1)	No cleavage	No cleavage
4	HO-GG (class 2)	No cleavage	No cleavage

'a': In all these cases there is glycine in the 1st position (glycyll leaving group) of GLP.

Table 5: Attempted cleavage of dipeptides added to the N terminus of $G^7, GLP(8-36)CEX$

Based on the results shown in Table 5, it was concluded that the amide bond is very difficult to cleave under physiological conditions either by 2,5-diketopiperazine (DKP) or 2,5-diketomorpholine (DMP) formation. This is independent of the nucleophiles and leaving groups tested, even under elevated temperature. The focus of this study then moved to esters which were anticipated to be easier to cleave as compared to the amides.

IV) Depsi-peptides and Esters

Depsi-peptides were synthesized through addition of dipeptides to the hydroxyl group at the N terminus of another peptide via an ester linkage (Figure 9). The coupling procedures are described in the experimental section and they proved highly effective. As before, dipeptides of differential tendency for intramolecular cyclization (diketopiperazine formation) and release of the parent drug (N-terminal hydroxyl peptide) were studied. While adding the dipeptide, both Class 3 (an amine nucleophile cleaving an ester bond) and Class 4 (a hydroxyl nucleophile cleaving an ester bond – Figure 10) compounds were prepared and studied.

The initial work began with imidazole-lactic acid (OH-His) as the terminal amino acid and subsequent leaving group. The HO-His⁷,GLP(8-37) was synthesized. It was a full agonist with 25% the potency of native GLP-1. There were several attempts to add a dipeptide to the α hydroxyl group of HO-His⁷,GLP(8-37) and test for the cleavage of the new ester bond. However, there was a problem in selectively acylating the α -hydroxyl group of this peptide. As “protected” imidazole lactic acid was not commercially available, we decided initially to work with the compound where the imidazole group

was unprotected. As a result, the “unprotected imidazole” was inadvertently acylated along with the hydroxyl group. A synthetic scheme for the preparation of HO-His⁷,GLP(8-37), its subsequent acylation and the formation of multiple side-products is depicted in Appendix VIII.

Consequently, Phenyllactic acid (OH-phenylalanine) was chosen in this initial test as it was readily available, and the return to a protected HO-His would be conducted if the work with HO-Phe proved successful.

V) Adding dipeptides to the OH terminus of HO-F⁷,GLP(8-36)-CEX

The HO-F⁷,GLP(8-36)-CEX peptide was synthesized from the GLP(8-36)-CEX PAM resin (the synthetic scheme is represented in Figure 16A) and served as the parent drug for these experiments. This peptide has an EC₅₀ value of 0.008nM (gold color in Figure 16B) while native GLP has an EC₅₀ value of 0.011nM. Therefore, the HO-F⁷,GLP(8-36)-CEX was found to be at least as potent as the native GLP-1. This is a most important and a somewhat unexpected observation that the histidine can be substituted by phenyllactic acid. This warranted additional validation. Subsequent experiments yielded identical results. The possibility exists that this result is a function of the CEX extension in the HO-F⁷,GLP(8-36)-CEX. In this regard, it has been reported that the C-terminal region of exendin-4 increases its affinity to the GLP receptor⁷⁸.

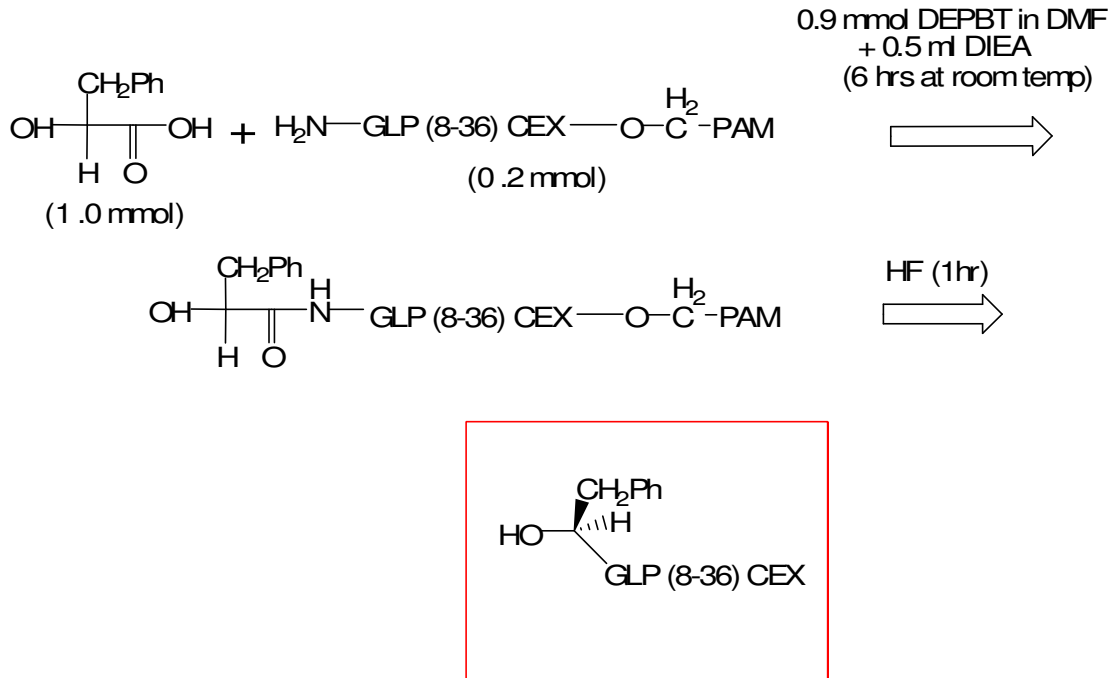


Figure 16A: Schematic synthesis of HO-F⁷,GLP(8-36)-CEX

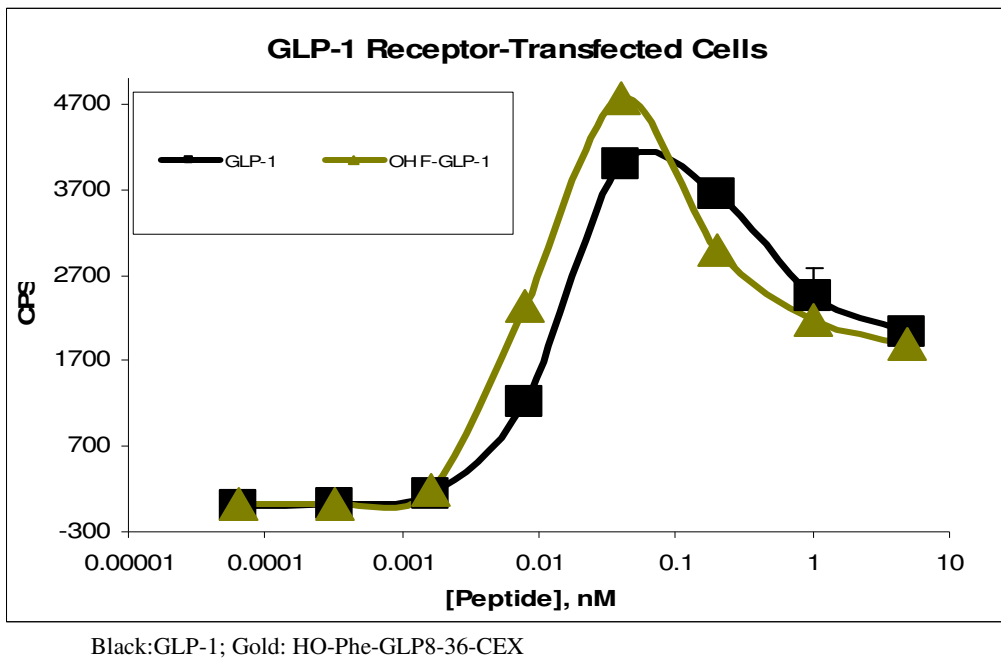


Figure 16B: Bioassay results of HO-F⁷,GLP(8-36)-CEX

The α hydroxyl group of HO-F⁷,GLP(8-36)-CEX was acylated and both Class 3 (an amine nucleophile cleaving an ester bond; Figure 17A) and Class 4 (a hydroxyl nucleophile cleaving an ester bond; Figure 17B) compounds were prepared and studied. Along with the 2,5-diketopiperazine (amine nucleophile) or 2,5-diketomorpholine (hydroxyl nucleophile), the biologically active HO-F⁷,GLP(8-36)-CEX is released as shown in Figure 17C.

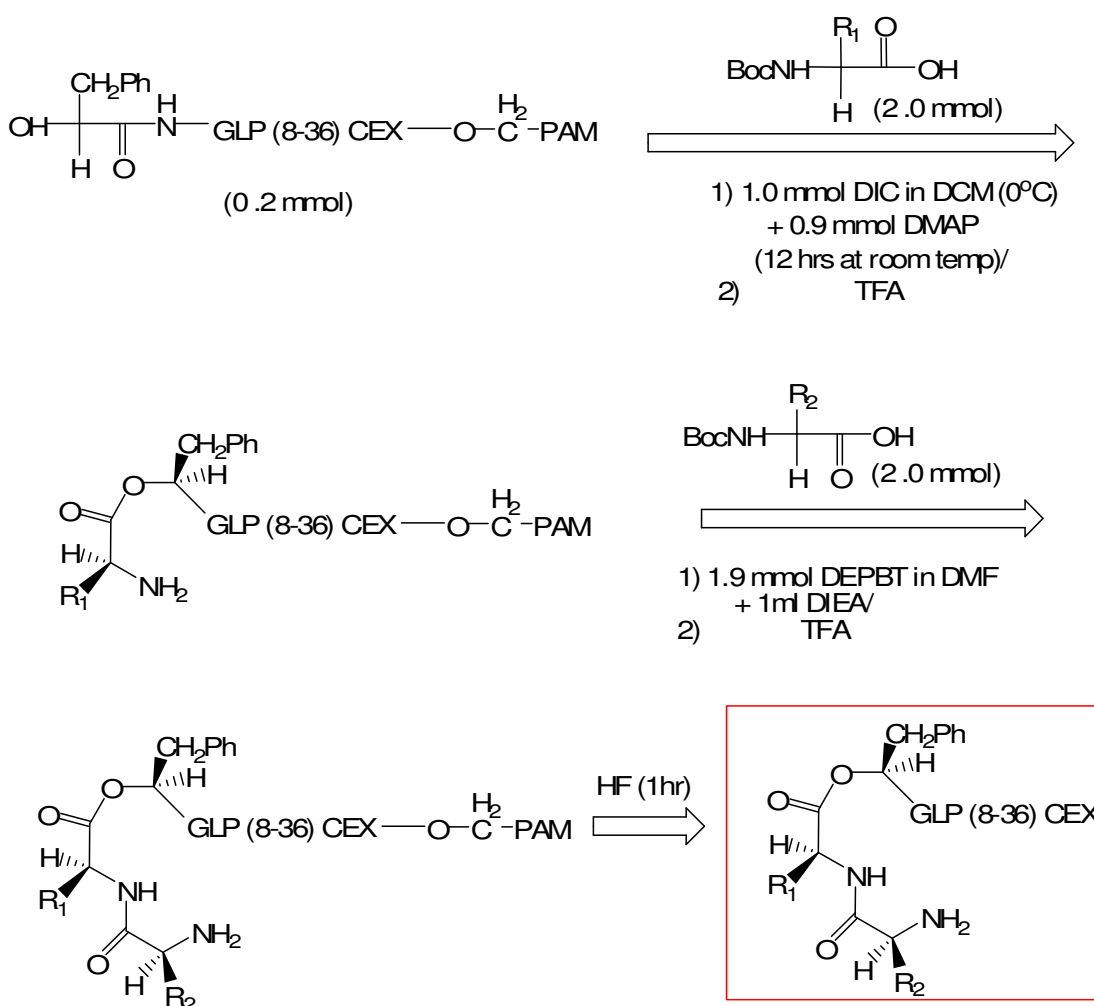


Figure 17A: Schematic synthesis of Class III prodrugs

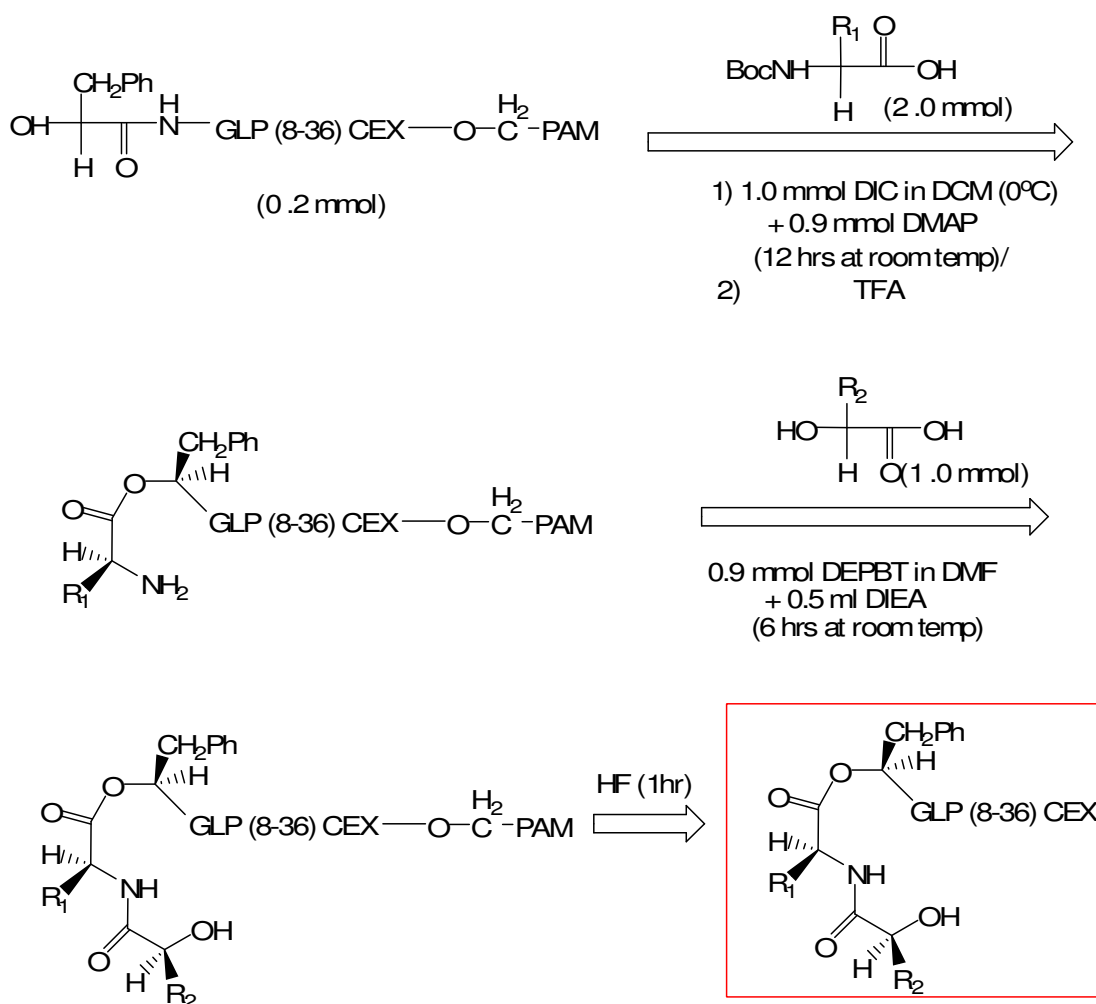
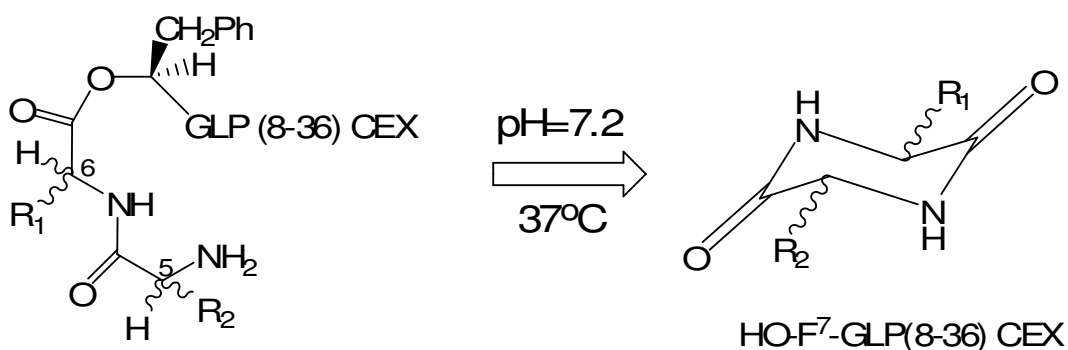


Figure 17B: Schematic synthesis of Class IV prodrugs

A) Amine cleaving ester (Class 3):



B) Hydroxyl cleaving ester (Class 4):

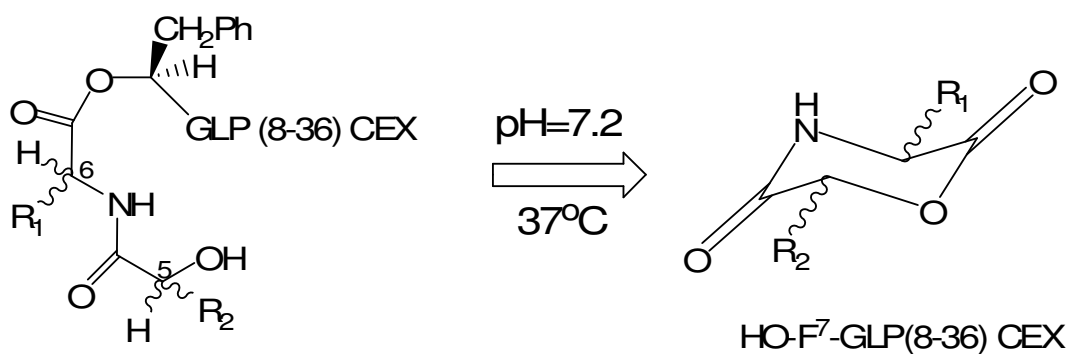


Figure 17C: Cleavage of A) Class III and B) Class IV prodrugs

To explore the possible formation of 2,5-diketopiperazine (DKP) or 2,5-diketomorpholine (DMP) and the simultaneous generation of HO-F⁷,GLP(8-36)-CEX, the prodrug was incubated in PBS buffer at 37°C for approximately a week. The peptide was also heated at 100°C to determine the susceptibility to cleavage (Table 6). The structures of the peptides in Table 6 are illustrated in Appendix VI.

Serial No	Peptide (Yaa1Xaa2-O-Phe ⁷ -GLP-8-36-CEX)	t _{1/2} * of cleavage at 37°C
1	Gly-Gly (class 3)	0.87 hrs
2	HO-Gly-Gly (class 4)	1.13 hrs
3	HO-Phe-Val (class 4)	No cleavage
4	HO-Phe-dVal (class 4)	50.58 hrs
5	HO-Phe-Ala (class 4)	2.83 hrs
6	HO-Phe-dAla (class 4)	2.41 hrs
7	HO-Phe-Gly (class 4)	2.46 hrs
8	HO-Phe-Phe (class 4)	33.31 hrs
9	HO-Phe-dPhe (class 4)	7.65 hrs
10	Phe-Val (class 3)	64.0 hrs

* t_{1/2} is the time required for 50% release of the HO-Phe-GLP8-36-CEX at 37°C in PBS (pH7.2). It is calculated by a standard first order reaction plot. All these esters, including #3 cleaved at 100°C. In all these cases, there is HO-Phe in the 1st position (hydroxy phenylalanyl leaving group) of GLP.

Table 6: Cleavage of dipeptide extended HO-F⁷,GLP(8 36)-CEX

The first two peptides shown in Table 6 (Peptides 1 and 2) were analyzed to determine if either of the nucleophiles (amine or hydroxyl) could cleave the ester bond by DKP or DMP formation respectively. The results validated our expectation that the esters are more susceptible to cleavage than the amides. The relatively slower rate of cleavage of peptides 3, 4, 8, 9 and 10 seem to suggest that the bulk of the dipeptide extensions (Phe or Val) greatly affect the rate of dissociation of the prodrug. While there is virtually no difference between a methyl and a hydrogen side chain (5, 6 and 7), the presence of an isopropyl group (β branching) greatly attenuates the rate of ester cleavage as evidenced in

peptides 3, 4 and 10. Peptide 10 dissociates faster than peptide 3 as the amine is a stronger nucleophile as compared to the hydroxyl, a point corroborated by peptides 1 and 2 as well. Finally, the large difference in the $t_{1/2}$ between peptides 8 and 9 indicates that the side chain interactions in the dipeptide (R1 and R2 in Figure 17C) play an important role as well. This same effect is shown by peptides 3 and 4. In both instances, the L,D-dipeptide diastereoisomer cleaves faster than the corresponding L,L- diastereoisomer.

Peptides 3 to 9 are represented as shown in Figure 18A. The observed half life of the prodrug increases as the substituent X gets bulkier (3, 4, 8, 9 and 10 in Table-6). This is probably because the transition state (TS) is more sterically hindered as the size of X increases. Consequently, the energy of activation increases thereby increasing the half life of the prodrug (Refer to Figure 22).

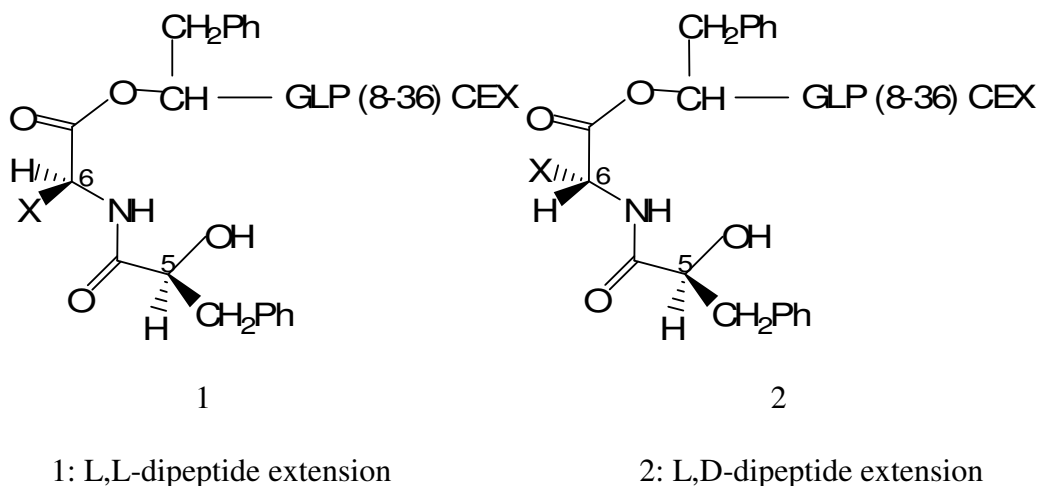


Figure 18A: HO-F⁵X⁶-O-F⁷,GLP(8-36)-CEX structures

This is especially exemplified for the two pairs of stereoisomers (3 and 4; 8 and 9). Here, by changing the stereochemistry of a single amino acid in the C-terminus of the

dipeptide extension, a huge difference in rate was observed. The steric hindrance of the corresponding transition states is far greater in a L,L-dipeptide diastereoisomer (Analog 1 in Figure 18A) as compared to a L,D- diastereoisomer (Analog 2 in Figure 18A). Hence, 3 has a greater $t_{1/2}$ as compared to 4, and 9 has a $t_{1/2}$ greater than 10.

Compound 10 is F⁵V⁶-O-F⁷,GLP(8-36)-CEX (Figure 18B). This has a $t_{1/2}$ of 64 hrs and represents the longest duration peptidic prodrug to cleavage under physiological conditions, reported to date. The transition state in this case is sizably hindered because of the steric interaction between the phenylalanyl and the valyl side chain.

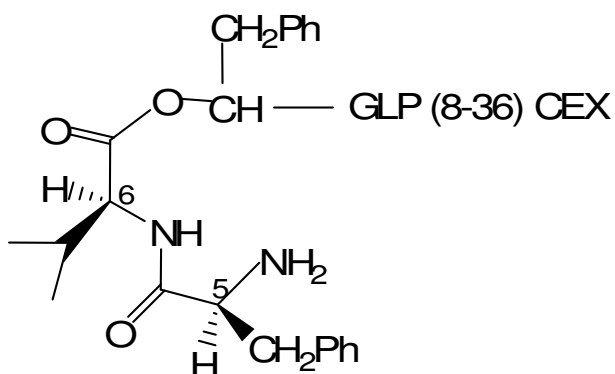
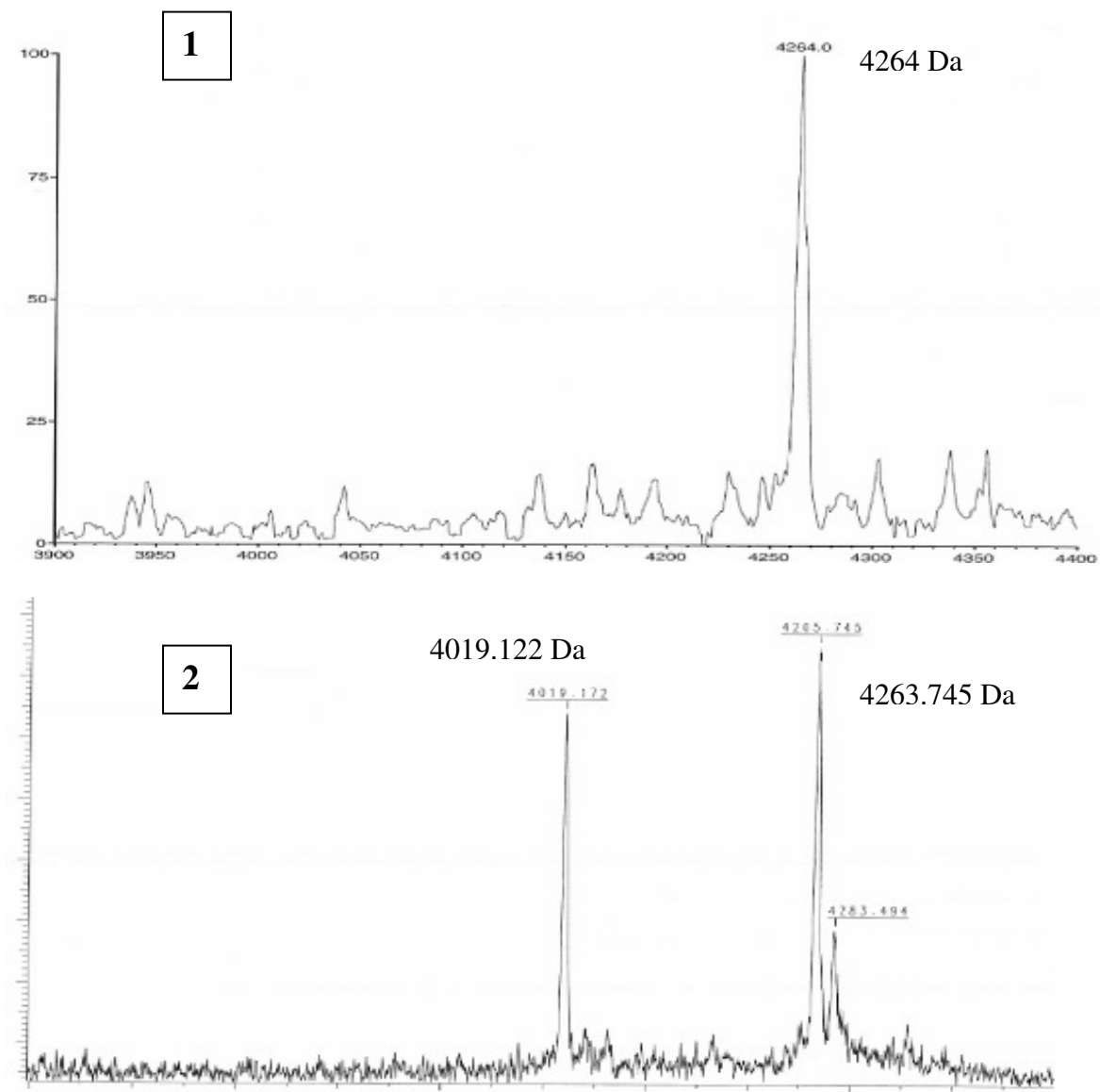


Figure 18B: F⁵V⁶-O-F⁷,GLP(8-36)-CEX ($t_{1/2}$ =64 hrs)

The experimental data supporting the cleavage of compound 10 (Figure 18B) (4264 Da) to form the parent drug HO-F⁷,GLP(8-36)-CEX (4019 Da) is shown in Figure 19. Since the reaction studied is an intramolecular cyclization, it is assumed that the presence of other impurities in the sample does not affect the rate of internal dissociation. In addition, both our molecules of interest (the prodrug and the drug) have been followed with a MALDI analysis even in the midst of contaminating material.



Phe-Val-O-F⁷-GLP8-36 CEX (4264Da) in PBS at 37°C at 0 min. 2) Phe-Val-O-F⁷-GLP8-36 CEX (4264Da) cleaving to the parent HO-F⁷-GLP 8-36 CEX (4019 Da) after incubation in PBS at 37°C for 64 hours.

Figure 19: Cleavage of F⁵V⁶-O-F⁷,GLP(8-36)-CEX to form HO-F⁷,GLP(8-36)-CEX

A second set of analogous depsipeptides were also studied to further examine the effects of the dipeptide extension structure upon the rate of cleavage (Table 7). Their

synthesis follows the same pattern as outlined in Figure 17A and 17B. The major difference is that in this case, the R2 or Y site is a less hindered hydrogen (glycyl residue) instead of a bulky phenylalanyl as used previously (refer to Figure 17C and Figure 20). In this case a glycolic acid (OH-glycine) or a glycine were used at the terminal end of the peptidic prodrug. The structures of the peptides in Table 7 are illustrated in Appendix VII.

Serial No	Peptide (Yaa1Xaa2-O-Phe ⁷ -GLP-8-36-CEX)	t _{1/2} of cleavage at 37°C
1	Gly-Gly (class 3)	0.87 hr
2	HO-Gly-Gly (class 4)	1.13 hrs
3	HO-Gly-Val (class 4)	4.70 hrs
4	HO-Gly-dVal (class 4)	5.13 hrs
5	HO-Gly - ¹ AIB (class 4)	0.75 hrs
6	HO- Gly - ² PhG (class 4)	0.49 hrs
7	HO- Gly - ³ tBut (class 4)	Did not cleave
8	HO- Gly-Phe (class 4)	0.70 hrs
9	HO-Gly-dPhe (class 4)	0.93 hrs
10	Gly -Val (class 3)	20.38 hrs

t_{1/2} is the time required for 50% release of the HO-Phe-GLP8-36-CEX at 37°C in PBS (pH7.2). It is calculated by a standard first order reaction plot. All these esters cleaved at 100°C. In all these cases, there is OH-Phe in the 1st position (hydroxy phenylalanyl leaving group) of GLP.
¹AIB: α-aminoisobutyric acid; ²PhG: phenylglycine; ³tBut: tertiary butyl;

Table 7: Cleavage of ester bond in HO-G⁵X⁶-O-F⁷,GLP(8-36)CEX

The analysis was completed in the same manner as explained previously. The first two peptides shown in Table 6 (Peptides 1 and 2) were analyzed to determine if either of the nucleophiles (amine or hydroxyl) could cleave the ester bond by 2,5-diketopiperazine or 2,5-diketomorpholine formation respectively. These two peptides had been analyzed in Table 6 and were tested again to serve as a control. As expected, both of the nucleophiles studied could cleave the ester bond. This set of compounds (Analog 2 to 9 in Table 7) can be represented as shown in Figure 20.

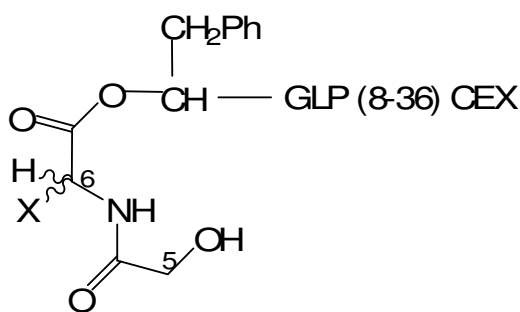


Figure 20: HO-G⁵X⁶-O-F⁷,GLP(8-36)CEX structures

These peptides are expected to cleave faster than in the previous case, as the steric bulk is removed (glycyl group in Figure 20 as compared to the phenylalanyl in Figure 18A). As the size of X becomes structurally bulkier, the transition state gets increasingly crowded. Consequently, the energy of activation increases thereby increasing the half life of the prodrug (Refer to Figure 22). This is what is seen in peptide 10 where X is an isopropyl (valine) group. When X is a tertiary butyl group (peptide 7), the compound does not cleave at all in PBS buffer (pH, 7.2) at 37°C (Figure 21). In Table 7, the pairs of stereoisomers (Analog 3 and 4; 8 and 9) dissociate at nearly the same rate. This is probably because the stereoisomers do not show a large difference in energy (purportedly

because of the non-chiral nature of glycine). Hence, in this case, both the glycyL,L-dipeptide extension and the glycyL,D-dipeptide extension have a comparable energetic transition state.

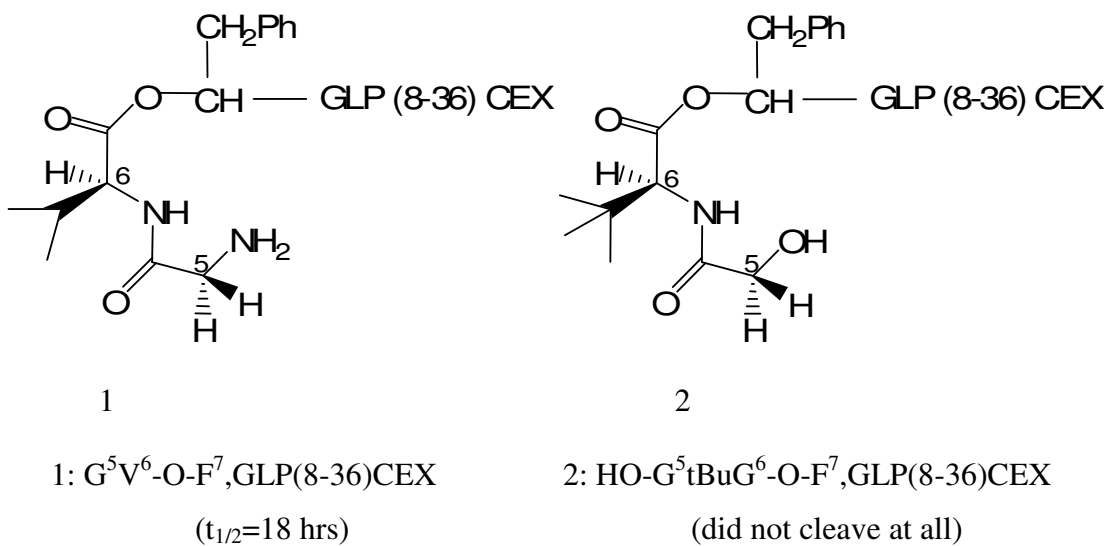


Figure 21: Dipeptide extended HO-F⁷,GLP(8-36)-CEX

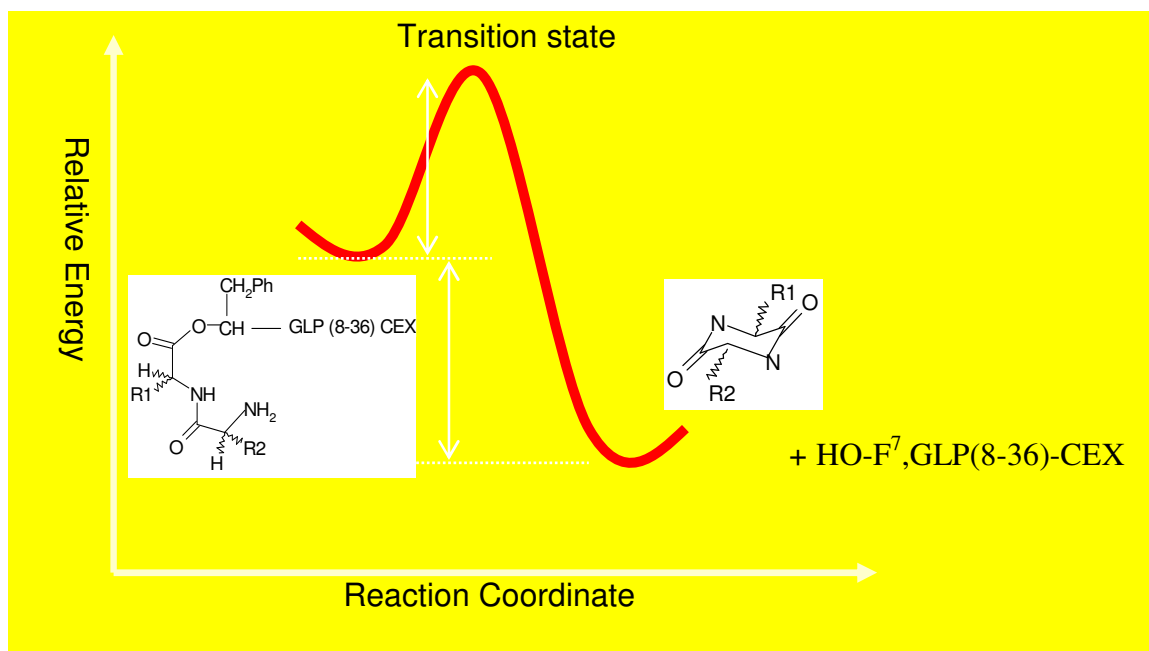


Figure 22: Transition State diagram

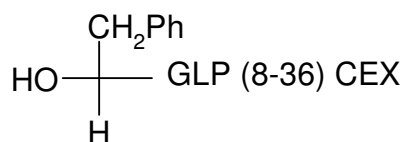
The observation that peptide 3 dissociates faster than peptide 10 seems to suggest that the hydroxyl is a stronger nucleophile as compared to the amine at a pH of 7.2 and 37°C. One possible explanation for this anomaly might be that the pKa of the N-terminal amine (which is normally approximately 7) is slightly increased in peptide 10. As a result, at a pH of 7.2, this amine nucleophile would be disproportionately protonated and thus account for the slower rate of dissociation of the prodrug. This is just one possibility to explain the observed results but additional study is needed to determine the exact basis of this observation.

Thus, our results suggest that the structural nature of the side chain (especially β branching as evidenced in dipeptides containing valine and tert-butyl glycine); the stereochemistry and the pKa of the nucleophile serve an important role in determining the relative rate of cleavage. Several fast and slow acting ester prodrug candidates have been

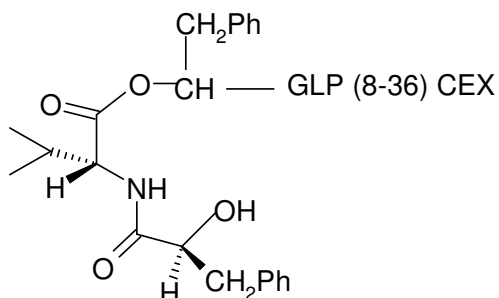
identified which were tested for their potency. As described earlier in our hypothesis, a prodrug should have minimal potency as compared to the drug, and its potency should increase consistent with the speed of cleavage of the dipeptide extension.

VI) Bioassays of selected longer-acting prodrug candidates

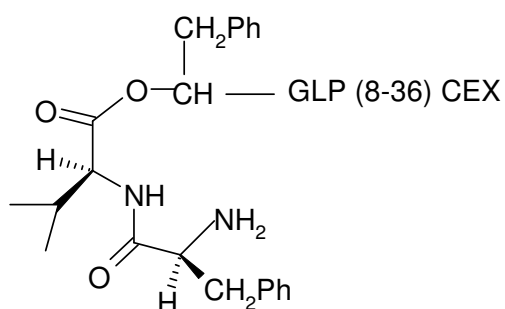
Four of the longer duration prodrugs were chosen for further analysis in the biopotency tests. Luciferase-based bio-assays were performed after purifying all these peptides by HPLC and confirming their masses by MALDI-MS analysis. Percent potency was calculated for purposes of comparing the mean EC_{50} of the parent with that of the respective prodrug. The results are tabulated in Table 8 and then pictorially represented in Figure 24A and B. The peptides tested in Table 8 are represented below in Figure 23. The syntheses of these prodrugs are schematically shown in Appendix I.



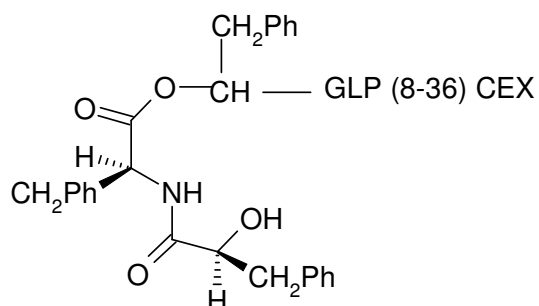
HO-F⁷,GLP(8-36)-CEX
(red)



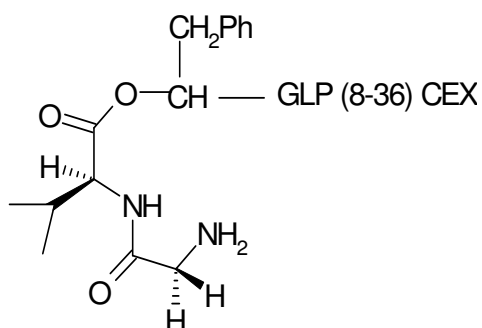
HO-F⁵dV⁶-O-F⁷,GLP(8-36)-
CEX ($t_{1/2}$ = 50.5 hr) (navy blue)



F⁵V⁶-O-F⁷,GLP(8-36)-CEX ($t_{1/2}$
= 64 hrs) (sky blue)



HO-F⁵F⁶-O-F⁷,GLP(8-36)-CEX
CEX ($t_{1/2}$ = 33.3 hr) (pink)



G⁵V⁶-O-F⁷,GLP(8-36)CEX ($t_{1/2}$
= 20.3 hr) (yellow)

Figure 23: Structures of the peptides represented in Figure 24 and Table 8

Serial No (Color)	Peptide (t_{1/2}): (Yaa1Xaa2-O-Phe-GLP-8-36-CEX)	EC₅₀ ± Std. deviation (nM)	% potency with respect to parent
1 (red)	HO-F ⁷ -GLP8-36 CEX (parent drug candidate)	0.028 ± 0.006	100% (parent drug)
2 (navy blue)	HO-Phe-dVal (t _{1/2} = 50.5 hrs)	0.40 ± 0.06	7%
3 (sky blue)	Phe-Val (t _{1/2} = 64.0 hrs)	2.070 ± 0.41	1.3%
4 (pink)	HO-Phe- Phe (t _{1/2} = 33.3 hrs)	0.771 ± 0.249	3.6%
5 (yellow)	Gly-Val (t _{1/2} = 20.3 hrs)	0.230 ± 0.10	12%

The color code refers to the respective peptides represented in the Figure 22. Percent potency calculations were done comparing the mean EC₅₀ of the parent with that of the prodrug.

Table 8: Bioassay of select longer-acting ester prodrugs

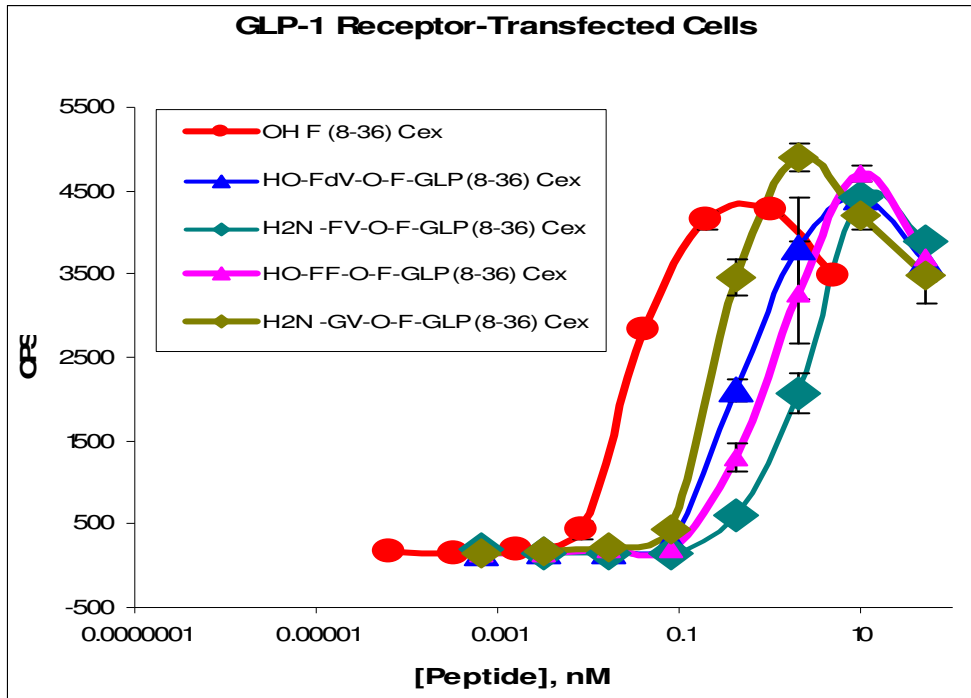
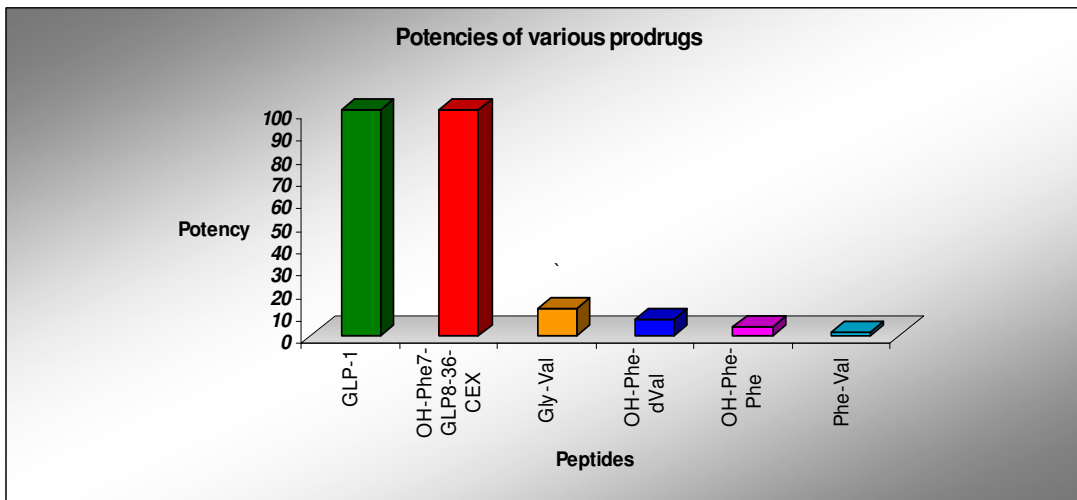


Figure 24A: Bioassay results of select longer-acting prodrugs



Green: GLP-1; Red: HO-F⁷,GLP(8-36)-CEX
 Yellow: G⁵V⁶-O-F⁷,GLP(8-36)CEX; Blue: HO-F⁵dV⁶-O-F⁷,GLP(8-36)-CEX
 Pink: HO-F⁵F⁶-O-F⁷,GLP(8-36)-CEX; Light blue: F⁵V⁶-O-F⁷,GLP(8-36)-CEX

Figure 24B: Histogram showing the potency of various prodrugs

These observations clearly show that addition of an ester linked dipeptide sequence to the terminal-hydroxyl group of the parent drug drastically reduces the potency of the drug. Two peptides were further analyzed to demonstrate that the prodrugs revert towards the potency of the parent drug following incubation for 24 hours, in PBS (pH, 7.2). The peptides chosen were analogs 4 and 5, based upon their physiologically relevant $t_{1/2}$ values being closest to 24 hours (Table 9).

These experiments were performed using HPLC purified samples with the luciferase-based assay. Percent potency calculations were done comparing the mean EC_{50} of the parent with that of the prodrug. The results are tabulated in Table 9 and then pictorially represented in Figure 25.

Serial No / (Color)	Peptide (t _{1/2}): (Yaa1Xaa2-O-Phe-GLP-8- 36-CEX)	EC ₅₀ ± Std. deviation (nM)	% potency with respect to parent
Black	HO-F ⁷ -GLP8-36-CEX (parent drug candidate)	0.023 ± 0.010	100% (parent drug)
5 ^(168 hrs) (red)*	Gly-Val (t _{1/2} = 20.3 hrs) incubated for 168 hrs.	0.024 ± 0.012	95.8 %
4 ^(0 hrs) (navy blue)	HO-Phe- Phe (t _{1/2} = 33.3 hrs) before incubation.	0.612 ± 0.270	3.7 %
4 ^(24 hrs) (sky blue)	HO-Phe- Phe (t _{1/2} = 33.3 hrs) incubated for 24 hrs.	0.134 ± 0.050	17.2 %
5 ^(0 hrs) (pink)	Gly-Val (t _{1/2} = 20.3 hrs) before incubation.	0.211 ± 0.072	10.9 %
5 ^(24 hrs) (gold)	Gly-Val (t _{1/2} = 20.3 hrs) incubated for 24 hrs.	0.05 ± 0.020	46 %

*- Peptide 5 after incubation in PBS for a week (potency almost completely restored).

⁰ – Time inside parenthesis refers to the time of incubation of the respective peptide

The color codes refer to the colors with which the respective peptides are represented in the Figure 23.

Table 9: Bioassay results that show the conversion of prodrugs to drugs

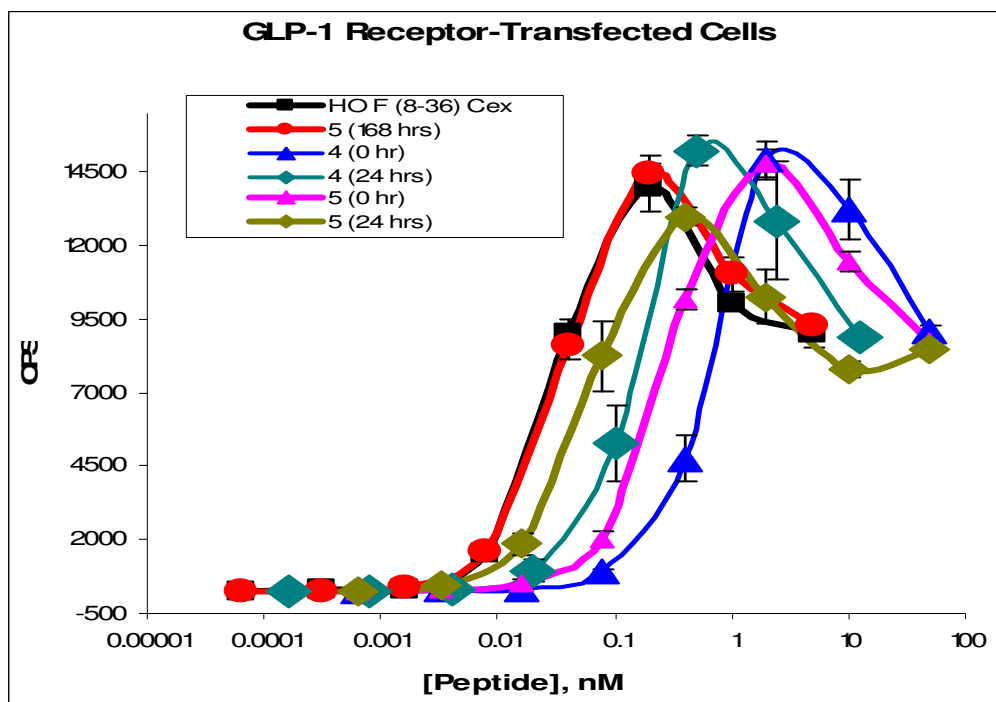


Figure 25: Bioassay results that show the reversal of prodrugs to drugs

Prodrug 5 has its potency converted close to that of the parent drug after incubation for a week (shown in red). Both prodrugs display a higher potency after being incubated in PBS for 24 hours due to gradual conversion to the parent drug. Thus the definition of a prodrug has been substantiated by our data. Prodrug 4 exhibited a 17.2% conversion (sky blue) after being incubated in PBS for 24 hrs. This is less than predicted by the calculated half-life of this prodrug (Table 8). The reason for this apparent disparity in the quantitative conversion rate of prodrug 4 has not yet been determined, though expected statistical variation in our bio-assay results and the instability of the parent drug in the bio-assay might account for this discrepancy. Future study of prodrug 4 will have multiple time points to help us understand this disparity.

VII) Ester prodrugs from internal sites of the peptide

a. Hypothesis

The prodrugs that we have synthesized spontaneously convert under physiological conditions (pH = 7.2 and temperature=37°C) to yield the parent drug. As explained in the hypothesis, the pH and temperature were relied upon for this conversion, as they are virtually invariant physiologically and this also eliminates the need for any specific enzyme mediated processing of the prodrug to its active form. The prodrug chemistry that has been established at the N-terminal end of GLP should also be translatable for use at other bio-active sites from which an ester prodrug can be prepared.

To make an ester prodrug, a judicious choice of serine/ threonine residue was explored at which the dipeptide could be added. The peptide must be biologically active before the addition of the dipeptide and inactive after the addition, in analogous fashion to our results at the terminal end of GLP-1. Hence, the peptide variants were tested for biological activity prior to pursuit of the prodrug modified forms.

b. Synthesis and analysis of prodrugs at internal sites

Two peptides were synthesized as possible starting points for development of internal prodrug candidates. The first peptide was (H7F),(E9Q),GLP(8-36)-CEX (Figure 26A) and the second one was (H7F),(E9Q),(T11S),GLP(8-36)-CEX (Figure 26B).

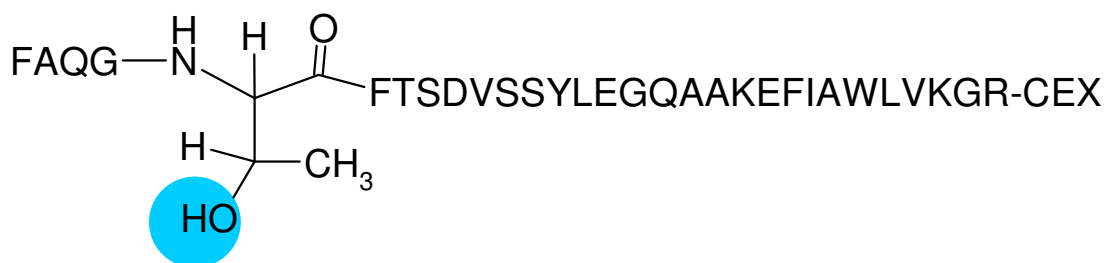
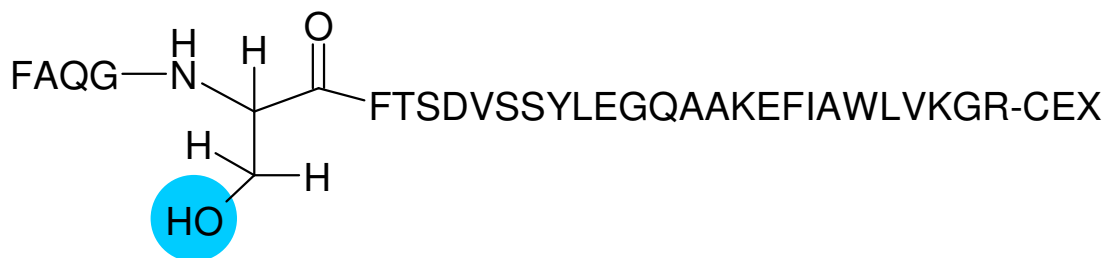


Figure 26A: (H7F),(E9Q),GLP(8-36)-CEX



*- The ester prodrug was synthesized at the circled hydroxyl group for both peptides.

Figure 26B: (H7F),(E9Q),(T11S),GLP(8-36)-CEX

The synthesis of an ester prodrug was attempted at the hydroxyl group of the 5th amino acid (threonine or serine side chain marked in Figure 26A and 26B respectively). For these molecules, a Boc benzyl-type synthesis on a PAM resin was conducted until the point of Phe at the 12th position. The rest of the synthesis was completed using Fmoc-based chemistry. This offered the opportunity to selectively remove the protecting group of the serine side chain, leaving all the other protecting groups intact. This allowed for the selective acylation on the free hydroxyl group of the serine at the 11th position.

More specifically a Boc-benzyl strategy could not be used throughout the synthesis as the hydroxyl protecting benzyl group of serine would require HF treatment for removal. Consequently, an ester prodrug could not be synthesized on the peptidic resin as the HF treatment would simultaneously remove the peptide from the resin. This is why, we added the Ser at the 11th position (Fmoc-O-t butyl-L-serine) and the subsequent Gly, Gln, Ala and Phe as Fmoc-protected amino acids. The t-butyl protecting group of the serine was selectively removed by treatment with TFA for 2 hours. The Boc-protected dipeptidic pro-moiety was added to this hydroxyl group to finish the synthesis of the ester prodrug. The final Boc-protecting group was removed by treatment with TFA and the N-terminal Fmoc group was removed by treatment with 20% piperidine in DMF. This was found to be a useful strategy to build the dipeptide esters from the hydroxyl side chain of serine and threonine residues. The glutamic acid residue at the 3rd position was also replaced with glutamine to prevent any unwanted coupling on the side chain carboxyl group. It was assumed that this would not lead to a loss of activity as previous reports have suggested that the 3rd position is not critical for GLP potency³⁵.

The luciferase bio-assay was conducted after purification of these peptides by HPLC, and confirmation of their masses by MALDI as described previously. Percent potency was calculated and the mean EC₅₀ of the peptide (drug candidate) was compared with that of native GLP-1. The results are tabulated in Table-10 and then shown in Figure 27.

Serial No / (Color)	Peptide ($t_{1/2}$)	EC ₅₀ ± Std. deviation (nM)	% potency with respect to GLP-1
1 (black)	GLP-1	0.02 ± 0.00	100%
2 (pink)	F ⁷ Q ⁹ S ¹¹ -GLP8-36 CEX	0.10 ± 0.02	20 %
3 (gold)	F ⁷ Q ⁹ T ¹¹ -GLP8-36 CEX	0.06 ± 0.02	33.33 %

GLP-1 was used as a standard. The color codes refer to the colors with which the respective peptides are represented in Figure25.

Table 10: Bioassay results of internal serine/ threonine drug candidates

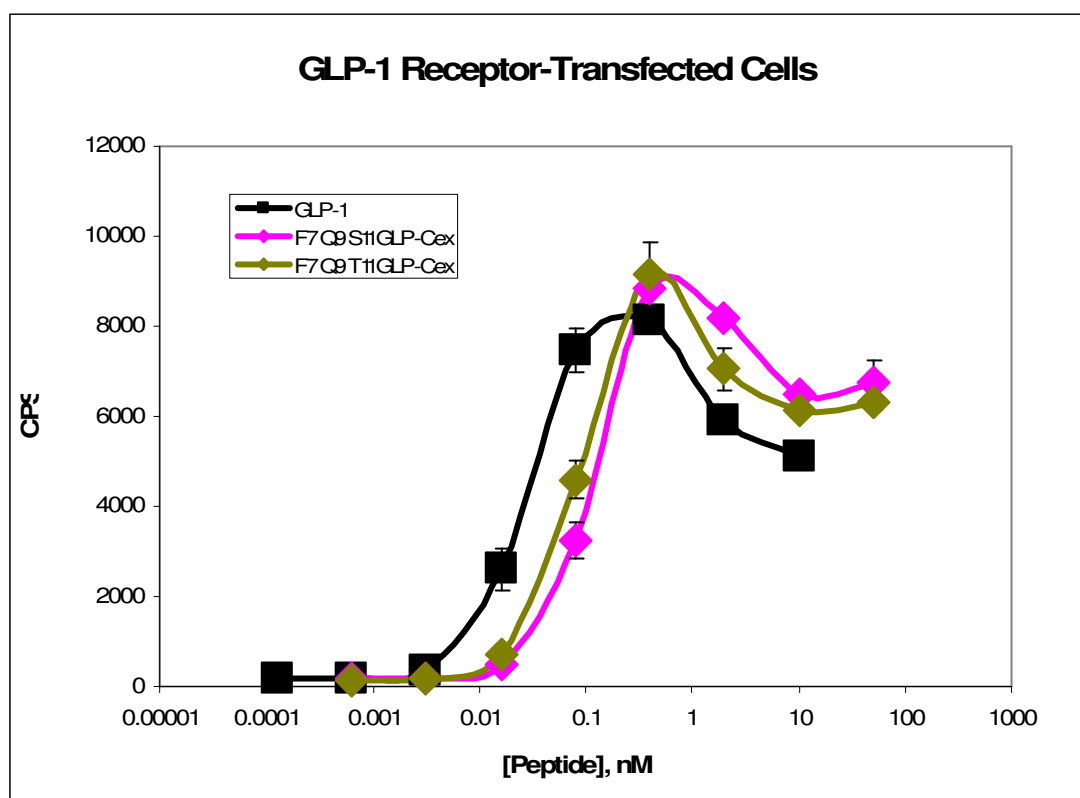


Figure 27: Bioassay of internal serine/ threonine ester prodrugs

The peptides (H7F),(E9Q),GLP(8-36)-CEX and (H7F),(E9Q),(T11S),GLP(8-36)-CEX were full agonists with 20% and 33.3% the potency of native GLP-1 respectively. It was decided that both these peptides were sufficiently potent for development as potential drug candidates.

The lower potencies of these GLP-CEX analogs as compared to GLP probably results from the H7F modification (as had been previously shown in this report). In this context, we assume that the E9Q modification does not lower the potency substantially (personal communication with John Day). However, previously reported structure-activity relationship data of GLP has been based on single substitution of the corresponding amino acid by alanine³⁵. In our case, both the H7F and E9Q modifications have been changed simultaneously in the same peptide and this might yield an unexpected result.

A Gly-Gly dipeptide was envisioned to be added to these GLP analogs to study the type of reaction as depicted in Figure 28. This dipeptidic pro-moiety was chosen as an initial case on the basis of its synthetic ease; not its extended half life. The hydroxyl group of the serine side chain was easier to acylate as compared to the bulkier threonine side chain. One potential prodrug (H7F),(E9Q),[T11S-O^β-(Gly-Gly)],GLP(8-36)-CEX was synthesized by adding a Gly-Gly dipeptide to the hydroxyl of the serine side chain as shown in Figure 26. In this regard, the $t_{1/2}$ of the Gly-Gly terminal ester prodrugs were ~1 hr (Table 7), whereas the $t_{1/2}$ of the internal ester prodrug was found to be approximately three times longer.

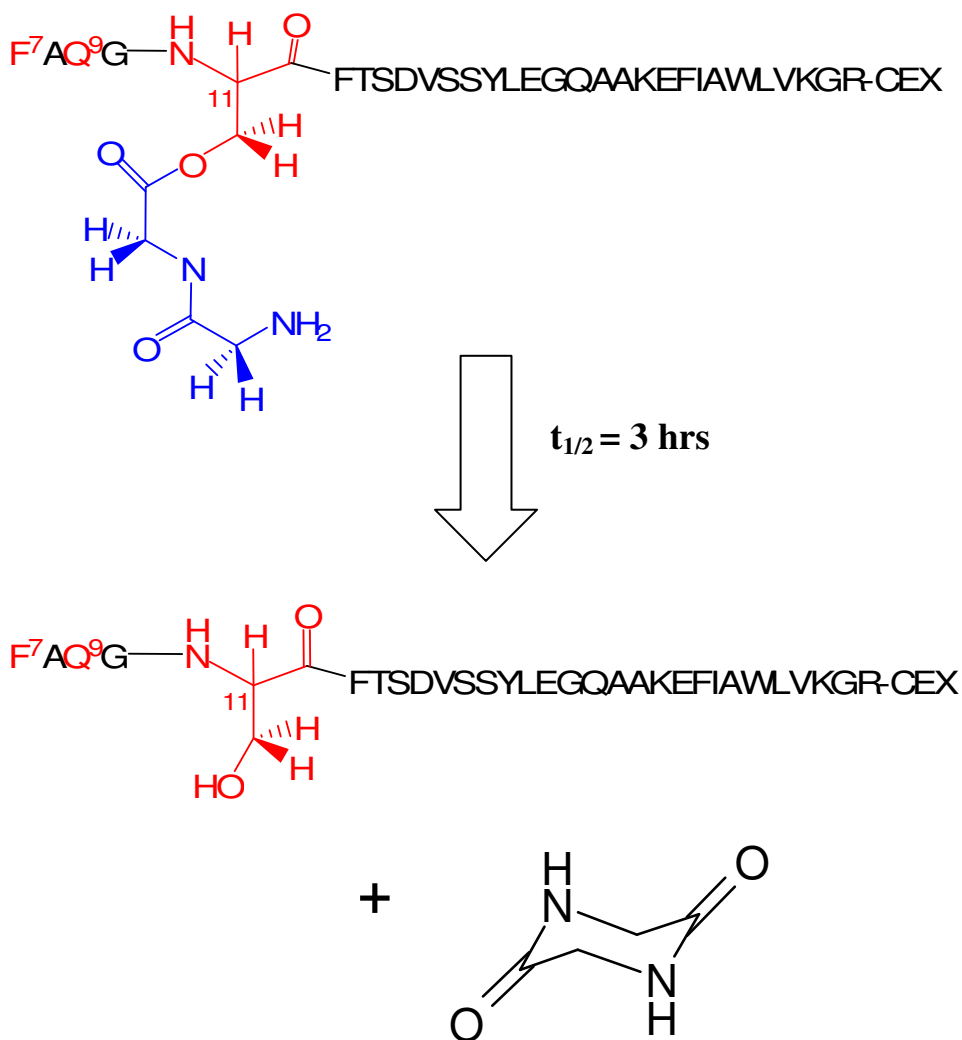


Figure 28: Conversion of serine ester prodrug (H7F),(E9Q),[T11S-O^β-(Gly-Gly)],GLP(8-36)-CEX to drug (H7F),(E9Q),(T11S),GLP(8-36)-CEX

Unfortunately, it was not possible to acylate the hydroxyl of the threonine side chain with a Gly-Gly dipeptide. This analogous addition of the dipeptide to Thr relative to Ser failed probably because of the steric restraints imposed by the methyl group at C-3 of the threonine side chain as compared to the hydrogen at C-3 of the serine side chain.

It was observed that the (H7F),(E9Q),[T11S-O^β-(Gly-Gly)],GLP(8-36)-CEX prodrug dissociated with a $t_{1/2} = 2.7 \text{ hrs}$ to yield the parent drug

(H7F),(E9Q),(T11S),GLP(8-36)-CEX along with the 2,5-diketopiperazine (DKP). We were unable to determine the absolute potency of this prodrug because its half life is lower than the incubation period of the prodrug in the cell culture based luciferase assay (5 hrs). The half life of the prodrug (2.7 hrs) indicates that approximately 70% of the prodrug would have converted to the active entity in 5 hours; hence the assay could not be accurately performed on this prodrug. However, we have nevertheless established the conversion of the internal serine prodrug to the active entity.

Since the conditions for the conversion of the prodrugs to the drug (pH = 7.2 and temperature=37°C) are virtually invariant physiologically, it was found that the prodrug chemistry that was established at the O-terminal end of GLP could be used to cleave from an internal site as well, specifically Ser but conceptually Thr. Thus our initial hypothesis is validated.

E) Conclusion:

Clinical studies have revealed that GLP-1 therapy is an effective treatment for Type II diabetes. In addition, it might be intrinsically safer than insulin therapy because of its glucose dependent action, thus eliminating the chances of hypoglycemia⁴⁹. So far no cases of hypoglycemia have been reported using treatment with a GLP-related drug.

An ideal prodrug should be stable to storage but must convert to the active drug under a specific set of conditions. The desired set of conditions for the activation of the prodrug will depend on its purpose and site of action. Detailed stability studies are important for the rigorous characterization of promising prodrugs. However, a rapid screening helps in the identification of such prodrug candidates. Such screening provides insights to the structure, stereochemistry and the site of attachment of the pro-moiety to the drug and how these affect the conversion of the inactive prodrug to the active drug. In the work presented here, the conditions for the conversion are a pH of 7.2 and temperature of 37°C. These conditions were used for the cleavage of the prodrugs as they are physiologically invariant and can thus be translated into other peptidic drugs as well. The relative potency of prodrug candidates to the parent drug were determined through a receptor-based cell culture assay.

Prodrug strategies have often been implemented to improve the efficacy and safety of important drugs in different diseases⁷⁹. In this report, the prodrug strategy has been used to increase the time action of the GLP analog by extending the half life of the prodrug. Although a number of different pro-moieties could be used, the 'dipeptide pro-moiety or the α hydroxyl dipeptide analog' which dissociated by the formation of

diketopiperazine (DKP) or diketomorpholine (DMP) along with the release of the active GLP analog over a wide time range was chosen.

Our strategy has a number of advantages. Firstly, a number of structurally diverse amino acids (aliphatic, aromatic, acidic, basic, neutral) and α hydroxyl amino acids are commercially available. Secondly, given the natural nature of amino acids there is likely to be fewer safety and immunogenic concerns regarding their use as pro-moieties. In this context, it should also be noted that the native amino acid sequence was maintained as far as possible, and this should minimize potential adverse immunogenic responses. However the magnitude and nature of such adverse reactions will need to be explored *in vivo*. Thirdly, the amino acid properties and peptide synthetic chemistries are well established. Finally, and most importantly the chemistry of diketopiperazine formation allowed at least four points where the structure could be stereochemically controlled to refine the formation rate of the active GLP analog. Prodrugs of varying half lives were synthesized by chemically modifying R1 and R2 in the context of different nucleophiles (Figure 6). This generated the novel chemoreversible prodrugs of GLP, which converted to the active entity via the intramolecular cyclization and subsequent release of 2,5-diketopiperazine (DKP) or 2,5-diketomorpholine (DMP). The large variance of half lives amongst the various prodrugs ranging from a $t_{1/2} = 0.5 - 64.0$ hrs underscores the great potential of this chemoreversible prodrug system in accurately tailoring the release of the parent drug under physiological conditions. The prodrug F⁵V⁶-O-F⁷,GLP(8-36)-CEX with a $t_{1/2} = 64$ hrs is the longest acting chemically defined peptidic prodrug reported to date.

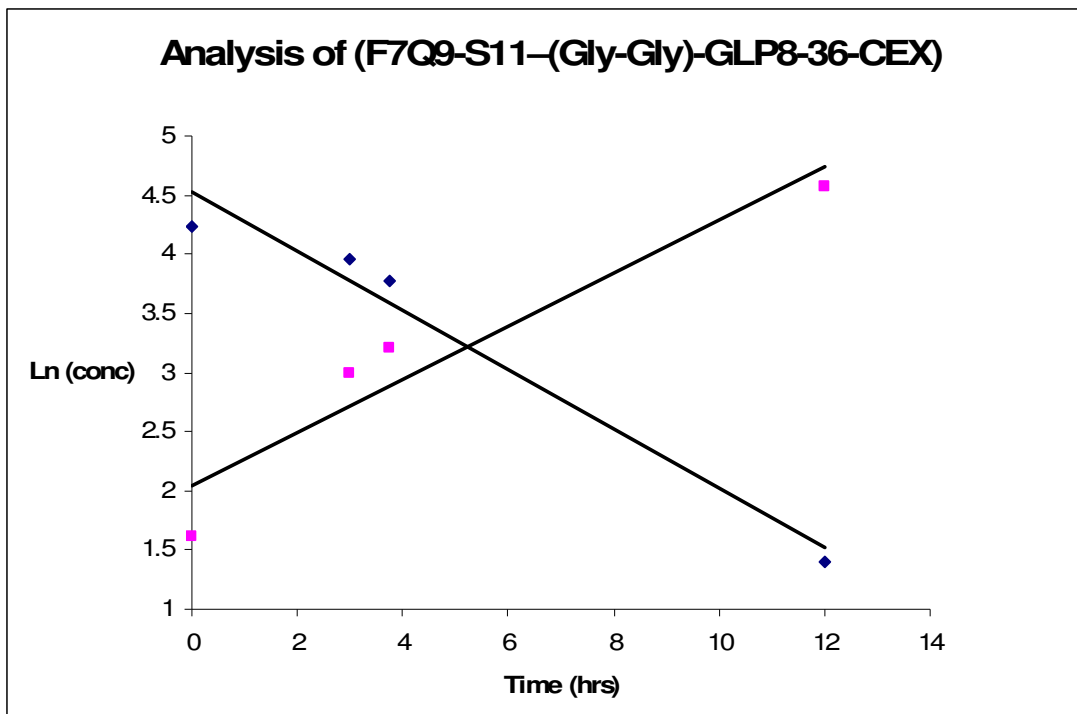
Four different varieties of prodrugs (Class 1, 2, 3 and 4) of GLP or biologically active GLP analogs were synthesized. Both the amide and the ester prodrugs were synthesized in good yield. In the beginning, the amide prodrugs were synthesized by adding a dipeptide to the amine group at the N-terminus. The cleavage of the amide bond of interest was attempted under physiological conditions with both an amine and a hydroxyl nucleophile (Table 4 and 5). Different leaving groups were employed, with a histidine (Table 2), phenylalanine (Table 3 and 4) and a glycine (Table 5) at the N-terminus of GLP analogs. For solubility purposes, we decided to work with a C-terminal modified GLP analog, GLP-CEX.

We observed that the amide bond could not be dissociated by 2,5-diketopiperazine (DKP) or 2,5-diketomorpholine (DMP) formation under physiological conditions. In fact, the amide bond could not be cleaved even when heated at 100°C at a pH=7.2. Consequently, an amide prodrug could not be synthesized using this approach. As a result, our attention focused on synthesizing ester prodrugs.

Two distinct classes of dipeptide esters were tested to study the cleavage of the ester bond. Class 3 variants employed an N-terminal amine nucleophile while Class 4 variants contained a hydroxyl nucleophile to cleave the ester bond (see Figure 10). Selectively acylating the α -hydroxyl group of HO-H⁷,GLP(8-36)-CEX proved to be very difficult in the absence of a “protected” imidazole peptide. Hence, we decided to work with phenyllactic acid and subsequently synthesized the HO-F⁷,GLP(8-36)-CEX which was found to be at least as potent as the native GLP in repetitive analysis. The ester prodrugs were synthesized using this parent drug as the scaffold.

The esters proved to be much more labile than the corresponding amides and most of the ester prodrugs dissociated to give the active drug under physiological conditions along with the assumed formation of 2,5-diketopiperazine (DKP) or 2,5-diketomorpholine (DMP). The degradation half lives of the respective prodrugs were calculated based on the first order kinetics ($t_{1/2} = .693/k$) where 'k' is the first order rate constant for the degradation of the prodrug. The disappearance of the prodrug and the appearance of the drug were both simultaneously analyzed and calculated using HPLC. Generally, there was an excellent mass balance between the loss of the prodrug and the appearance of the drug. However in our results, only the estimated half life of the disappearance of the prodrug has been reported.

A sample kinetic profile reflecting the disappearance of the prodrug (H7F),(E9Q),[T11S-O^β-(Gly-Gly)],GLP(8-36)-CEX and the appearance of the parent drug (H7F),(E9Q),(T11S),GLP(8-36)-CEX (Figure 28) under physiological conditions is shown in Figure 29. The slope of the first order plot (blue diamonds) represents the dissociation constant of the prodrug from which the half life was calculated to be 2.8 hrs. The experiment was performed over several half lives and the recovery of the parent compound was more than 90%.



Blue diamonds represent the disappearance of the prodrug.
Pink squares represent the appearance of the drug.
The logarithm of the concentrations of the prodrug (blue) and the drug (pink) were plotted on the y axis as a function of time on the x axis.

Figure 29: Typical kinetic profile showing the disappearance of a prodrug and the appearance of a drug

Of all the ester prodrugs that were studied, only two did not cleave and they are represented in Figure 30.

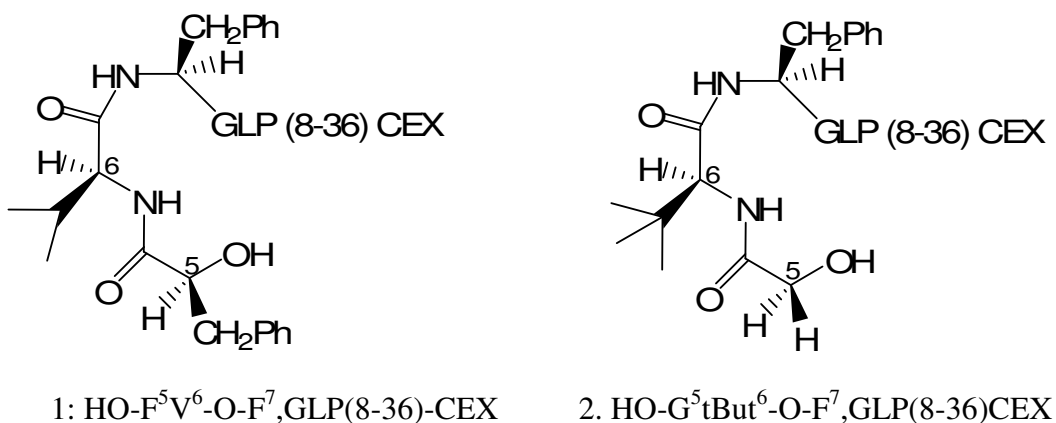


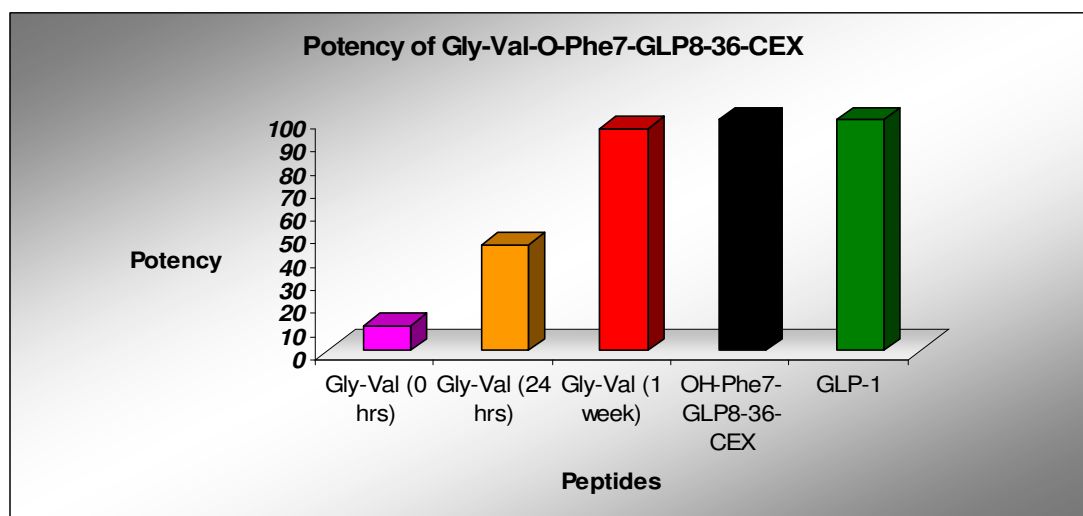
Figure 30: Ester prodrugs resistant to cleavage

The most likely reason for this is the increased size of the R1 and R2 in compounds 1 and 2 (Figure 30). The steric bulk of the isopropyl and tertiary butyl group crowds the transition state increasing the activation barrier for the intramolecular cyclization. As a result, the cyclization does not occur. When the hydroxyl nucleophile in compound 1 was replaced with the amine, the corresponding F⁵V⁶-O-F⁷,GLP(8-36)-CEX (Figure 18B) cleaved with a long half life of 64.0 hours. The presence of cleavage relative to the hydroxyl-peptide is because the amine is a stronger nucleophile, as compared to the hydroxyl. Thus it is seen that the chemical stability of the ester bond is influenced by the structure of the amino acid promoiety. The bulk of the side chain of the corresponding amino acids and the strength of the nucleophile play a role in the cleavage of the ester prodrugs. Additionally, stereochemistry of the two amino acids further influences the rate of cleavage. These results are consistent with related observations in the field of DKP-like prodrugs^{61,63}.

Our primary goal was to synthesize longer-acting prodrug candidates of GLP with a daily or even a weekly dosage. This is especially important as the longest acting DPP-

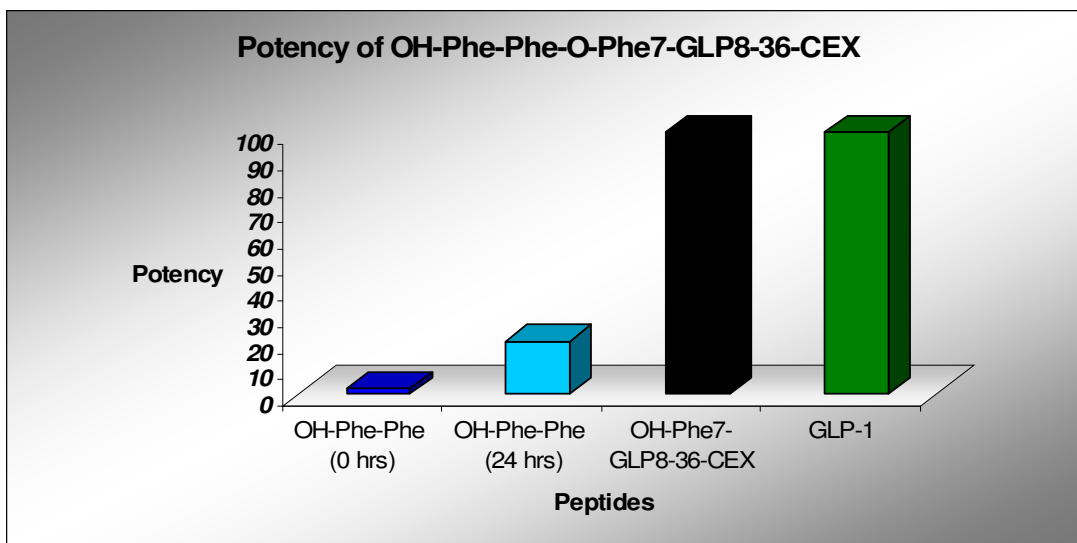
IV resistant GLP analog (Liraglutide) that is presently in Phase III trials has a biological half life of 10-14 hrs^{47,48}. Four prodrug candidates with varying half lives of 20.3hrs, 33.3hrs, 50.5 hrs and 64.0 hrs were successfully synthesized (Figure 23 and Appendix I). Each of these prodrug candidates should display extended duration of *in vivo* action and possibly constitute ‘once a week’ formulations, since this prolongation would be in addition to the natural time action of the parent drug.

The bio-assay we used is highly sensitive and reproducible. All the prodrugs have minimal inherent receptor potency relative to the parent drug (Table 8). The potency of $G^5V^6-O-F^7, GLP(8-36)-CEX$ is nearly restored quantitatively (Figure 31A), while that of $HO-F^5F^6-O-F^7, GLP(8-36)-CEX$ is only partial after incubation in PBS at 37°C for 24 hours (Figure 31B). The reason for latter observation is not immediately clear; and warrants further study.



Green: GLP-1; Black: $HO-F^7, GLP(8-36)-CEX$
 Red: $G^5V^6-O-F^7, GLP(8-36)CEX$ after incubation in PBS for 1 week;
 Yellow: $G^5V^6-O-F^7, GLP(8-36)CEX$ after incubation in PBS for 24 hours;
 Pink: $G^5V^6-O-F^7, GLP(8-36)CEX$ in PBS at 0 hours;

Figure 31A: Relative potency of $G^5V^6-O-F^7, GLP(8-36)CEX$



Green: GLP-1; Black: HO-F⁷,GLP(8-36)-CEX
 Light blue: HO-F⁵F⁶-O-F⁷,GLP(8-36)-CEX after incubation in PBS for 24 hours;
 Dark blue: HO-F⁵F⁶-O-F⁷,GLP(8-36)-CEX in PBS at 0 hours;

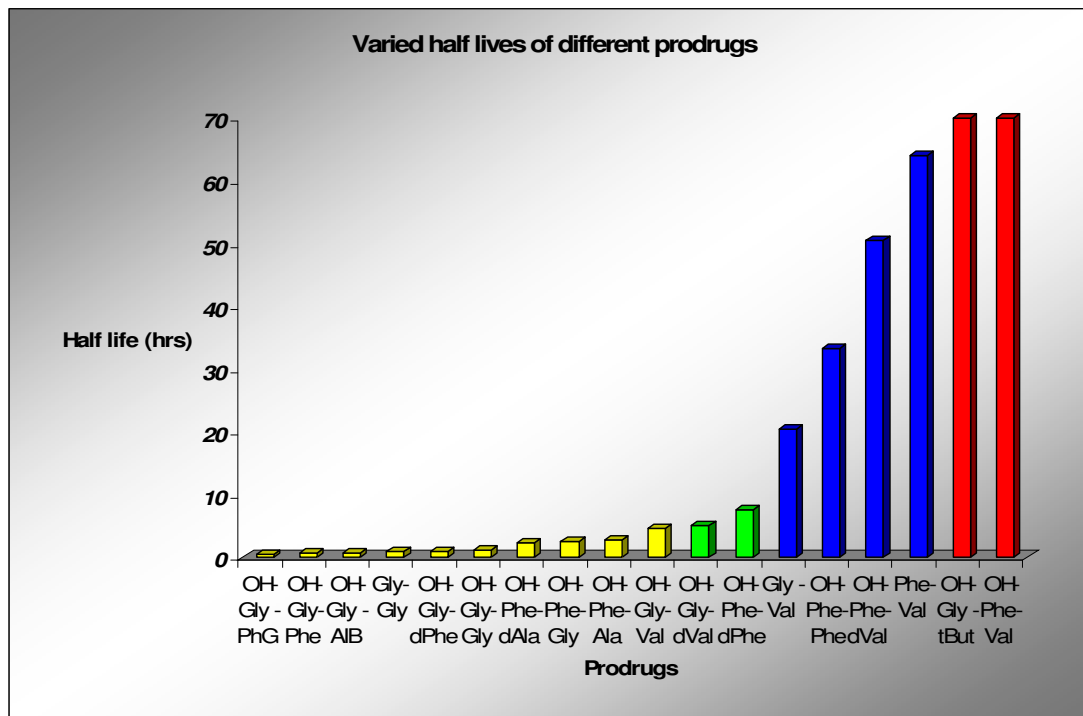
Figure 31B: Relative potency of HO-F⁵F⁶-O-F⁷,GLP(8-36)-CEX

The biological potency of the internal serine ester prodrug, (H7F),(E9Q),[T11S-O^β-(Gly-Gly)],GLP(8-36)-CEX could not be determined as its half life (2.8 hrs) is much shorter than the incubation period (5hrs) in the luciferase assay. However, its chemical conversion to the active (H7F),(E9Q),(T11S),GLP(8-36)-CEX (Figure 28 and 29) has been documented validating that the diketopiperazine chemistry is feasible from an internal ester site of the peptide. The internal ester prodrug (H7F),(E9Q),[T11S-O^β-(Gly-Gly)],GLP(8-36)-CEX cleaves with a half life that is longer than the terminal prodrug G⁵G⁶-O-F⁷,GLP(8-36)-CEX. The reason for this might be that the β-ester bond of the internal prodrug is more resistant to cleavage than the terminal α-ester bond.

In the overall context of things, we would have much preferred to have been able to cleave both the amide and ester bonds. This would provide the opportunity to utilize this prodrug chemistry at amine as well as hydroxyl containing drug candidates. One

central disadvantage of ester prodrugs is the ubiquitous presence of esterases *in vivo*; and hence the effective half life of the ester prodrug might be much faster in blood than reported here.

In conclusion, our prodrugs were extremely stable when stored as a powder at 4°C. They are soluble in physiological buffers, and exhibit differential conversion rates to the active drug under physiological conditions. This latter point is the central importance of my work. The results of this study clearly indicate that the *cis*-conformation of the dipeptide favors cleavage. Furthermore, that the overall structure (especially β branching as evidenced by the slow rates in pro-moieties containing valine), stereochemistry of the side chains, and the strength of the nucleophile play a profound role in affecting the rates of prodrug cleavage. It was also importantly shown that rate of conversion can be fine-tuned by selecting the structure of the pro-moieties. This is of utmost importance in the design of a properly functioning prodrug, as represented in Figure 32. The dynamic range in rate of cleavage ranged from an hour to almost half a week. This provides appreciable opportunity for choosing from a wide spectrum of potential prodrugs, each varying in duration of action. These prodrugs with their tailored rate of conversions can provide a versatile lead for further optimization of their pharmacological profiles.



Yellow: Prodrugs with $t_{1/2}$ under 5 hrs; Green: Prodrugs with $t_{1/2}$ under 10 hrs
 Blue: Prodrugs with $t_{1/2}$ between 20 to 65 hrs; Red: Prodrugs that did not dissociate at all

Figure 32: Prodrugs with varying half lives

It is envisioned that the half lives of these prodrugs might be different when studied *in vivo* than reported in our *in vitro* experiments. This will probably be as a result of the action of the esterases and other enzymes, but unlikely a change in the chemical rate of conversion. Hence, an *in vivo* characterization of these prodrugs shall be necessary. Even if the prodrugs display the required half life *in vivo*, it might be required to slow their renal clearance (the renal threshold is 38,000 Da while the prodrugs have a molecular weight of ~4500). This can be done by pegylating the prodrugs at appropriate residues.

A place for additional investigation is the identification of methods to cleave amide prodrugs under physiological conditions. The amide prodrugs will presumably

have an enhanced half life relative to that of the ester prodrugs. However, the increased flexibility of using amine-based drugs and their prodrugs to escape what might be selective degradation by esterases warrants further investigation.

We have observed a number of prodrugs that could be potentially administered on a ‘once a week’ basis. Even longer acting prodrug candidates might be desired. Those will be prodrugs that can be administered on a ‘once a month’, or even in a ‘once a year’ formulation. However, it is worth noting that there are many other mechanisms beyond ‘diketopiperazine formation’ by which the prodrugs can be destroyed *in vivo*. Since peptides intrinsically decompose *in vivo* under physiological conditions, there is a limit set to the “time of action” of a specific peptide-based drug. However, our ability to use inverted stereochemistry of the dipeptide with no change in rate of chemical cleavage is a huge advantage in minimizing enzymatic destruction of the prodrug element.

The studies of the structure of additional pro-moieties and how they affect the rate of conversion will provide additional diversity in prodrug chemistry for future use. This might then lead to a more effective structure-activity correlation study which can be subsequently used to synthesize prodrugs of optimal stability and pharmacokinetic profiles.

Bibliography

- 1) Majumdar, S. K. (2001) Bulletin of the Indian Institute of the History of Medicine
Hyderabad 31(1): 57-70
- 2) Pendergrass, M. (2007) Nature Endocrinology and Metabolism 3(1): 1
- 3) <http://www.diabetes.org>
- 4) Cryer, P. E. (2007) Nature Endocrinology and Metabolism 3(1): 4-5
- 5) Onkamo, P., et al. (2000) Diabetologia 43(10): 1334–1336
- 6) Kishiyama, C. M., Chase, H., and Barker, J. M. (2006) Reviews in Endocrine and
Metabolic Disorders 7(3): 215-224
- 7) The Diabetes Control and Complications Trial Research Group (1998) Annals of
Internal Medicine 128(7): 517-523.
- 8) Cavaghan, M.K. et al. (2000) The Journal of Clinical Investigation 106: 329–333
- 9) Sadikot, S.M., Jaslok Hospital and Research Centre, Mumbai
<http://diabetesindia.com/>
- 10) United Kingdom Prospective Diabetes Study (1995) Diabetes 44: 1249–1258
- 11) <http://www.diabetes.org/gestational-diabetes.jsp>
- 12) Banting, F. G., et al. (1922) Canadian Medical Association Journal 12: 141-146.
- 13) Banting, F. G. and Best, C. H. J. (1922) Journal of Laboratory and Clinical Medicine
7: 464-472.
- 14) Sanger, F. (1959) Science 129(3359): 1340-1344.
- 15) Lepore, M., et al. (2000). Diabetes 49(12): 2142-2148.
- 16) De León, D.D. and Stanley, C.A, (2007) Nature Clinical Practice Endocrinology &
Metabolism 3: 57 – 68

- 17) The Diabetes Control and Complications Trial Research Group. (1993) The New England Journal of Medicine 329(14): 977-986
- 18) Nicholas G. A., and Gomez-Camirero, A. (2007) Diabetes, Obesity and Metabolism 9(1): 96-102
- 19) Johnston, L. W., and Weinstock, R. S. (2006) Mayo Clinic Proceedings 81(12): 1615-1620
- 20) Nauck, M.A., et al. (2002) The Journal of Clinical Endocrinology & Metabolism 87(3): 1239-1246
- 21) Schmidt W. E., Siegel, E. G., and Creutzfeldt, W. (1985) Diabetologia 28(9): 704-707
- 22) Green B. D. et al., (2003) Biological Chemistry 384: 1543-1551.
- 23) Holst, J. J. (1999) Trends in Endocrinology and Metabolism 10: 229 –234
- 24) McCormack, J.G. (2006) Biochemical Society Transactions 34: 238–242
- 25) Orskov, C., et al. (1996) Wourld Journal of Gastroenterology 31: 665– 670
- 26) Daniel, J., et al., (2006) The Lancet 368(9548): 1696-1705
- 27) Giorgino, F., et al. (2006) Diabetes Research and Clinical Practice 74(2): S152-S155
- 28) Butler, A. E., et al., (2003) Diabetes 52: 102–110
- 29) Nauck, M., et al., (1986) Diabetologia 29: 46 –52
- 30) Drucker, D. J., et al., (1987) Proceedings of the National Academy of Science 84: 3434–3438
- 31) Holz, G. G., et al. (1999) Journal of Biological Chemistry 274: 14147–14156
- 32) Gromada, J., et al., (1998) Pflugers Archiv. European Journal of Physiology 435: 583–594

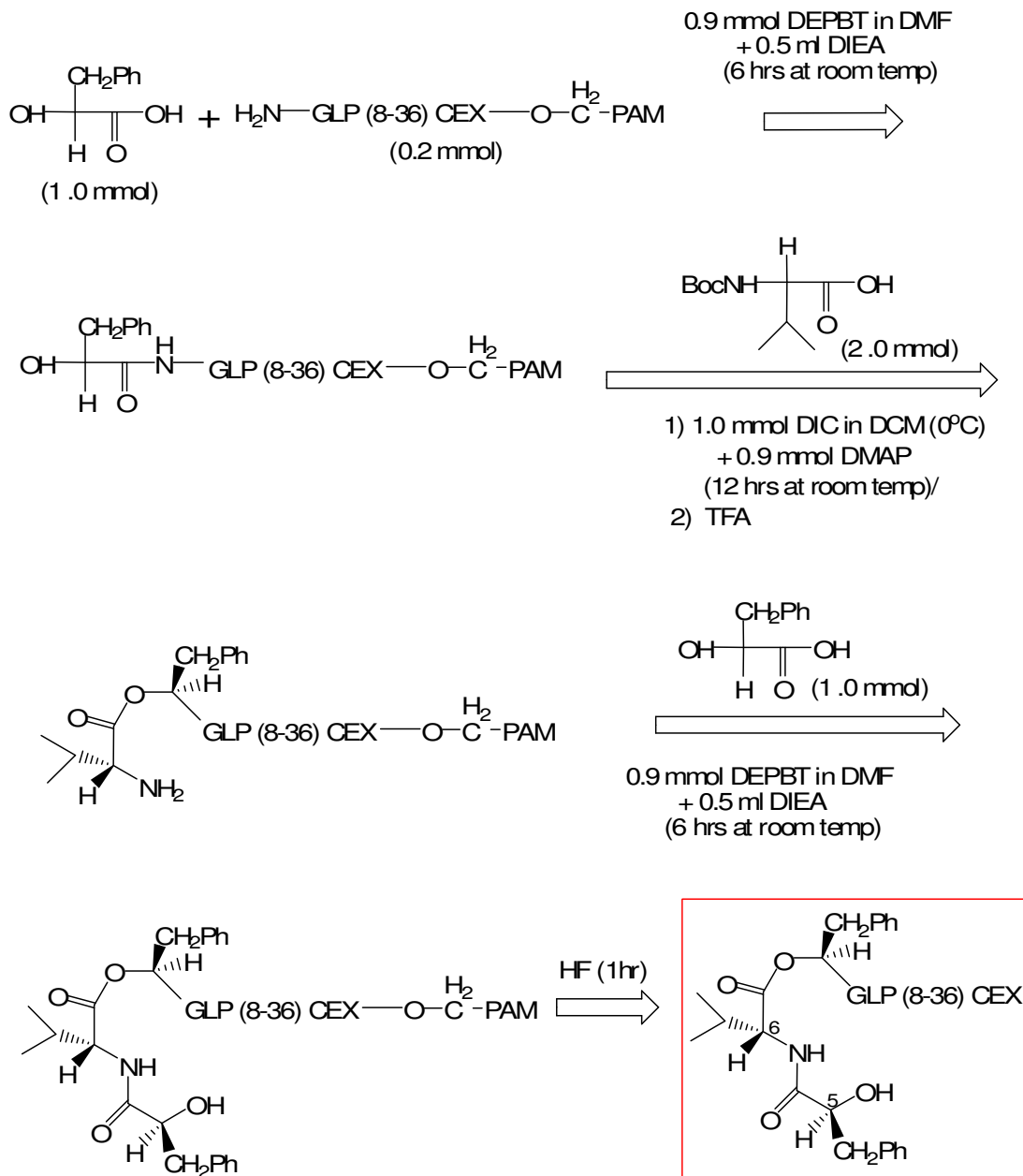
- 33) Weir, G. C. et al., (1989) *Diabetes* 38: 338–342
- 34) Rabenhoj, L., et al., (1994) *Diabetes* 43(4): 535-539
- 35) Adelhorst, K., et al., (1994) *Journal of Biological Chemistry* 269(9): 6275-6278
- 36) Larsen, J., et al., (2001) *Diabetes Care* 24: 1416–1421
- 37) Ørskov, C., Wettergren, A., and Holst, J. J. (1993) *Diabetes* 42: 658–661
- 38) Deacon, C. F. et al., (1995) *Journal of Clinical Endocrinology and Metabolism* 80:
952–957
- 39) Knudsen, L.B., and Pridal, L. (1996) *European Journal of Pharmacology* 318: 429–
435
- 40) Holst, J. J., and Deacon, C. F. (1998) *Diabetes* 47(11): 1663-1670.
- 41) Åhren, B., et al., (2004) *Journal of Clinical Endocrinology and Metabolism* 89: 2078–
2084
- 42) Stuart A. R., Gulve, E. A., and Minghan, W. (2004) *Chemical Reviews* 104(3): 1255
-1282
- 43) Thorens, B., et al., (1993) *Diabetes* 42(11): 1678–1682
- 44) Eng, J. Et al., (1992) *Journal of Biological Chemistry* 267(11): 7402-7405
- 45) Kolterman, O. G., et al., (2005) *American Journal of Health System Pharmacy* 62:
173–181
- 46) Kendall, D. M., et al., (2005) *Diabetes Care* 28: 1083–1091
- 47) Knudsen, L. B., et al., (2000) *Journal of Medicinal Chemistry* 43: 1664–1669
- 48) Bjerre, Knudsen et al., (2005) *Diabetes* 52(1): 321–322
- 49) Deacon, C.F. (2004) *Diabetes* 53: 2181-2189
- 50) IUPAC *Pure & Applied Chemistry* (1998) 70(5): 1129–1143

- 51) Albert, A., (1958) *Nature* 182: 421–423
- 52) Jiunn, H. L., and Lu, A.Y. H. (1997) *Pharmacology Review* 49: 403–449
- 53) Stańczak, A., and Ferra, A. (2006) *Pharmacological Reports* 58: 599-613
- 54) Beaumont, K., et al., (2003) *Current Drug Metabolism* 4: 461-485
- 55) Humphrey, M. J., and Ringrose, P. S. (1986) *Drug Metabolism Reviews* 17: 283-310
- 56) Saffran, M., et al., (1988) *Journal of Pharmaceutical Sciences* 77: 33-38
- 57) Lee, S. H. et al., (2005): *Bioconjugate Chemistry* 16: 377-382
- 58) Poijarvi-Virta, P. (2006) *Current Medicinal Chemistry* 13(28): 3441-3465
- 59) Bundgard, H., and Moss, J. (1990) *Pharmaceutical Research* 7(9): 885-892
- 60) Oliyai, R., and Valentino J. S. (1993) *Annual Review of Pharmacology and Toxicology* 33: 521-544
- 61) Bundgard, H., and Moss, J. (1990) *Journal of Pharmacy and Pharmacology* 42: 7-12
- 62) Goolcharran, C. and Borchardt, R. T. (1998) *Journal of Pharmaceutical Sciences* 87(3): 283-288
- 63) Borchardt, R. T., and Cohen, L. A. (1972) *Journal of the American Chemical Society* 94: 9166-9174
- 64) Larsen, S. W., Anderson, M., Larsen, C. (2004) *European Journal of Pharmaceutical Sciences* 22(5): 399-408
- 65) Balvinder, S., et al., (2003) *Pharmaceutical Research* 20(9): 1381-1388
- 66) Hamada, Y., et al., (2004) *Bioorganic & Medicinal Chemistry* 12: 159–170
- 67) Hamada, Y., et al., (2002) *Bioorganic & Medicinal Chemistry* 10: 4155–4167
- 68) Santos, C., et al., (2005) *Bioorganic & Medicinal Chemistry Letters* 15:1595–1598
- 69) Hamel, A. R. et al., (2004) *Journal of Peptide Research* 63: 147-154

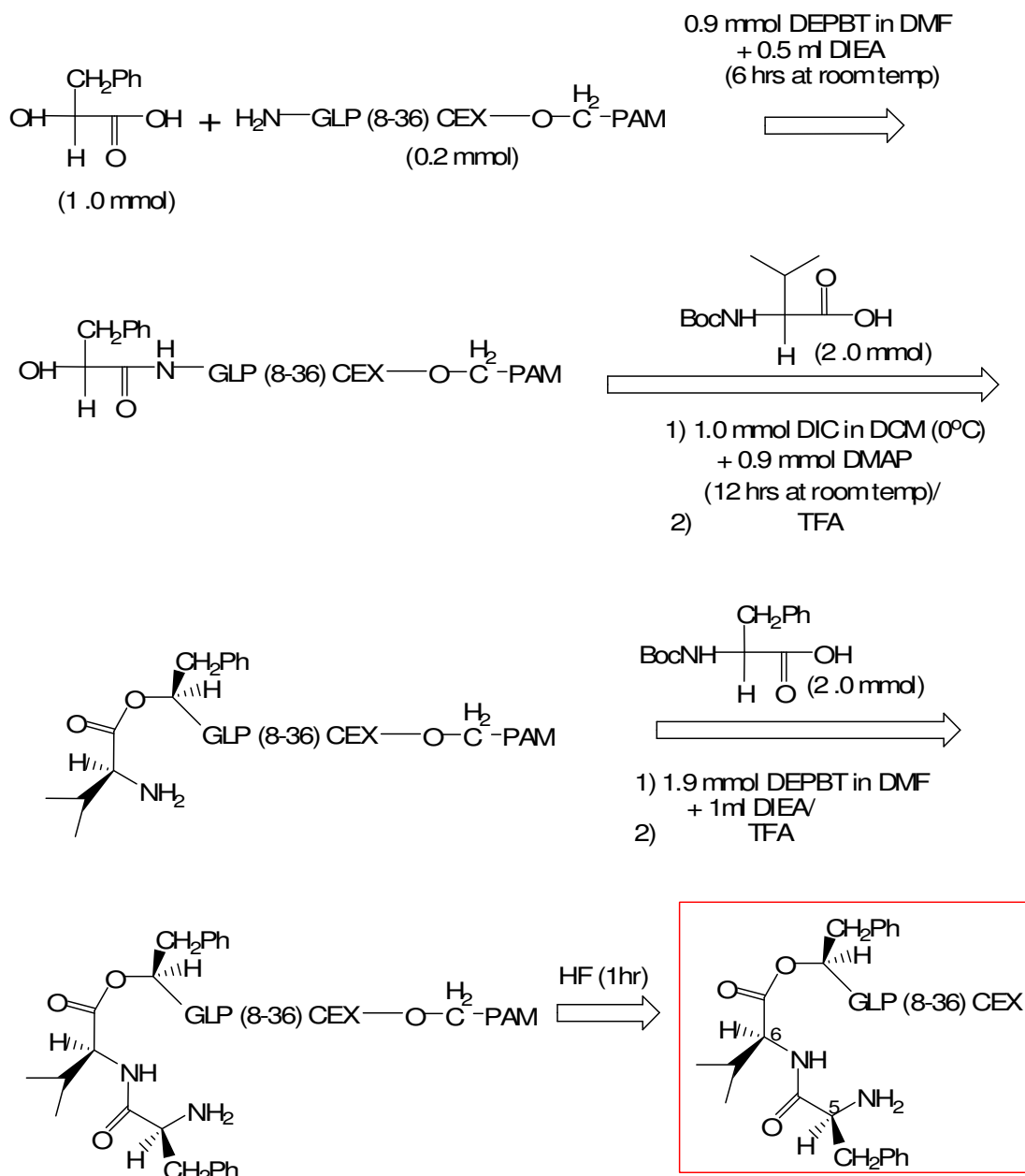
- 70) Hamel, A.R., Hubler, F., and Mutter, M., (2005) *Journal of Peptide Research* **65**: 364-374
- 71) Suggs, J. W., and Pires, R. M. (1997): *Tetrahedron Letters* **38**: 2227-2230
- 72) Fischer, P. M. (2003) *Journal of Peptide Science* **9**(1): 9-35
- 73) Louise, H. N. (1999) *Biochemical Pharmacology* **58**: 749–757
- 74) Williams, C. (2004) *Nature Reviews, Drug Discovery* **3**: 125-135
- 75) Schnolzer, M., et al., (1992) *Int J Pept Protein Res* **40**(3-4):180-193
- 76) “Personal Communications” – with Prof. Phil Dawson (Scripps Research Institute, San Diego, California)
- 77) Samantha, E. G., Peter, J. B., and Louise, H. N. (1997) *Journal of Biomolecular Screening* **2**(4): 235-240
- 78) Donnelly, D., (2003) *Journal of Biological Chemistry* **278**: 10195-10200
- 79) Denny, W. A. (2001) Prodrug strategies in cancer therapy. *European Journal of Medicinal Chemistry* **36**: 577–595
- 80) Menger, F. M., Ladika, M. (1988) *Journal of American Chemical Society* **110**(20): 6794-6796

Appendix I: Schematic synthesis of longer-acting prodrugs

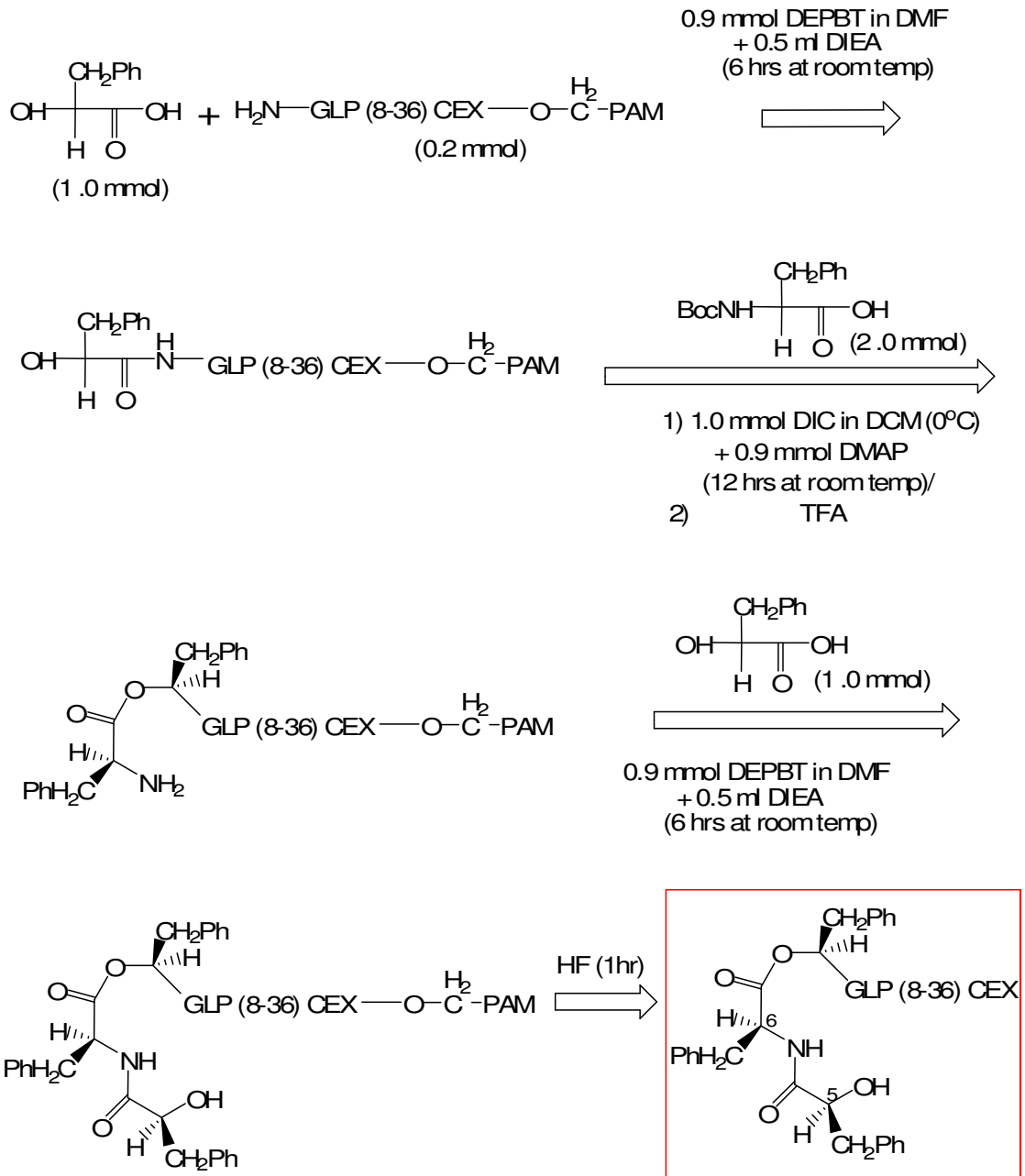
A) Synthesis of HO-F⁵dV⁶-O-F⁷,GLP(8-36)-CEX



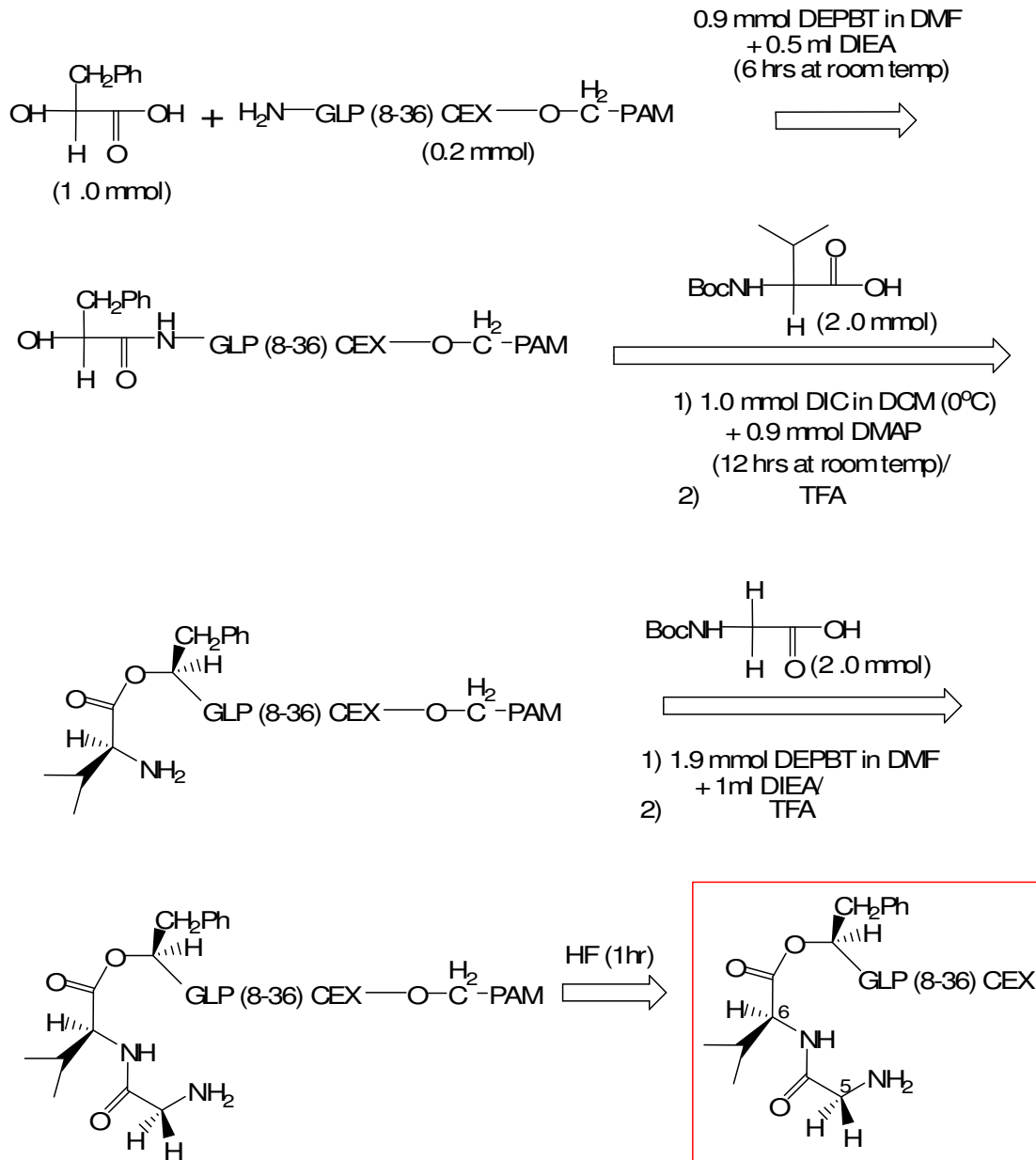
B) Synthesis of F⁵V⁶-O-F⁷,GLP(8-36)CEX



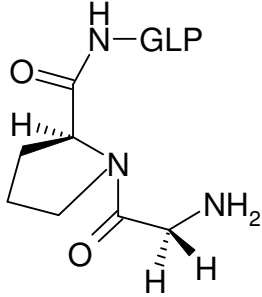
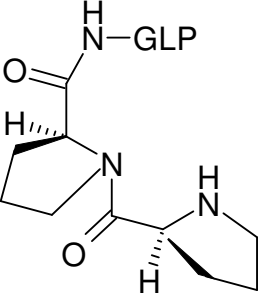
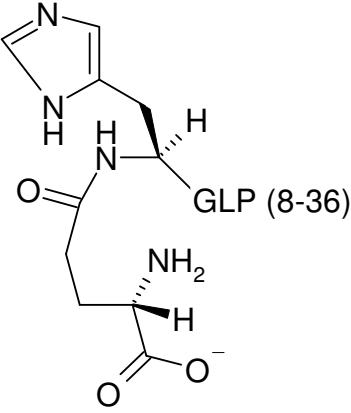
C) Synthesis of HO-F⁵F⁶-O-F⁷,GLP(8-36)-CEX

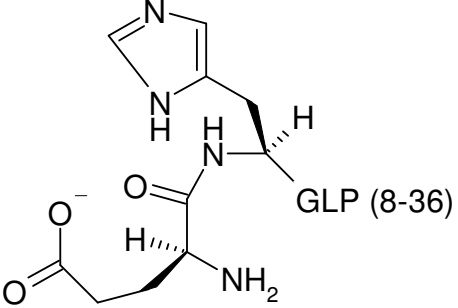
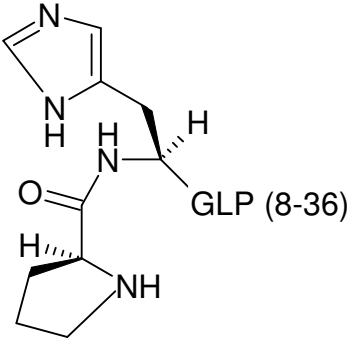
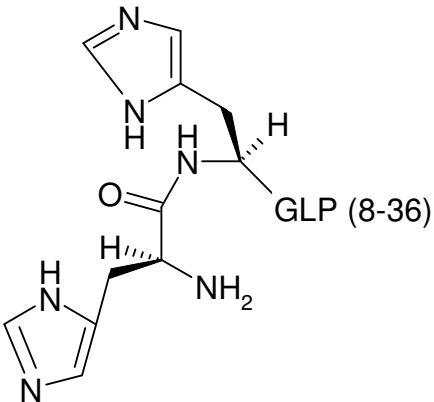


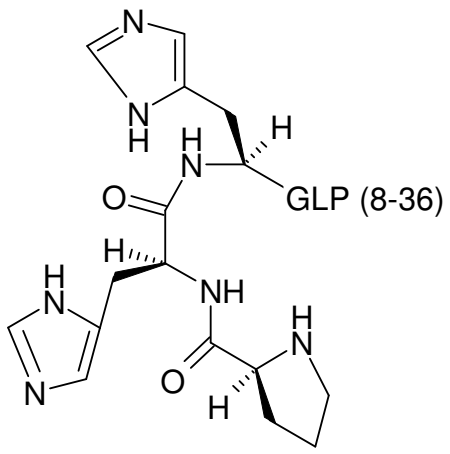
D) Synthesis of G⁵V⁶-O-F⁷,GLP(8-36)CEX



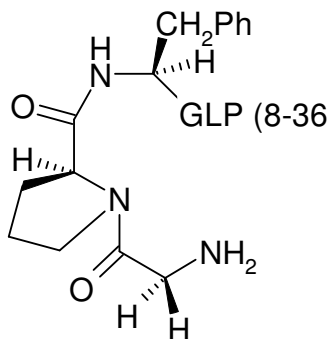
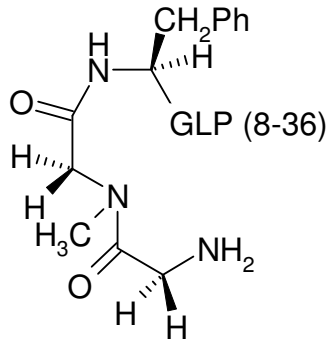
Appendix II: Structure of peptides in Table 2

Serial No	Structure
1.	
2.	
3.	

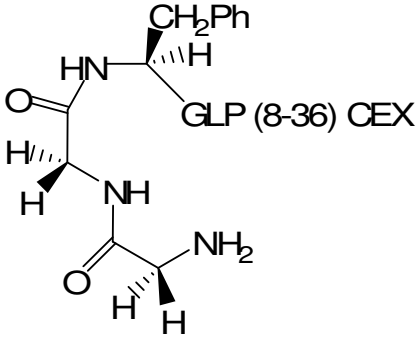
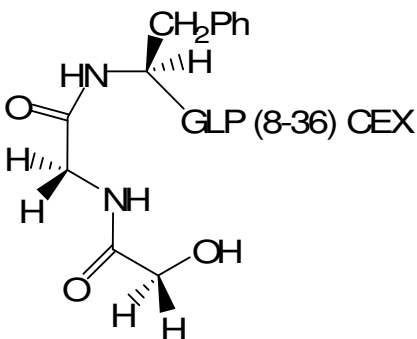
Serial No	Structure
4.	 <p>Chemical structure of L-tryptophan, showing the indole ring system attached to the alpha-carbon of the amino acid backbone. The beta-carbon is substituted with a carboxylate group (COO⁻). The structure is labeled with "GLP (8-36)".</p>
5.	 <p>Chemical structure of L-tryptamine, showing the indole ring system attached to the alpha-carbon of the amino acid backbone. The beta-carbon is substituted with a primary amine group (NH₂). The structure is labeled with "GLP (8-36)".</p>
6.	 <p>Chemical structure of 5-hydroxytryptamine (5-HT), showing the indole ring system attached to the alpha-carbon of the amino acid backbone. The beta-carbon is substituted with a primary amine group (NH₂). The structure is labeled with "GLP (8-36)".</p>

Serial No	Structure
7.	 <p>GLP (8-36)</p>

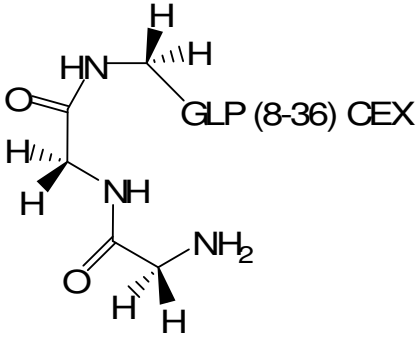
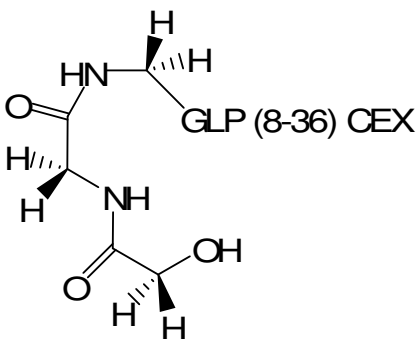
Appendix III: Structure of peptides in Table 3

Serial No	Structure
1.	 <p>Chemical structure of a cyclic peptide derivative. The structure shows a five-membered ring containing a nitrogen atom. One nitrogen atom is part of an amide group with a carbonyl oxygen (O) and a hydrogen atom (H). The adjacent carbon atom is bonded to a hydrogen atom (H) and a CH_2Ph group. The other nitrogen atom is part of an amide group with a carbonyl oxygen (O) and a hydrogen atom (H). The adjacent carbon atom is bonded to a hydrogen atom (H) and an NH_2 group. The label "GLP (8-36)" is placed near the CH_2Ph group.</p>
2.	 <p>Chemical structure of a cyclic peptide derivative, similar to structure 1 but with a methyl group (H_3C) attached to the nitrogen atom. The structure shows a five-membered ring containing a nitrogen atom. One nitrogen atom is part of an amide group with a carbonyl oxygen (O) and a hydrogen atom (H). The adjacent carbon atom is bonded to a hydrogen atom (H) and a CH_2Ph group. The other nitrogen atom is part of an amide group with a carbonyl oxygen (O) and a hydrogen atom (H). The adjacent carbon atom is bonded to a hydrogen atom (H) and an NH_2 group. A methyl group (H_3C) is attached to the nitrogen atom. The label "GLP (8-36)" is placed near the CH_2Ph group.</p>

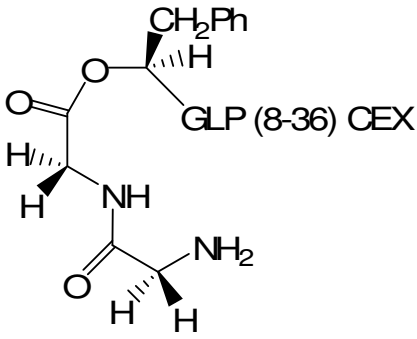
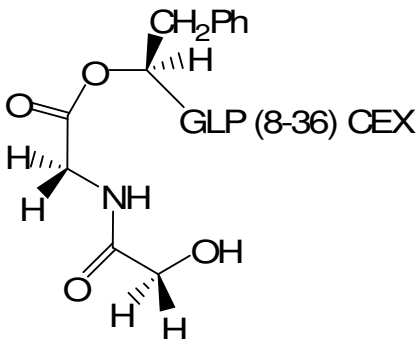
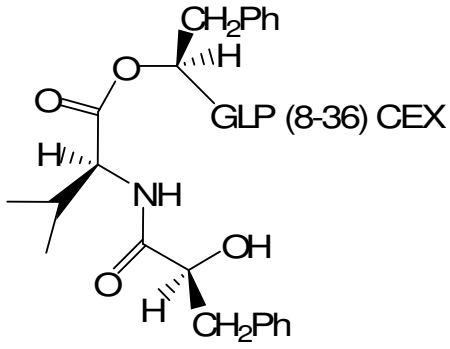
Appendix IV: Structure of peptides in Table 4

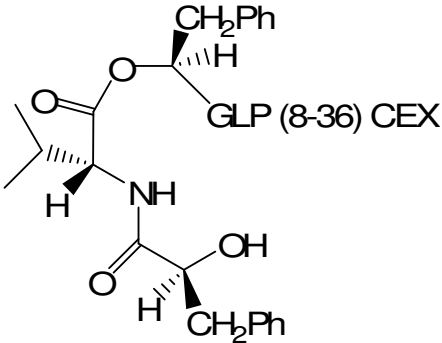
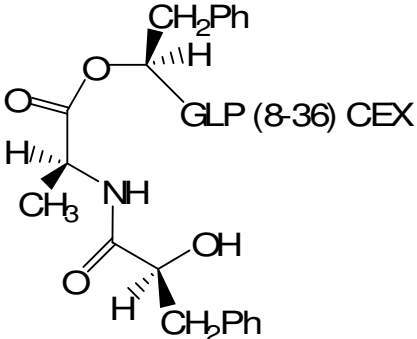
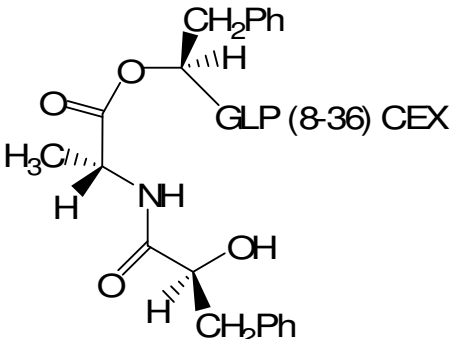
Serial No	Structure
1.	 <p>Chemical structure of a dipeptide derivative. The structure shows a central peptide backbone with a benzyl group (CH₂Ph) and a hydrogen atom (H) on the alpha carbon. The beta carbon is substituted with an amino group (NH₂). The structure is labeled "GLP (8-36) CEX".</p>
2.	 <p>Chemical structure of a dipeptide derivative. The structure shows a central peptide backbone with a benzyl group (CH₂Ph) and a hydrogen atom (H) on the alpha carbon. The beta carbon is substituted with a hydroxyl group (OH). The structure is labeled "GLP (8-36) CEX".</p>

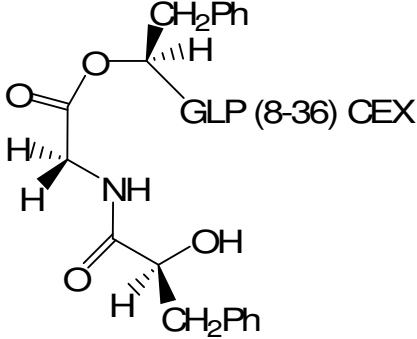
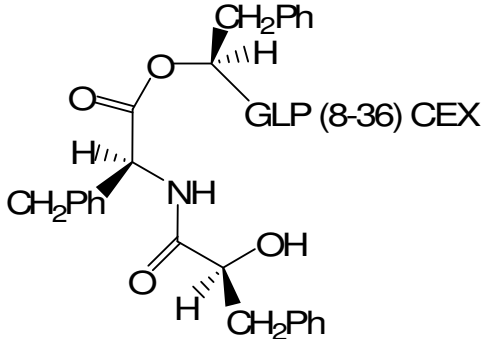
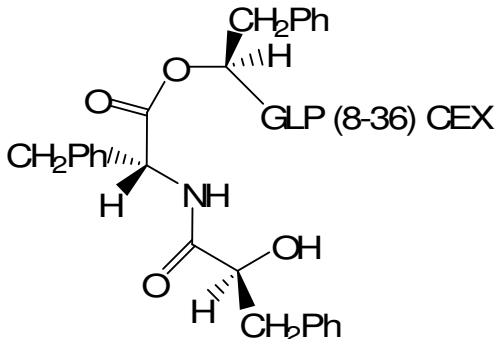
Appendix V: Structure of peptides in Table 5

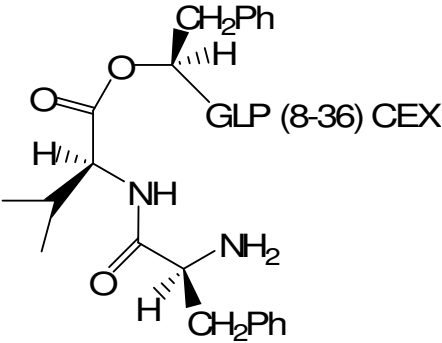
Serial No	Structure
1.	 <p>The chemical structure shows L-glutamine, a five-carbon amino acid. It features a central alpha-carbon bonded to a hydrogen atom (wedge), an amino group (NH, dash), and a carboxylate group (C=O, wedge; O, dash). The side chain consists of a beta-carbon bonded to a hydrogen atom (wedge), another hydrogen atom (dash), and a gamma-carbon bonded to a hydrogen atom (wedge), another hydrogen atom (dash), and an amino group (NH₂, dash). The text "GLP (8-36) CEX" is positioned to the right of the structure.</p>
2.	 <p>The chemical structure shows L-glutamic acid, a five-carbon amino acid. It features a central alpha-carbon bonded to a hydrogen atom (wedge), an amino group (NH, dash), and a carboxylate group (C=O, wedge; O, dash). The side chain consists of a beta-carbon bonded to a hydrogen atom (wedge), another hydrogen atom (dash), and a gamma-carbon bonded to a hydrogen atom (wedge), another hydrogen atom (dash), and a hydroxyl group (OH, dash). The text "GLP (8-36) CEX" is positioned to the right of the structure.</p>

Appendix VI: Structure of peptides in Table 6

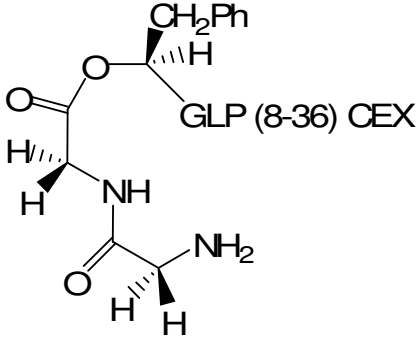
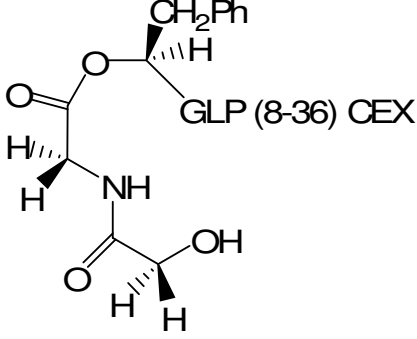
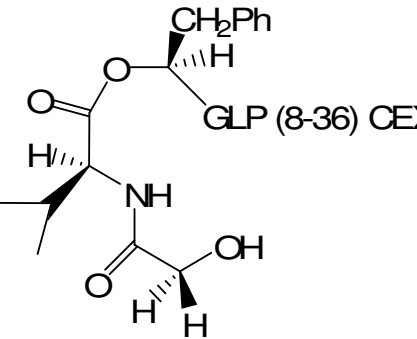
Serial No	Structure
1.	 <p>Chemical structure 1: A cyclic peptide derivative. The ring consists of a carbonyl group, an oxygen atom, a CH₂Ph group (wedge), and a hydrogen atom (dash). The nitrogen atom is bonded to a hydrogen atom (wedge) and a hydrogen atom (dash). The nitrogen is also bonded to a carbonyl group, which is further bonded to a CH₂ group (wedge) and a hydrogen atom (dash). The CH₂ group is bonded to an NH₂ group (wedge) and a hydrogen atom (dash).</p>
2.	 <p>Chemical structure 2: A cyclic peptide derivative. The ring consists of a carbonyl group, an oxygen atom, a CH₂Ph group (wedge), and a hydrogen atom (dash). The nitrogen atom is bonded to a hydrogen atom (wedge) and a hydrogen atom (dash). The nitrogen is also bonded to a carbonyl group, which is further bonded to a CH₂ group (wedge) and a hydrogen atom (dash). The CH₂ group is bonded to a hydroxyl group (OH, wedge) and a hydrogen atom (dash).</p>
3.	 <p>Chemical structure 3: A cyclic peptide derivative. The ring consists of a carbonyl group, an oxygen atom, a CH₂Ph group (wedge), and a hydrogen atom (dash). The nitrogen atom is bonded to a hydrogen atom (wedge) and a hydrogen atom (dash). The nitrogen is also bonded to a carbonyl group, which is further bonded to a CH₂ group (wedge) and a hydrogen atom (dash). The CH₂ group is bonded to a hydroxyl group (OH, wedge) and a CH₂Ph group (wedge).</p>

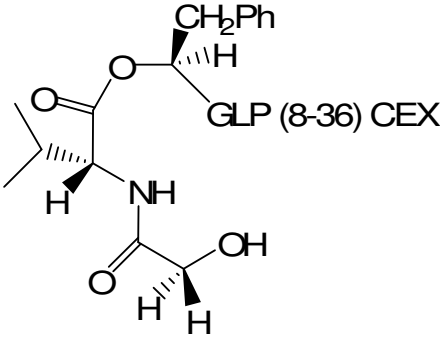
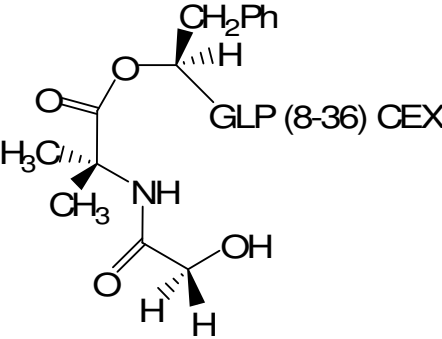
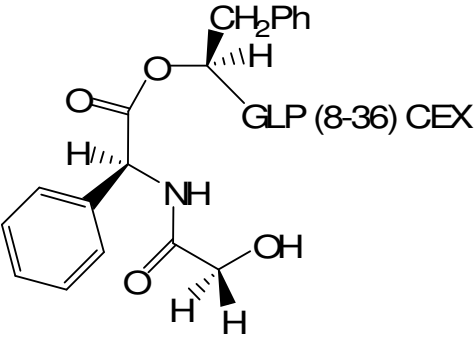
Serial No	Structure
4.	 <p>The structure shows a cyclic peptide derivative. The main ring is a six-membered ring containing an oxygen atom and a carbonyl group. The alpha carbon of the ring has a methyl group (CH₃) attached with a dashed bond and a hydrogen atom (H) with a wedged bond. The nitrogen atom of the ring is attached to a side chain consisting of a carbonyl group, a chiral carbon with a hydroxyl group (OH) and a benzyl group (CH₂Ph) attached with wedged bonds, and a hydrogen atom (H) with a dashed bond. The oxygen atom of the ring is attached to a benzyl group (CH₂Ph) with a wedged bond and a hydrogen atom (H) with a dashed bond. The label "GLP (8-36) CEX" is placed to the right of the structure.</p>
5.	 <p>The structure shows a cyclic peptide derivative. The main ring is a six-membered ring containing an oxygen atom and a carbonyl group. The alpha carbon of the ring has a hydrogen atom (H) attached with a dashed bond and another hydrogen atom (H) with a wedged bond. The nitrogen atom of the ring is attached to a side chain consisting of a carbonyl group, a chiral carbon with a hydroxyl group (OH) and a benzyl group (CH₂Ph) attached with wedged bonds, and a hydrogen atom (H) with a dashed bond. The oxygen atom of the ring is attached to a benzyl group (CH₂Ph) with a wedged bond and a hydrogen atom (H) with a dashed bond. The label "GLP (8-36) CEX" is placed to the right of the structure.</p>
6.	 <p>The structure shows a cyclic peptide derivative. The main ring is a six-membered ring containing an oxygen atom and a carbonyl group. The alpha carbon of the ring has a methyl group (H₃C) attached with a dashed bond and a hydrogen atom (H) with a wedged bond. The nitrogen atom of the ring is attached to a side chain consisting of a carbonyl group, a chiral carbon with a hydroxyl group (OH) and a benzyl group (CH₂Ph) attached with wedged bonds, and a hydrogen atom (H) with a dashed bond. The oxygen atom of the ring is attached to a benzyl group (CH₂Ph) with a wedged bond and a hydrogen atom (H) with a dashed bond. The label "GLP (8-36) CEX" is placed to the right of the structure.</p>

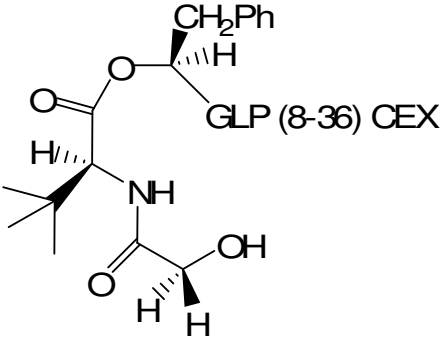
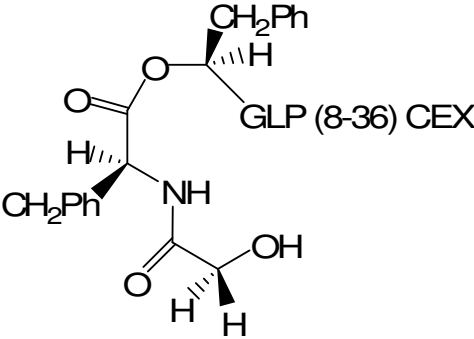
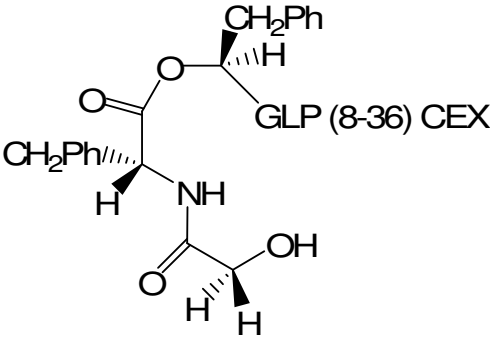
Serial No	Structure
7.	 <p>Chemical structure of a cyclic peptide derivative, labeled GLP (8-36) CEX. The structure shows a cyclic backbone with a benzyl group (CH₂Ph) attached to the C-terminus. The stereochemistry is indicated by wedged and dashed bonds. The structure is shown in a chair-like conformation.</p>
8.	 <p>Chemical structure of a cyclic peptide derivative, labeled GLP (8-36) CEX. The structure shows a cyclic backbone with a benzyl group (CH₂Ph) attached to the N-terminus. The stereochemistry is indicated by wedged and dashed bonds. The structure is shown in a chair-like conformation.</p>
9.	 <p>Chemical structure of a cyclic peptide derivative, labeled GLP (8-36) CEX. The structure shows a cyclic backbone with a benzyl group (CH₂Ph) attached to the N-terminus. The stereochemistry is indicated by wedged and dashed bonds. The structure is shown in a chair-like conformation.</p>

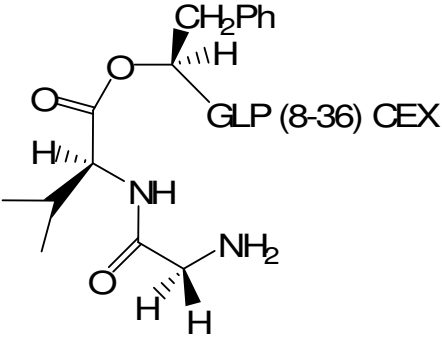
Serial No	Structure
10.	 <p>The chemical structure shows a peptide backbone with a benzyl group (CH₂Ph) attached to the side chain. The structure is labeled "GLP (8-36) CEX". The amino acid residues are shown with their respective side chains and stereochemistry. The structure is a cyclic peptide derivative with a benzyl group (CH₂Ph) attached to the side chain. The structure is labeled "GLP (8-36) CEX".</p>

Appendix VII: Structure of peptides in Table 7

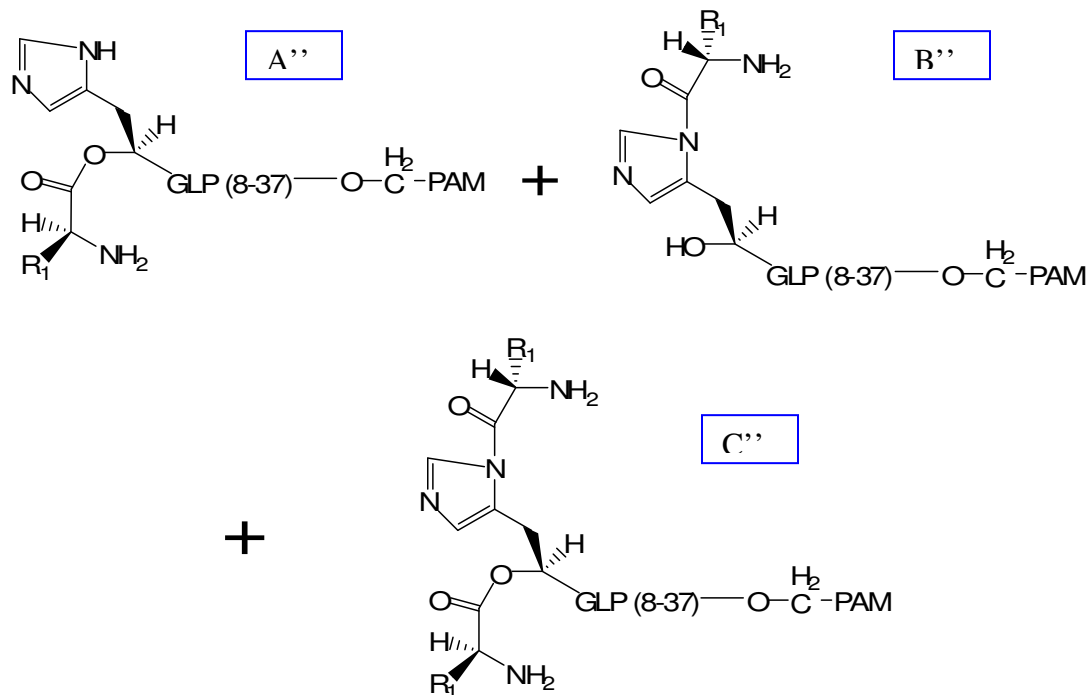
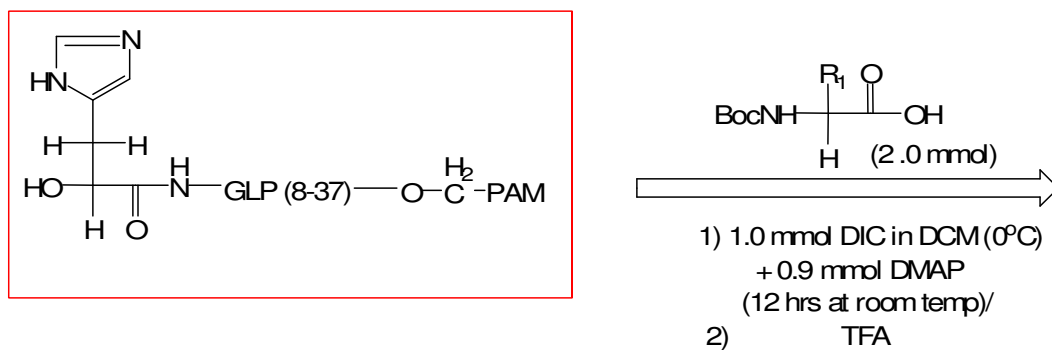
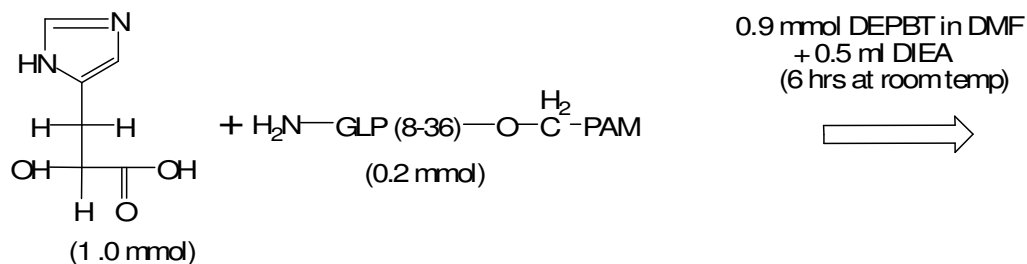
Serial No	Structure
1.	 <p>The structure shows a dipeptide, L-phenylalanyl-L-glutamine. The phenylalanine residue is on the left, with its side chain represented as CH_2Ph. The glutamine residue is on the right, with its side chain represented as NH_2. The peptide backbone consists of a central amide bond (NH) and two carbonyl groups (C=O). Stereochemistry is indicated with wedges and dashes: the α-carbon of phenylalanine has a hydrogen atom on a dashed bond, and the α-carbon of glutamine has a hydrogen atom on a dashed bond. The label "GLP (8-36) CEX" is positioned to the right of the structure.</p>
2.	 <p>The structure shows a dipeptide, L-phenylalanyl-L-glutamic acid. The phenylalanine residue is on the left, with its side chain represented as CH_2Ph. The glutamic acid residue is on the right, with its side chain represented as OH. The peptide backbone consists of a central amide bond (NH) and two carbonyl groups (C=O). Stereochemistry is indicated with wedges and dashes: the α-carbon of phenylalanine has a hydrogen atom on a dashed bond, and the α-carbon of glutamic acid has a hydrogen atom on a dashed bond. The label "GLP (8-36) CEX" is positioned to the right of the structure.</p>
3.	 <p>The structure shows a dipeptide, L-phenylalanyl-L-glutamic acid, with an additional methyl group attached to the α-carbon of the phenylalanine residue. The phenylalanine residue is on the left, with its side chain represented as CH_2Ph. The glutamic acid residue is on the right, with its side chain represented as OH. The peptide backbone consists of a central amide bond (NH) and two carbonyl groups (C=O). Stereochemistry is indicated with wedges and dashes: the α-carbon of phenylalanine has a hydrogen atom on a dashed bond and a methyl group on a wedge, and the α-carbon of glutamic acid has a hydrogen atom on a dashed bond. The label "GLP (8-36) CEX" is positioned to the right of the structure.</p>

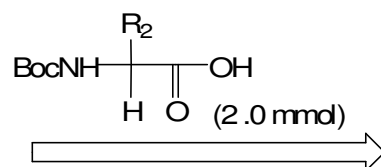
Serial No	Structure
4.	 <p>The structure shows a cyclic peptide derivative. It features a seven-membered ring containing an oxygen atom and a carbonyl group. A benzyl group (CH_2Ph) is attached to the ring with a wedged bond, and a hydrogen atom (H) is attached with a dashed bond. The label "GLP (8-36) CEX" is positioned to the right of the ring. A side chain is attached to the ring, consisting of a methylene group (CH_2), a carbonyl group (C=O), and a chiral center with a hydroxyl group (OH) on a wedged bond and two hydrogen atoms (H) on dashed bonds.</p>
5.	 <p>The structure shows a cyclic peptide derivative similar to the one in row 4. It features a seven-membered ring containing an oxygen atom and a carbonyl group. A benzyl group (CH_2Ph) is attached to the ring with a wedged bond, and a hydrogen atom (H) is attached with a dashed bond. The label "GLP (8-36) CEX" is positioned to the right of the ring. A side chain is attached to the ring, consisting of a methyl group (CH_3), a carbonyl group (C=O), and a chiral center with a hydroxyl group (OH) on a wedged bond and two hydrogen atoms (H) on dashed bonds.</p>
6.	 <p>The structure shows a cyclic peptide derivative similar to the one in row 4. It features a seven-membered ring containing an oxygen atom and a carbonyl group. A benzyl group (CH_2Ph) is attached to the ring with a wedged bond, and a hydrogen atom (H) is attached with a dashed bond. The label "GLP (8-36) CEX" is positioned to the right of the ring. A side chain is attached to the ring, consisting of a phenyl group (C_6H_5), a carbonyl group (C=O), and a chiral center with a hydroxyl group (OH) on a wedged bond and two hydrogen atoms (H) on dashed bonds.</p>

Serial No	Structure
7.	 <p>Chemical structure 7 shows a cyclic peptide derivative. The structure features a benzyl group (CH_2Ph) and a hydroxyl group (OH) attached to the ring. The label "GLP (8-36) CEX" is present. Stereochemistry is indicated with wedges and dashes.</p>
8.	 <p>Chemical structure 8 shows a cyclic peptide derivative. The structure features two benzyl groups (CH_2Ph) and a hydroxyl group (OH) attached to the ring. The label "GLP (8-36) CEX" is present. Stereochemistry is indicated with wedges and dashes.</p>
9.	 <p>Chemical structure 9 shows a cyclic peptide derivative. The structure features two benzyl groups (CH_2Ph) and a hydroxyl group (OH) attached to the ring. The label "GLP (8-36) CEX" is present. Stereochemistry is indicated with wedges and dashes.</p>

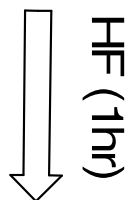
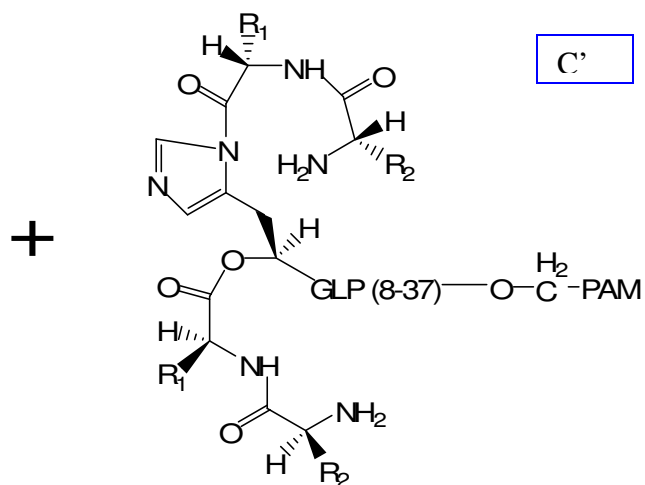
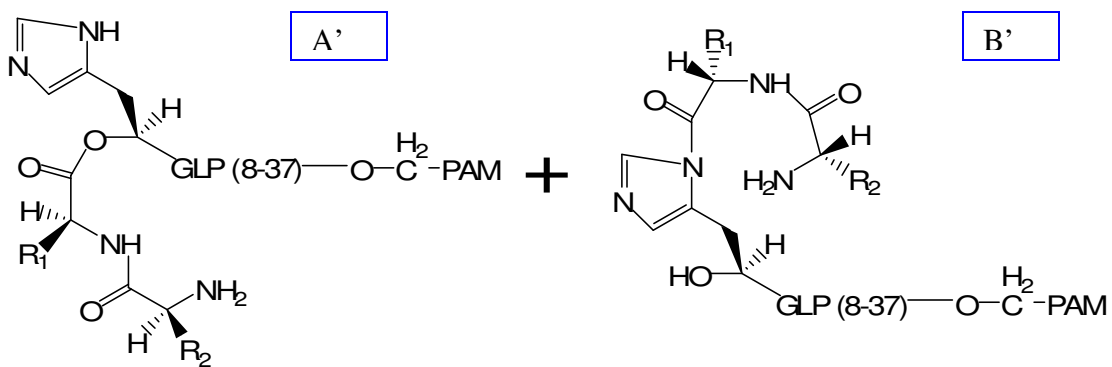
Serial No	Structure
10.	 <p>The chemical structure is a cyclic peptide derivative labeled "GLP (8-36) CEX". It features a seven-membered ring containing an oxygen atom and a carbonyl group. A benzyl group (CH₂Ph) is attached to the ring with a wedge bond, and a hydrogen atom (H) is attached with a dash bond. A methyl group (CH₃) is attached to the ring with a wedge bond, and a hydrogen atom (H) is attached with a dash bond. The ring is connected to a side chain consisting of an amide group (NH) and a primary amine group (NH₂). The amide group is attached to a carbon atom that has a hydrogen atom (H) attached with a dash bond. The primary amine group is attached to a carbon atom that has two hydrogen atoms (H) attached with dash bonds.</p>

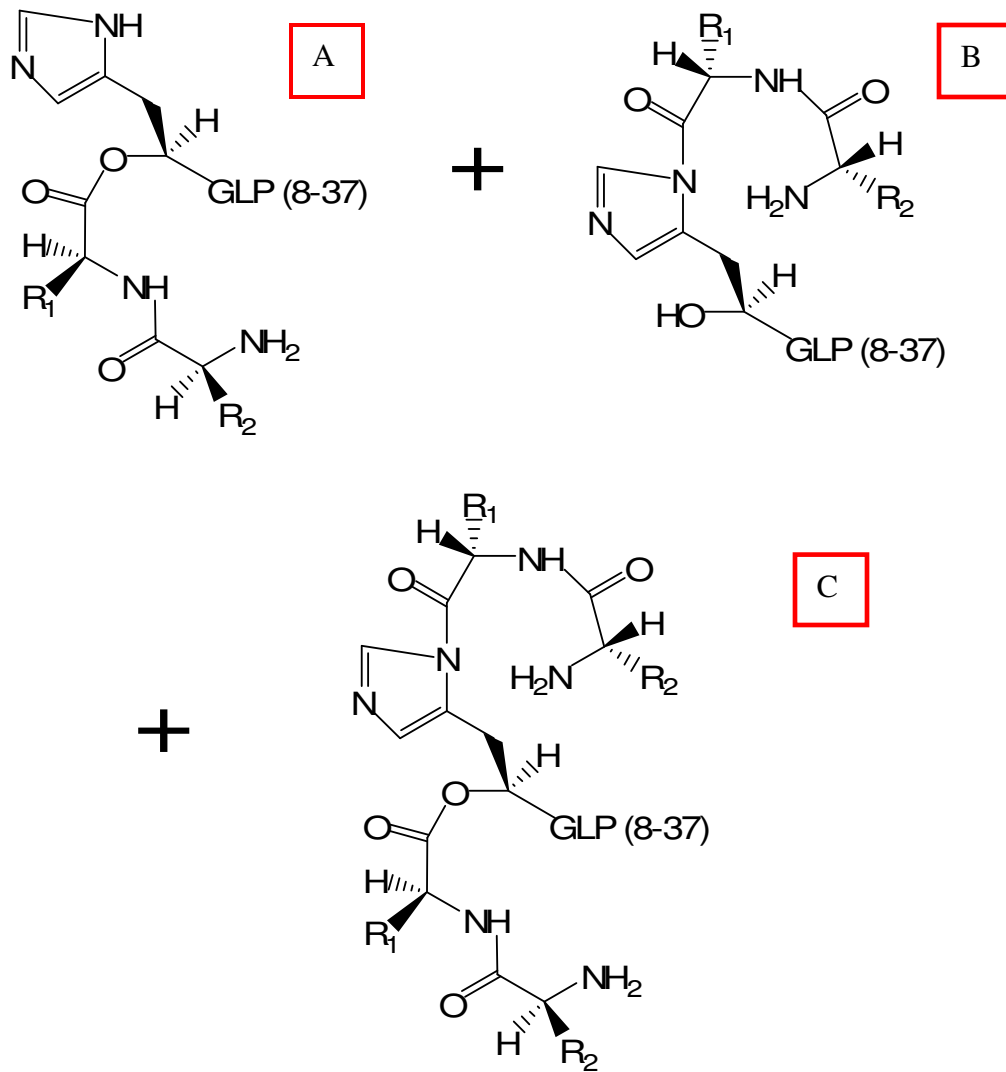
Appendix VIII: Acylation of HO-His⁷,GLP(8-37)





- 1) 1.9 mmol DEPBT in DMF
+ 1 ml DIEA
- 2) TFA





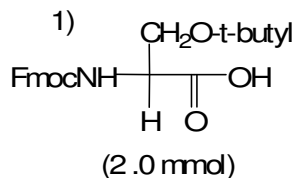
Appendix IX: Synthesis of (H7F),(E9Q),(T11S),GLP(8-36)-

CEX



i) 1.9 mmol DEPBT in DMF
+ 1ml DIEA/

ii) 20% piperidine in DMF



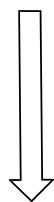
2) 2.0 mmol Fmoc-Gly i) 1.9 mmol DEPBT in DMF
+ 1ml DIEA/
ii) 20% piperidine in DMF

3) 2.0 mmol Fmoc-Gln i) 1.9 mmol DEPBT in DMF
+ 1ml DIEA/
ii) 20% piperidine in DMF

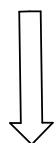
4) 2.0 mmol Fmoc-Ala i) 1.9 mmol DEPBT in DMF
+ 1ml DIEA/
ii) 20% piperidine in DMF

5) 2.0 mmol Fmoc-Phe i) 1.9 mmol DEPBT in DMF
+ 1ml DIEA/





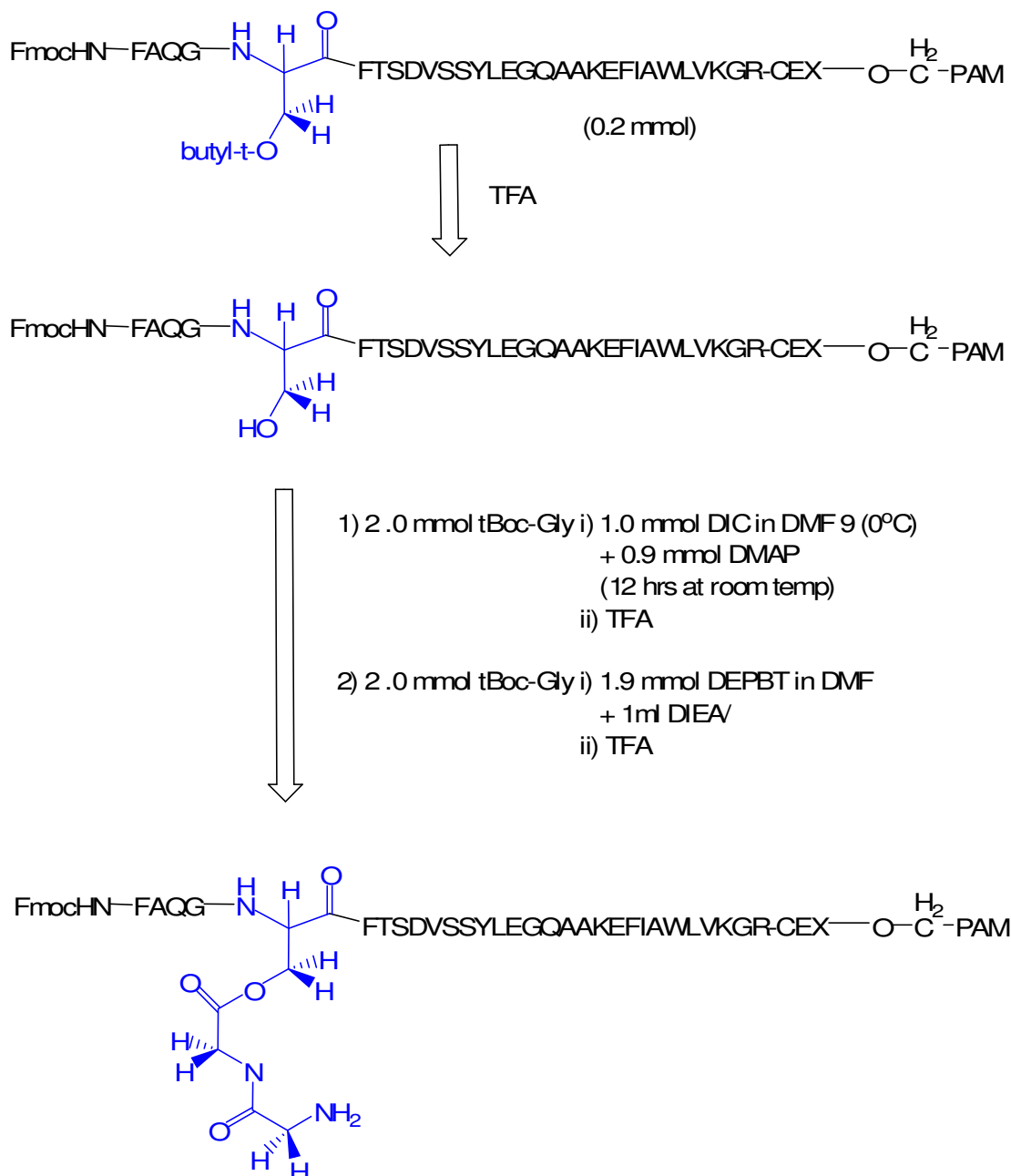
- 1) TFA for 2 hrs
- 2) 20% piperidine



HF cleavage

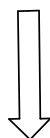
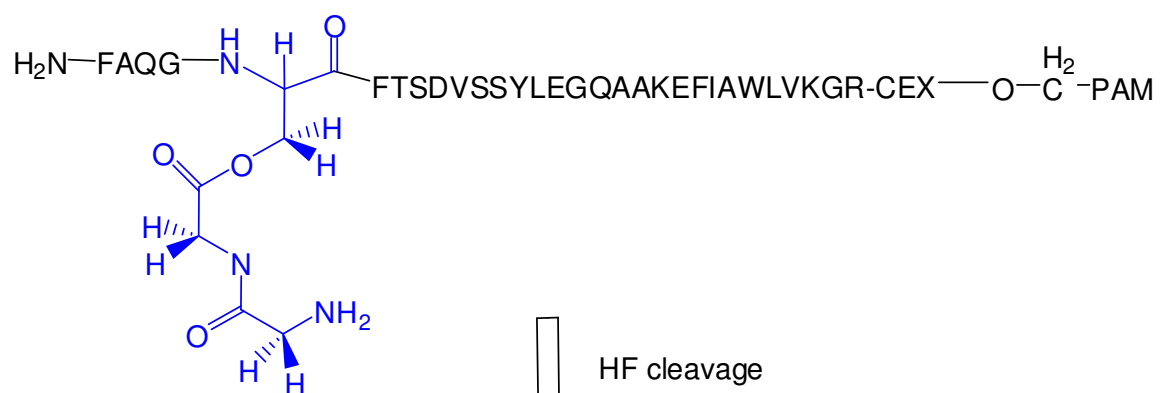


Appendix X: Synthesis of (H7F),(E9Q),[T11S-O^β-(Gly-Gly)],GLP(8-36)-CEX

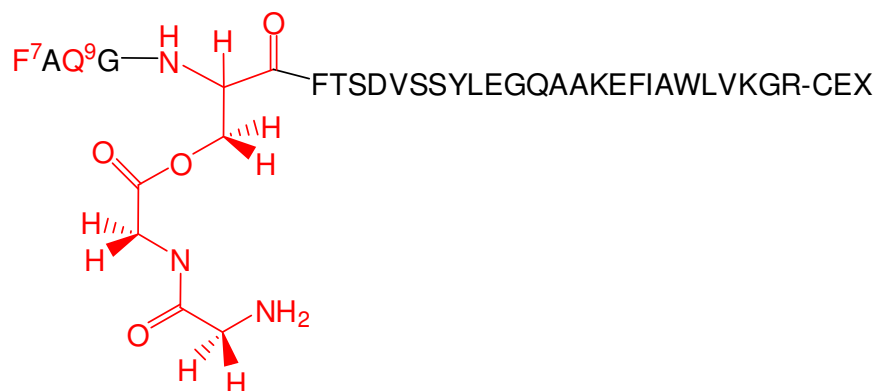




20% piperidine



HF cleavage



Appendix XI: A note on nomenclature

- A. Native GLP-1(7-37)-acid has been listed as GLP throughout this thesis. Its sequence is:

HAEGTFTSDVSSYLEGQAAKEFIAWLVKGRG-acid

- B. F⁷,GLP(8-37) refers to the GLP analog where the His at the 7th position has been replaced by Phe. The analog is:

FAEGTFTSDVSSYLEGQAAKEFIAWLVKGRG-acid

- C. The GLP(7-36)-CEX amide has been designated as GLP(7-36)-CEX throughout this thesis. The CEX sequence (in red) is the C-terminal nine amino acids of exendin-4 where the C terminus is a serine amide. Its sequence is:

H⁷AEGTFTSDVSSYLEGQAAKEFIAWLVKGRPSSGAPPPS-amide

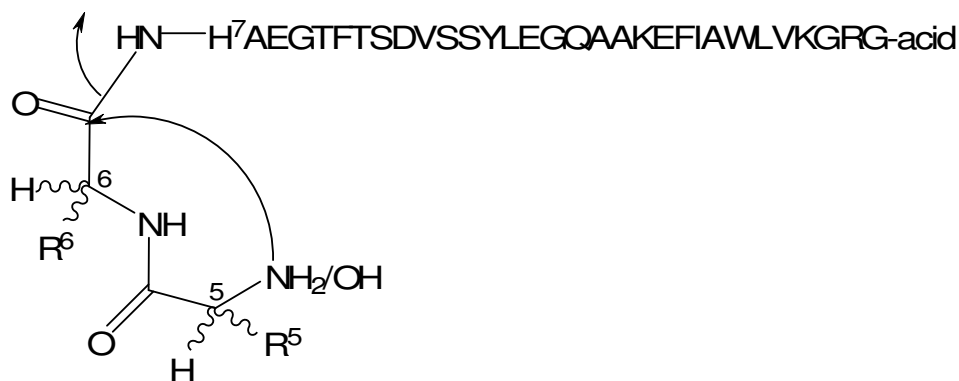
Changes have been made to the nomenclature to signify analogous peptides. For example, the sequence of HO-F⁷,GLP(8-36)-CEX is:

HO-F⁷AEGTFTSDVSSYLEGQAAKEFIAWLVKGRPSSGAPPPS-amide

- D. The amide prodrugs designated as X⁵Y⁶H⁷,GLP(8-37) and X⁵Y⁶F⁷,GLP(8-37) refers to the prodrugs synthesized on the native GLP and F⁷,GLP(8-37) respectively. The sequence of X⁵Y⁶H⁷,GLP(8-37) is shown below:

X⁵Y⁶H⁷AEGTFTSDVSSYLEGQAAKEFIAWLVKGRG-acid

The structure of such amide prodrugs (amine and hydroxyl nucleophile) is represented below:



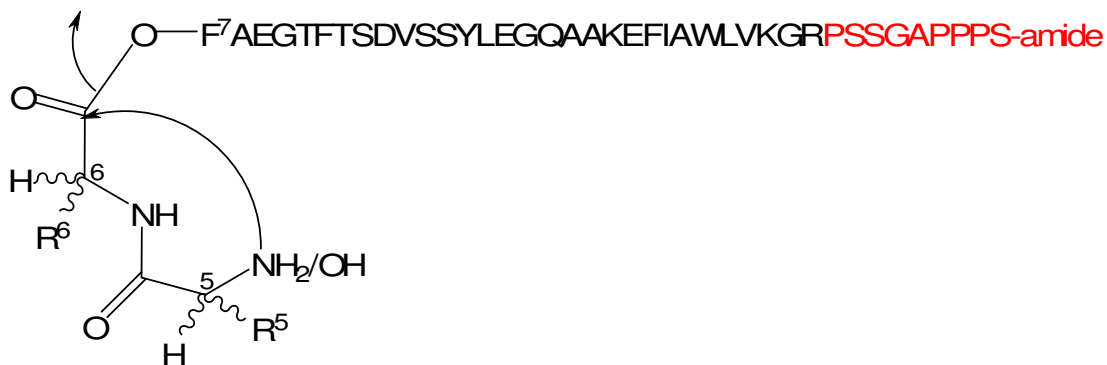
E. The ester prodrugs are designated as $X^5Y^6-O-F^7$,GLP(8-36)-CEX with an amine nucleophile:

$X^5Y^6F^7$ AEGTFTSDVSSYLEGQAAKEFIAWLVKGRPSSGAPPPS-amide

and $HO-X^5Y^6-O-F^7$,GLP(8-36)-CEX with a hydroxyl nucleophile respectively.

$HO-X^5Y^6-O-F^7$ AEGTFTSDVSSYLEGQAAKEFIAWLVKGRPSSGAPPPS-amide

The structure of such ester prodrugs (amine and hydroxyl nucleophile) is represented below:



F. The preliminary peptides for the synthesis of the internal ester prodrugs are

(H7F),(E9Q),GLP(8-36)-CEX and (H7F),(E9Q),(T11S),GLP(8-36)-CEX. The

mutations from the native sequence are represented in parenthesis and shown in red. The sequence of (H7F),(E9Q),GLP(8-36)-CEX is :

F⁷AQ⁹GTFTSDVSSYLEGQAAKEFIAWLVKGRPSSGAPPPS-amide

and the sequence of (H7F),(E9Q),(T11S),GLP(8-36)-CEX is:

F⁷AQ⁹GS¹¹FTSDVSSYLEGQAAKEFIAWLVKGRPSSGAPPPS-amide

The structure of (H7F),(E9Q),(T11S),GLP(8-36)-CEX is given by:



- G. The internal ester prodrug designated as (H7F),(E9Q),[T11S-O^β-(Gly-Gly)],GLP(8-36)-CEX was synthesized from the serine at the 11th position of (H7F),(E9Q),(T11S),GLP(8-36)-CEX. The (Gly-Gly) dipeptide pro-moiety (shown in red) was added to the S11. The sequence of (H7F),(E9Q),[T11S-O^β-(Gly-Gly)],GLP(8-36)-CEX is given by:

F⁷AQ⁹GS¹¹FTSDVSSYLEGQAAKEFIAWLVKGRPSSGAPPPS-amide
 |
 GG

The structure of (H7F),(E9Q),[T11S-O^β-(Gly-Gly)],GLP(8-36)-CEX is

